# Aspects of effective dynamics for nonequilibrium systems

**Simi R. Thomas**

Dissertation presented in partial
fulfillment of the requirements for the
degree of Doctor in Science

September 2013

# Aspects of effective dynamics for nonequilibrium systems

**Simi R. THOMAS**

Supervisory Committee:
Prof. Dr. Antoine van Proeyen, chair
Prof. Dr. Christian Maes, supervisor
  (KU Leuven)
Prof. Dr. Joseph Indekeu, KU Leuven
Prof. Dr. Mark Fannes, KU Leuven
Prof. Dr. Enrico Carlon, KU Leuven
Prof. Dr. David S. Dean
  (Université de Bordeaux)
Dr. Matthias Krüger
  (Universität Stuttgart & Max Planck Institute
for Intelligent Systems)

September 2013

*Quand tu veux construire un bateau, ne commence pas par rassembler du bois, couper des planches et distribuer du travail, mais reveille au sein des hommes le desir de la mer grande et large - Antoine de Saint-Exupéry*

The front and back covers are designed by M. Michel Tursis.

The cover designs depict a nonequilibrium background - The Waves and The Wind. A large probe is placed in this environment - The Boat and The Wind turbine, which follows the motion of the background.

# Preface

*The Force will be with you, always - Obi-Wan Kenobi to Luke Skywalker*

## Forces: Then & Now

The ability of human mind to learn from old experiences, to string them logically as cause and effect, to develop meaningful patterns and then to be able to alter the cause to manipulate the effect in its favor has been the reason behind mankind's continuing prosperity and dominance over other life forms on earth.

One experience out of the many layers accumulated over 200,000 years of existence of Homosapiens has been the ability to cause and perform motion in many forms. Motion, which in modern thought is understood as change in position, speed, direction, shape or configuration or abstractly a change in "**State**".

The questions attached -
- "What is motion ? "
- "Why is there motion ? "
- " How is there motion ? "

sound today ridiculously simple-minded.

Yet, we thrive on the accumulated systematic thought process which has been ongoing since wo/man exerted her/his curious mind on nature and natural process.

We start with the Greeks, who are known to have developed the notion that nature is comprehensible through logic. And among the Greeks was Aristotle - "The Philosopher". For him - *Motion <u>is</u> the problem of force and vice versa.* Aristotle, who gave the description of nature in terms of four fundamental

elements, believed that - Each element has its **natural motion** and its necessary destination of a **natural state**.

Thus mud, constituted of water and earth, if dropped, follows the path of the dominant element - earth and seeks its natural state at the center of the earth.

The core of his idea was the following: motion is caused, when a force is exerted by an agent and ceases as soon as the acting force stops too. Any body constrained out of its natural state, on the removal of the constraint will execute motion until it reaches its natural state.

Archimedes, a physicist and engineer in modern terms, was one of the first to see **rest** and not just motion worthy of attention. He concluded that the natural state of a body is one where - opposing forces balance (this was probably one of the first understandings of superposition of forces ) [6] and an unbalance of forces causes motion out of the equilibrium or stable state.
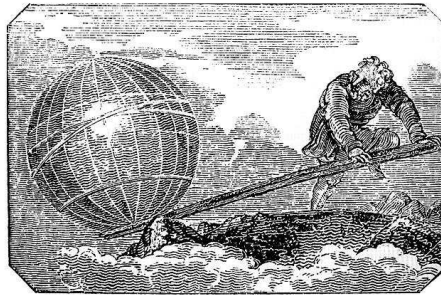
Figure 1: Give me a place to stand and I will move the earth - Archimedes on the lever.

Two thousand years later Galileo Galilei, a pioneer experimentalist from Padua threw canon balls from the crow's nest of moving ships, dropped them down high towers and along inclined planes to discover laws and test conjectures. His observations told him-

A body set in motion continues in its state of motion, without the aid of any force and unless there are forces which resist its motion. This he called **inertia**.

Galileo understood that the state of a body in constant velocity was equivalent to its state at rest and both did not require application of force. Here was created a digression from Aristotelian thought that a natural state of a body is the state of rest and that for a body to continue in a state of motion requires constant application of force.

Fifty year had passed when Isaac Newton presented the three famous laws of

motion in his thesis *Philosophiæ Naturalis Principia Mathematica* and together with it also gave the Universal Law of Gravitation. These laws related force to mass and to the concept of momentum. They also presented a new and then uncomfortable scenario, since the laws of gravitation were interactions acting over a distance.

Today our knowledge about forces is far more detailed and sophisticated. We know that forces can not only cause motion but forces hold matter together. The gravitational force keep us from floating away into space and keeps the earth orbiting around the sun. We have managed to systematize our knowledge about forces and have grouped them into 4 fundamental categories

- Gravitation
- Electromagnetism
- Strong Nuclear Interactions
- Weak Nuclear Interactions

These forces hold electrons inside an atom; protons and neutrons inside a nucleus and cause the radioactive decay of certain nuclei.

We further understand that different forces act at various range or distances and have very different strengths. E.g. gravitational force between nucleons inside an atom is almost negligible compared to the nuclear interaction between them. On the other hand at astronomical distances gravity is the most significant force holding our solar system together.

We have also encountered forces which do not fall in the above categories. Their action does not depend on the atomic or chemical nature of objects exerting them or being exerted on. Rather, these are forces that exist only at certain scales of description and not on others. These forces do not have a microscopic meaning and manifest only at mesoscopic and macroscopic scales. Such forces form the subject matter of our interest in this work. They depend on and originate from the action of large numbers.

To understand the origin of such forces we pass over into the realm of Thermodynamics and Statistical physics. In Chapter 1 we discuss the definition of effective forces coming from a thermodynamic point of view and then look at their statistical interpretation. We discuss some problems that make a similar definition difficult in nonequilibrium.

Chapter 2 deals with basic theory of stochastic processes and in particular time-dependent Markov process and Arrhenius rate law. The application of time-dependent dynamics is seen in the context of the No-go theorem in Chapter 3.

Chapter 4 is a review of the Large Deviation Theory and its applications in statistical mechanics. We discuss its particular application in Markov processes. The Large Deviation rate functions can be related to effective potentials and forces in equilibrium. We discuss this with the help of an example: The Entropic Spring

We end with a more serious study of statistical forces and try to extract some of their general characteristics with the help of exploratory models. We discuss how to derive effective dynamics of a slow parameter using systematic coarse graining methods like the Projection operator technique. We apply these arguments to derive the buoyant force in granular matter.

We look at nonequilibrium extensions of Statistical forces with the help of a Markov jump model of coupled systems on 3 state space and a diffusion model of the Rouse polymer.

# Gratias vobis ago

*Piglet noticed that even though he had a very small heart, it could hold a rather large amount of gratitude. - A.A. Milne, Winnie-the-Pooh*

This is the last addition that I make to my thesis. Before the curtain falls, I would like to take this opportunity to thank all those who stood by me for the past 4 years.

The work in this thesis is unequivocally a result of the vision of my adviser Prof. Christian Maes. I consider myself fortunate, Christ, to have you as my guide for the past four years. I have learned not only the subtleties of nonequilibrium physics from you, but more importantly, I have tried to learn your perseverance in face of hard questions. Thank you.

I especially thank the members of my examination committee who took time to read my thesis and gave useful suggestions.

Amma, Appa, my achievements stand on the foundation of your sacrifices and love. I feel proud to be your daughter. This thesis is dedicated to my parents Rajan Thomas and Aleyamma Rajan.

My dear brother, I thank you for all the discussions about life, the laugh and play we had as kids. They have made me a strong and better human. I thank you Stalin for coming into my life.

Apart from my family, there is one constant of my universe and that is you Shruti. For the past fifteen years your presence has inspired me. I thank you for always encouraging me to do my best and loving me for who I am.

Our long distance relation has no twin. We have met exactly once in person. Shayista, your friendship and love has been my strength for the past 6 years.

My friends say that I smile more since I met you. You have held me together at difficult times. My partner and love, Raph, thank you for all the happiness and love.

Monique, Michel, Véro, my god child Arthur, Maurice, Chantal, Pascal, Virginie, Damien et Ben - Merci du fond du coeur pour l'accueil que vous m'avez réservé et pour m'avoir témoigné autant d'affection qu'à votre ami, votre soeur ou votre fille. Je suis on ne peut plus heureuse de vous avoir comme famille. Et Michel, merci encore pour vos superbes dessins qui illustrent la couverture de cette thèse.

Thank you all, my Belgian family...

Eliran & Bram : Office 06.10 rocked because of you. You surely unlocked a few doors in my mind. Soghra, Winny, Urna, Alberto for answering my questions and for being there.

Filip, for picking me from the airport, I thank you now. For beers & trips and for being the sweetest IT person I have known (sorry Raph! ). Anneleen, for being miss dependable.

Pri, Nick, Izaak, Ale, Bert - you are the twinkling lights on the Christmas tree, the icing on the cake. Thank you for your friendship. Jean-Charles, thank you for introducing me to mindfulness and teaching me to be calm and balanced.

Myriam, you are a step away from being my big sister. Thank you for your patience, love and good counsel.

Lastly, but not the least I thank my teachers. You helped me grow.

Teachers of St. Paul's Academy, Dr. Bikram Phookun, St. Stephen's college, Dr. T R. Seshadri, Delhi University and Dr. Ashoke Sen, HRI Allahabad.

# Abstract

In this work we present a few general and some specific aspects of effective dynamics of macroscopic observables, obtained through the study of some models. The work presented here is based on results already published in [92, 95, 96].

It is usually observed that time-dependence in external driving is sufficient to generate non-zero effective currents. We discuss the peculiarities of some special time-dependent driving, where the effective, time-averaged current in the system remains zero. This we call the No-go theorem. We compare this with the usual time-dependence seen, say in case of ratchets, which do create non-zero time averaged currents.

The purpose of statistical physics is to build connections between microscopic variables (which are enormous in number and usually fast in "speed") and the macroscopic variables (usually fewer and slower compared to the microscopic variables). Much can be inferred about the microscopic state of a system from the nature of a well defined macroscopic observable defined on it. Hence, the temperature of a gas is a pointer towards the average of the squares of the velocities of the molecules of the gas. The main question which drives this thesis work is : How the effective dynamics is connected to the microscopic or the internal description in nonequilibrium ?

Forces in the internal dynamics can induce effective forces and result in currents in the effective description. We are interested in the direct question about, how to arrive at these effective forces and currents starting from the microscopic picture. The inverse question is of greater interest about, given the effective forces and currents how one can reconstruct aspects of the internal dynamics and the potentials and forces acting here.

In our explorations, we visit the questions: "Is Archimedes' Law true for granular matter ? " In the pretext of this question, we discuss various regimes where granular matter behaves like fluids and the systematic corrections that

appear when it behaves like a solid instead. We show that the forces exerted by the granular system on the colloids immersed in them are different in the different regimes. We present the emergence of a drag force in the far-from-fluid regime.

We enter into the realm of nonequilibrium with the aid the very relevant subject of Rouse polymer dynamics. The motion of a tagged monomer in nonequilibrium conditions has been widely studied in the polymer physics community, yet the nonequilibrium (as far as we know) has always been on the coarse grained effective level of the tagged monomer. We explore in this work, the significance of nonequilibrium force like shearing, when it exists in the bath instead. Making a distinction between out-of-equilibrium in the system or in its environment is of importance when building models to describe the behavior of tagged particles in nonequilibrium baths e.g., the motion of a macromolecule inside a living cell. The breaking of detailed balance in the bath not only leads to the violation of the first fluctuation-dissipation relation but also leads to the breaking of **local detailed balance** and hence violation of the second fluctuation-dissipation relation. The corrections to the second fluctuation-dissipation relation is a still an open topic of research.

We also explore how effective dynamics is in general influenced by breaking of detailed balance in the bath. And what one can infer about the bath by looking at the nonequilibrium statistical forces.

# Beknopte samenvatting

In deze tekst staat de studie centraal van enkele effectieve dyamica's in de niet-evenwichts statistische mechanica.We bestuderen zowel specifieke als algemene en meer conceptuele aspecten binnen bepaalde modellen. Het hier gepresenteerde werk vindt zijn grondslag terug in al gepubliceerde resultaten [92, 95, 96].

Eén van de fundamentele gevolgen van het uit evenwicht drijven van een systeem is het optreden van stromen. Echter, opdat er zich een netto effective stroom zou voordoen in een systeem is het niet voldoende dat de potentiaal tijdsafhankelijk is. We bestuderen daarom enkele speciale gevallen van tijdsafhankelijke potentialen (en velden) waarbij er geen netto gemiddelde stroom geproduceerd wordt. We noemen dat ook wel het No-go theorema. We maken ook de vergelijking met enkele gekende tijdsafhankelijkheden (zoals bijvoorbeeld in *ratchets*) die w'el een effectieve (tijdsgemiddelde) stroom induceren.

Het doel van statistische mechanica is een brug te bouwen tussen de microscopische beschrijving, waar het aantal variabelen meestal erg groot is, en de macroscopische beschrijving door middel van meestal een klein aantal variablen. Zo geeft de temperatuur van een gas (in evenwicht) informatie over de gemiddelde snelheid van de gasdeeltjes. De motivatie voor deze thesis is het beter willen verstaan van hoe informatie omtrent de effectieve dynamica van bepaalde observabelen zoals stroom zich relateert met de microscopische beschrijving van het onderliggende systeem.

Zo kan men zich bijvoorbeeld de vraag stellen of de wet van Archimedes ook geldig is voor granulaire systemen. Granulaire system kunnen zich gedragen als vloeistoffen maar ook als vaste stoffen. Intuitief kan men zich de overgang tussen beide regimes op de volgende manier voorstellen: zonder het aanbrengen van externe krachten staan alle deeltjes stil en gedraagt het granulair systeem

zich als een vaste stof. Begint men het granulair systeem te schudden door het aanleggen van externe krachten, dan zal het vloeistofkarakter zich meer en meer manifesteren. Krachten die door een granulair systeem op colloidale deeltjes uitgeoefend worden, hangen dan ook in sterke mate af van het regime waarin het granulaire systeem zich bevindt.

Het bestuderen van de dynamica van een Rouse-polymeer brengt ons bij niet-evenwichtsfysica. In de literatuur wordt wrijving van deeltjes in een reservoir meestal beschreven door een effectieve kracht die men aanbrengt op het deeltje. Dat is het gecombineerde effect van de omliggende baddeeltjes op het gekozen doeldeeltje. Hier willen we een stap verder gaan, namelijk door in plaats van een kracht op het doeldeeltje aan te brengen, enkel een kracht op de baddeeltjes aan te leggen. Dat geeft aanleiding tot een effectieve kracht op het doeldeeltje. De microscopische dynamica wordt in evenwicht gegeven door de Boltzmann-verdeling (via de voorwaarde van microscopische reversibilieit of *detailed balance*). De effectieve dynamica van een deeltje is simpelweg het wegintegreren van de vrijheidsgraden van het reservoir. Buiten evenwicht echter is de stationaire verdeling niet gekend, er is geen *detailed balance.* We bestuderen daarom ook hoe het breken van deze conditie de effectieve dynamica van deeltjes beïnvloed. In het bijzonder willen we weten of de daarbij geïnduceerde niet-evenwichts statistische krachten belangrijke informatie omtrent het reservoir bevatten.

# Contents

# List of Figures

# Chapter 1

# Introduction

*In all affairs it's a healthy thing now and then to hang a question mark on the things you have long taken for granted. - Bertrand Russell (Philosopher, Mathematician)*

*It's not a silly question if you can't answer it. - Jostein Gaarder, Sophie's World*

## 1.1 Thermodynamics

The world accessible to human senses, even the depths where our microscopes can dig into, is made of not one, two or tens but close to $10^{23}$ number of particles. To be able to describe this world and navigate through it we need a language appropriate to its size. For instance, on a warm day you let the windows of your rooms open to let some cool air in. The knowledge that the air outside is cooler than the air in your room precedes your judgment that leaving the windows open would eventually cool your room. Irrespective of which city (village) in the world you live in and its corresponding air quality, you would expect the same outcome.

Heat flows from high temperature to low temperature. Food cooks faster in a pressure cooker. Gas expands when heated at a constant pressure. Experiences that remain true no matter the chemical nature or the atomic structure of the constituents involved.

The set of principles which govern such phenomena in systems with a large number of particles fall under Thermodynamics. The laws of thermodynamics describe the state of a system in terms of - not the details of position and momentum of the individual particles constituting it, but rather in terms of global parameters like pressure $P$, volume $V$, temperature $T$, number of particles $n$. The change in state of a system is dictated by quantities like internal energy $U$, work $W$, heat $Q$, entropy $S$, free energy $\mathcal{F}$.

Assuming that the laws of thermodynamics and the various relations between global parameters are known, we want to talk about the forces which are exerted by and exerted on these systems. Just as Aristotle spoke of a **natural state** of a system and the **natural motion** as the change in the state of the system until it reaches its natural state. The thermodynamic "natural state" of a system is called its **equilibrium** state. Away from equilibrium, thermodynamic forces act to evolve the system state towards equilibrium. The second law of thermodynamics tells us that for an isolated system equilibrium is defined as the state which has maximum entropy and a system would spontaneously evolve towards this state. If the system is in contact with an environment, with which it exchanges energy, the equilibrium state is the one for which the free energy is minimized, such that the entropy of the universe is maximized.

If $dS_u$ is the change in entropy of the universe, which consists of the system, with entropy change $dS$ and the environment with entropy change $dS_E$, then

$$dS_u = dS + dS_E$$

For fixed volume and number of particles of the environment, the changes in entropy of the system and the environment, when there is no work done, are:

$$dS \geq \frac{1}{T}dU, dS_E \geq \frac{1}{T}dU_E$$

where $dU$ is the change in energy of the system in contact with an environment at fixed temperature $T$. Since the energy in the universe is conserved, the energy change in the system is negative of the change in energy of the environment $dU_E$,

$$dU = -dU_E$$

$dS_E \geq \frac{1}{T} - dU > -dS$. Therefore,

$$dS_u \geq \frac{1}{T}(dU - TdS)$$

$$\geq \frac{1}{T}d\mathcal{F} \tag{1.1}$$

where $d\mathcal{F}$ is the change in Helmholtz free energy

$$\mathcal{F} := U - TS \tag{1.2}$$

of a system. Hence, for an arbitrary system with fixed volume, temperature and number of particles, the direction of increasing entropy of the universe $dS_u > 0$ is the same as decreasing the Helmholtz free energy $d\mathcal{F} < 0$.

There are other markers of the equilibrium state, depending on the manner in which the system interacts with its environment. E.g., if in addition to exchanging heat at constant temperature, there is change in volume $V$ of the system at constant pressure $P$, the entropy of the universe is maximized when the Gibbs free energy

$$G := U + PV - TS$$

is minimized.

The free energies are in general called **Thermodynamic Potentials** and are general indicators towards the direction of evolution.

We can also define a **Grand Potential**

$$\phi := U - TS - \mu N$$

In chemical reactions and systems with two or more phases in equilibrium, the constituent number of particles in each subsystem can change. The increase in the Gibbs free energy of a system on addition of one particle while temperature and pressure are held fixed is called the chemical potential $\mu$ of the system.

## 1.1.1 Thermodynamic Forces and Generalized displacements

Given the definitions of the thermodynamic potentials above and using the first law of thermodynamics, we arrive at the following expression for the change in internal energy of the system
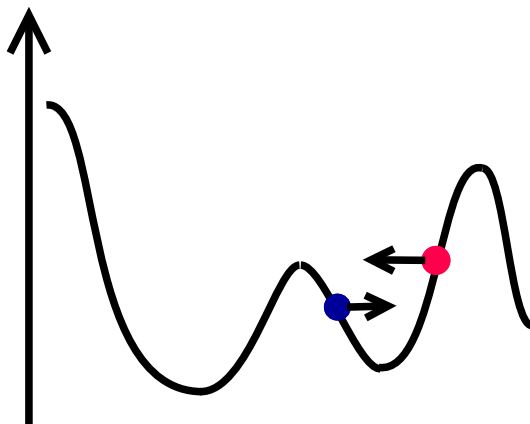
**Forces as gradients along the free energy landscape**

Figure 1.1: Free Energy Landscape in configuration space

$$dU = TdS - PdV + \mu dN$$

where $PdV$ is the mechanical work done by the system and $-\mu dN$ is the chemical work. Using this expression in eq. (1.2) yields the following identities

$$
\begin{aligned}
S &= -\left(\frac{\partial \mathcal{F}}{\partial T}\right)_{V,N} \\[2ex]
P &= -\left(\frac{\partial \mathcal{F}}{\partial V}\right)_{T,N} \\[2ex]
\mu &= \left(\frac{\partial \mathcal{F}}{\partial N}\right)_{T,V}
\end{aligned}
\tag{1.3}
$$

Pressure $P$ and chemical potential $\mu$ are the thermodynamic forces associated with the generalized displacements in volume $V$ and number of particles $N$. Figure 1.1 makes the action of these forces quite apparent. The thermodynamic forces drive the system in the direction which minimizes its free energy. In the state where the free energy is minimized, the force is zero.

**Example:** Consider $N$ particles of supersaturated steam in a box of volume $V$, maintained at temperature $T$. In equilibrium what is the number of particles which remain in vapor state and how many particles condense into liquid state ?

For a system at constant temperature and volume the appropriate thermodynamic potential to consider is the Helmholtz free energy

$$d\mathcal{F} = -PdV + \mu dN$$

Assuming that the total volume $V$ is equal to the volume of the water vapor. If $N_s$ and $N_l$ are the number of steam and liquid particles respectively, then $N = N_s + N_l$ and $dN_s = -dN_l$. If the chemical potentials of liquid and steam are $\mu_l$ and $\mu_s$ respectively, then

$$\mu dN = \mu_s dN_s + \mu_l dN_l$$

$$= (\mu_s - \mu_l)dN_s \tag{1.4}$$

Using eq. (1.3), at constant $T$ and $V$

$$\mu_s - \mu_l = \left(\frac{\partial \mathcal{F}}{\partial N_s}\right)_{T,V}$$

In equilibrium, the free energy is minimum, thus in equilibrium the number of liquid and water vapor particles are such that the chemical potentials of liquid and water vapor are equal.

$$\mu_s = \mu_l$$

in equilibrium.

*We conclude that an imbalance in thermodynamic forces cause generalized displacements in the direction where thermodynamic potentials are minimized.*

The formalism of forces in Equilibrium Thermodynamics is very well understood. It is nevertheless true that the validity of Equilibrium Thermodynamics is strictly limited. It requires systems to transition between equilibrium states and the dynamics to be either reversible or at least non-dissipative. This formalism does not apply to most machines, motors and chemical reactions

which undergo irreversible changes at finite speeds, with dissipative forces like the frictional force acting on them.

Some developments have been made to describe irreversible processes, away from equilibrium, still using principles close to Equilibrium Thermodynamics. These developments are summed up under Nonequilibrium Thermodynamics. The purpose of the next section is not to be an extensive discussion on the principles and results of Nonequilibrium Thermodynamics, but to illustrate the usage of forces in nonequilibrium situations.

## 1.2 Nonequilibrium Thermodynamics (NET)- Fluxes and Forces

The purpose of NET is to study the change in state of a system, not only through its initial and final values, but to monitor the behavior as a function of time. It describes the approach to equilibrium, through irreversible paths, of a system that has been driven far from equilibrium.

NET is based on the assumption of local equilibrium, which widely stated, says that a system which is undergoing fluxes or currents and is out of equilibrium can be split into many subsystems each of which is assumed to be small enough to be locally in equilibrium. In other words, the time of relaxation to equilibrium of each subsystem is assumed to be much smaller than the time of relaxation of relevant observables. This assumption is of course not valid for systems like polymers in which the time of relaxation of each subsystem is comparable to the whole system.

NET also assumes that all quantities defined in equilibrium retain their meaning in nonequilibrium, like entropy, temperature; but they are allowed to change with time and space. Together with these assumptions, there exists also an empirical relation between fluxes and forces which is a starting point of NET. This relation is similar to the equilibrium thermodynamic equations.

### 1.2.1 Transport Equations

The three famous transport equations (Fourier's Law, Fick's Law and Ohm's Law) have been proposed from experimental considerations and are as follows:

$$\mathbf{q} = -\lambda \nabla T \tag{1.5a}$$

$$\mathbf{J} = -D \nabla c \tag{1.5b}$$

$$\mathbf{I} = \sigma \nabla \psi \qquad (1.5c)$$

These equations state that the heat flux $\mathbf{q}$ (amount of energy flowing per unit time per unit area through a conductor), matter flux $\mathbf{J}$ and charge flux $\mathbf{I}$ are related linearly to thermodynamic forces which are caused by inhomogeneities in temperature $T$, mass concentration $c$ and electric potential $\psi$. The constants of proportionality are $\lambda$, the material's thermal conductivity, $D$, the diffusion constant and $\sigma$, the charge conductivity.

In general,

$$\mathbf{J}_\alpha = \sum_\beta \mathbf{L}_{\alpha\beta} \nabla X_\beta$$

where $\mathbf{J}_\alpha$ are the generalized fluxes and $\nabla X_\beta$ are the generalized forces, which are changes in some intensive variables $X_\beta$ and which can again be represented as gradients of some generalized free energies with respect to some extensive variables, in the same manner as in equilibrium thermodynamics.

## 1.3 Statistical forces - It is an elementary matter (of numbers)

Thermodynamics describes the macroscopic world around us - in terms of macro observables such as pressure, temperature, volume etc. The Laws of Thermodynamics dictate the relations between various macroscopic quantities and the manner and direction in which change in them could occur to be consistent with observations (reality). Yet, these laws of Thermodynamics must be a consequence of the intense activity of atoms and molecules at the microscopic scale. Hence, to be able to truly appreciate what the laws of thermodynamic tell us, as well as to be able to understand and predict the behavior of systems on which the aspects of equilibrium thermodynamics are not applicable any more, it is paramount that we explore the relations between the microscopic and macroscopic world.

Statistical mechanics is the link between the microscopic "invisibles" and the macroscopic "visibles" ( observables).

Consider an mole ($10^{23}$) non-interacting gas particles (i.e. an ideal gas) released into the corner of a large room. If we follow the motion of each of these particles separately, nothing spectacular happens. Each particle follows its trajectory unscrupulously. Yet, instead if we forget about individual particles for a while

and focus our attention on the number density of particles in the room, we notice that the density has evolved from almost a delta function, concentrated at the corner of the room to a uniform density spread across the volume.

Why did this happen ? – It is a simple matter of numbers. In the lack of any biasing forces, like gravity, acting on the gas particles, there are on average more particles moving from the corner to the rest of the volume than vice versa.

Hence there seems to be a trend on average towards uniform density. There is an apparent lack of force to push this trend, but the statistical world is a democratic world and the power of numbers prevails. We would like to define a force called *Statistical force* to reflect the tendency of the system to relax towards the state of maximum entropy.

How could you measure this force ? – Like any force, this force can be measured by its action on a probe. As a probe, we introduce a wall which constrains the motion of the particles along a certain direction. From our experience of thermodynamics we know that the gas particles do exert a force on the wall, which on a unit area we call *pressure* of the gas. We will arrive later at the conclusion that this force is statistical in nature.

### 1.3.1    Entropy - The link

In the year 1877, Ludwig Boltzmann was able to establish the link between the microscopic world and the macroscopic world through his famous equation

$$S = k_B \log \Omega$$

He connected the thermodynamic entropy $S$ to the phase space volume $\Omega$ (or the probability ) of the macrostate. $k_B$ is the Boltzmann constant.

**Microstate:** The microscopic description of the system is given in terms of its microstate (represented by $\eta$). For a system of $N$ gas particles in a room of volume $V$, the microstate of the system is a point in $6^N$ dimensional phase space - 3 dimensions each of position and momentum.

**Macrostate:** The macrostate describes the observable state of the system. It could be total energy, total angular momentum etc.

**Volume of the Macrostate:** is the volume in phase space, occupied by all those microstates which have a given value for the macroscopic observable.

*The most probable state or equivalently the equilibrium (macro)state is the one for which the volume in phase space $\Omega$ is maximum.*

This is indeed consistent with our thermodynamical definition of equilibrium state, which maximizes the entropy of the universe.

Following these considerations further, for a system in contact with a heat bath at temperature $T$, one comes to the conclusion that for a fixed temperature and volume, in equilibrium the microstates are distributed with a Gibbs-Boltzmann probability distribution ($P()$):

$$P(E_s) = \frac{1}{Z(\beta)} e^{-\beta E_s}$$

$Z(\beta) = \int e^{-\beta E_s} \mathrm{d}\Omega$ is called the partition function, $\beta = \frac{1}{k_B T}$ is called inverse temperature.

The average energy of the system

$$\bar{E} = \int P(E_s) E_s \mathrm{d}\Omega = -\frac{\partial}{\partial \beta} \log Z(\beta)$$

is the internal energy $U$ we speak about in thermodynamics. As is quite clear from the equation above, the average energy does not depend on the microscopic details of the gas particle dynamics, but only on some global properties of the system.

For a system at constant temperature, the pressure in the microstate $s$ is given by $\pi_s = -\frac{\partial E_s}{\partial V}$.

The average pressure of the system in equilibrium state is then

$$\bar{P} = \int \pi_s P(E_s) \mathrm{d}\Omega$$

After some manipulations we find that the average pressure

$$\bar{P} = \frac{1}{\beta} \left( \frac{\partial}{\partial V} \log Z \right)_T$$

is also a statistical quantity.

The statistical entropy $S = -k_B \int P(E_s) \log P(E_s) \mathrm{d}\Omega$ can be derived from similar arguments and making use of the thermodynamics relations

$$\mathrm{dU} = \mathrm{TdS} - \mathrm{PdV}$$

The free energy $\bar{\mathcal{F}} = \bar{E} - TS$ can be calculated using these expressions and we find back again the relation between the statistical force $\bar{P}$ and the free energy $\bar{\mathcal{F}}$

$$\bar{P} = - \left( \frac{\partial \bar{\mathcal{F}}}{\partial V} \right)_T$$

We see that in general the Statistical observables $\bar{P}$, $\bar{E}$ etc. are obtained from the microstate $\eta$, by an appropriate **averaging out** or **coarse graining** of the microstates, with some probabilistic weights.

We thus propose, in general, for a joint system with a generalized macro variable $X$ and micro variables $\eta$ distributed according to the joint probability distribution $\rho(\eta, X)$ the **Statistical force** on the macro variable, is given by

$$F_{\mathrm{Stat}}(X) = \int \rho_X(\eta) \left( -\frac{\partial H(X, \eta)}{\partial X} \right) \mathrm{d}\eta \tag{1.6}$$

where $H(X, \eta)$ is the joint energy of the $\{X, \eta\}$ system and $\rho_X(\eta)$ is the probability density of the microstate $\eta$, for a fixed value of the macro variable at $X$.

**In Equilibrium**

The statistical force which the microscopic degrees of freedom exert on the macroscopic degrees of freedom results when a coupling is inserted between the two systems. This coupling would in practice be some kind of constraint on the microscopic dynamics in presence of the macroscopic system. E.g., if the macroscopic observable is the mean value of the microscopic variables ($\eta$), then the phase space of the micro variables is confined to a subspace of the available phase space such that their mean is fixed to $X$. In general, to find the new stationary distribution of the micro variables under constraint is not trivial. When working with systems with an equilibrium dynamics though, life is a lot simpler. One can show that new stationary distribution $\rho_X(\eta)$, the probability of the microscopic state $\eta$ for a given value of the macro observable, $X$ is simply equal to conditional probability $\rho(\eta|X)$ of the old joint distribution $\rho(\eta, X)$ being in this subspace.

$$\rho_X(\eta) = \rho(X|\eta)$$

Hence, in equilibrium $\rho_X(\eta) = \frac{e^{-\beta H(X,\eta)}}{Z(\beta)}$

Substituting this in eq. (1.6) gives us back the thermodynamic definition of forces

$$F_{\text{Stat}}(X) = -\frac{\partial \bar{\mathcal{F}}}{\partial X}$$

as gradients of generalized thermodynamic potentials.

**In Nonequilibrium**

It has been shown in [14] that when the microscopic dynamics is out of equilibrium, then in general

$$\rho_X(\eta) \neq \rho(X|\eta)$$

Thus, we do not have a simple way to relate Statistical forces with the thermodynamic potentials.

**A simple example**

Consider a particle hopping on a ring with $N$ sites ($i$). The jump rates are asymmetric with the rate to jump clockwise as $p$ and anti-clockwise as $q$. For all rates such that $p \neq q$, the dynamics is non equilibrium and there is a non-zero current

$$j(i, i+1) = \frac{p-q}{N}$$

flowing through it.

The stationary distribution $\rho(i) = \frac{1}{N}$ is a constant.

Suppose now we constrain the dynamics by taking away one site, say $m$, from the ring. The motion is now confined to a subspace of the original phase space. The stationary distribution of the new process with rates $p$, $q$ for all sites $i \neq m$ and zero for jumps into and out of site $m$, can be calculated by solving the Master equation with the new rates. We find that

$$\rho_m(i) = \begin{cases} \frac{1}{Z}(p/q)^i & \text{if } i \neq m \\ 0 & \text{otherwise} \end{cases}$$

where $Z = \sum_{i=1}^{N-1} (p/q)^i$

The dynamics is infarct turned into detailed balance now.

On the other hand, the conditional probability of the joint system under constraint is

$$\rho(i|m) = \begin{cases} \frac{1}{N-1} & \text{if } i \neq m \\ 0 & \text{otherwise} \end{cases}$$

This example clear shows that out-of-equilibrium there is no simple way to relate the original dynamics to the new constrained dynamics. When $p = q$ we get back the equality between the two cases in equilibrium.

Further discussion on the nature of statistical forces with some examples has been made in Chapters 5 and 6. Parts of the discussions about thermodynamics and statistical physics in this chapter have been inspired from [60, 117, 85]. Some historical parts were taken from [120].

# Chapter 2

# Stochastic processes and Markov systems

*A man must have chaos yet within him to be able to give birth to a dancing star.*

*- Friedrich Nietzsche, Thus Spake Zarathustra*

*Who could ever calculate the path of a molecule? How do we know that the creations of the worlds are not determined by the falling grains of sand?*

*- Victor Hugo, Les Miserables*

## 2.1 Introduction

Classical uncertainty came naturally to human thought from the idea that we are too small and the universe is too large and interrelated for a thorough deterministic description. Anything from hydrogen atom to baseball is tinged, to a greater or lesser degree, with uncertainty. This uncertainty may lie in defining their initial conditions or in their dynamics itself. This uncertainty is a result of insufficient information about the workings of a system and is due to the choice of *coarse-graining* or *macroscopic* definition which we attach to the variables describing the system.

Classical uncertainty is a result of insufficient information. Think of the question, what will be the outcome of one single experiment of coin toss, *Heads* or *Tails* ? Or which number out of *one to six* would appear on the face of die in one throw ? These are physical phenomena governed by *Newtonian Mechanics* and we can give a precise answer to these questions, if we have information about the initial state of the coin or the die (its configuration in three dimensional space), initial velocity and angular momentum imparted to it, the force of gravity, of course the impact on the dynamics due to the millions of surrounding air particles as well as the force and the nature of impact once it touches the ground. Even for very simple questions like above, there seems to be a lot of considerations to be accounted for.

We handle these matters in a more pragmatic but "imprecise" manner, in the language of probability. We ask the question whether the coin or die is fair, and if that is so, then we evoke the arguments of symmetry to say that since the two faces of the coin are equivalent for all practical purposes and all the six faces of the die are dynamically similar, there is a one in two chance of seeing Heads as an outcome of a coin flip and one in six chance of seeing say number two as an outcome of a die throw.

To predict the probabilities of various states which a system could acquire, it is important to know beforehand not only the nature of the system but also the nature of the experiment due to be performed. Certainly, some experiments are designed in a way that only a subset of states in the total state space are accessible.

While posing the question, what the probability is of a *Heads* or *Tails* in an experiment of coin toss, it is not enough to say that the two faces of the coin are equivalent, but one must also mention the mechanism of the flip. If the flip is such that the coin can take all possible orientations in 3-D space then for a significant area of the coin circumference, there exists a non-zero probability of the coin landing on its edge rather than on any of the two faces. Mahadevan and Yong in [97] show that there is more to the story than the said "fairness" of the coin. They visited the question of a "fair" three sided coin (non-zero thickness), and showed that the probability is a function of the aspect ratio [1] and angle between the angular momentum vector and initial orientation of the normal to the coin face. They also showed that a fair three sided coin must have an aspect ratio of $1/\sqrt{3}$.

While formulating a problem probabilistically, the state of the system is described by a *random variable* which can take any value out of a set called the state space, with a certain probability. In the next section (2.2) we shall go through a short historical overview of random processes in physics. In section

---

1. ratio of its width to its height

2.3 we will start with a mathematical formulation of stochastic process and in section 2.4 we shall study in detail the nature of Markov systems. In chapter 3.2 we shall look at an intriguing application of time-dependent Markov process in molecular machines.

## 2.2 Historical Elements

The theory of stochastic processes, at least in terms of its application to physics, was accelerated with the twentieth century explanations of *peculiar character in motions of the particles of pollen in water*, first observed as early as 1785 by Dutch physician Jan Ingenhousz and later rediscovered and studied in some detail by Scottish botanist Robert Brown in 1827 [54, 23]. At about the same time, in 1822, Joseph Fourier came up with the heat conduction equation, on the basis of which A. Fick set up the diffusion equation in 1855 [51].

A. Einstein's ingenious microscopic derivation of the diffusion equation: *Concerning the motion as required by the molecular-kinetic theory of heat, of particles suspended in liquids at rest* [40, 41, 42] in 1905-1906 provided a description of the perpetual motion of small particles immersed in a fluid. In developing his theory Einstein developed many concepts which are, today, fundamental in the study of stochastic processes. Using modern terminology, he introduced the Markov chain model, discussed in section 2.4 to study the motion of a particle.

Paul Langevin in 1908, was the first to apply Newton's second law to a "Brownian particle" [84], on which the total force included a random component. His approach was based on single-stochastic realizations of the process. Subramaniam Chandrasekhar in 1943 was able to solve several dynamical problems in terms of random variables that evolved according to Langevin's version of $F = ma$ [26]. The approaches of Langevin and Einstein represent the two main approaches in the theory of stochastic processes.

The synthesis of the approaches leading to the understanding of how the properties of stochastic motions are connected to deterministic dynamics of the system and its heat bath were understood much later in works by Mark Kac, Robert Zwanzig and others [73, 55, 130]. The theory of stochastic processes was developed during the 20th century by several mathematicians and physicists including Fokker, Planck, Kramers, Klein, Wiener, Kolmogorov, Itô, Doob [53, 109, 78, 108, 80, 68, 37, 72, 87, 38].

## 2.3  Stochastic process

**A random variable** is a quantity that under given conditions(of experiment) can assume different values (outcome). It does not matter whether the randomness is intrinsic or unavoidable or an artifact of our ignorance.

**A state space** is the set of all possible outcomes of an experiment. Also called *sample space or configuration space* and is denoted by $\Omega$.

**Examples**

- The possible outcomes of the experiment of tossing a coin are H and T. The sample space is $\Omega = \{H, T\}$.
- The possible outcomes of the experiment of throwing a die are $1, 2, 3, 4, 5$ and $6$. The sample space is $\Omega = \{1, 2, 3, 4, 5, 6\}$. These are **discrete random variables**, which can take only countable number of values.
- The velocity of a Brownian particle in a colloidal solution is a continuous random variable. The sample space is $\Omega = \mathbb{R}^3$. This is a **continuous random variable**, which can take an uncountable number of values.

The word *stochastic* comes from the Greek word $\sigma\tau\acute{o}\lambda o\varsigma$, which means "aim". It also denotes a target stick; the pattern of arrows around a target stick stuck in a hillside is representative of what is stochastic.

**A stochastic process**: The time evolution of a random variable is called a random or *stochastic process*. Thus if $X$ is a random variable, then $\{X_t\}_{t \in \mathcal{T}}$ denotes a stochastic process. For brevity, we will also denote a stochastic process as $X(t)$. $\mathcal{T}$ is to be interpreted as time and is a subset of $(-\infty, \infty)$. When $\mathcal{T} = \mathbb{N}$, then $\{X_t\}_{t \in \mathcal{T}}$ is said to be a discrete time process and when $\mathcal{T} = \mathbb{R}$, then it is said to be a continuous time process.

**Example 1.3.2:**

- **Discrete time process:** A process in which the increment in time is deterministic and regular. The demand per week of a certain service over time, the closing price of HSBC stock between the period Dec. 2013 and Dec. 2014.
- **continuous time process:** A process in which the increment in time is stochastic and is itself governed by a probability density. The amount of radioactive uranium present on the earth's surface, number of cars in the city center between 08:00 and 10:00 in the morning.

### 2.3.1    Assigning probability and trajectories

A random variable $X$ is completely specified by the range of values $x$ it can assume and the probability $P(x)$ with which each value is assumed. That is to say, that the probabilities $P(X = x)$ for all possible values $x$ tells us everything there is to know about the random variable $X$. These probabilities are evaluated by conducting the same experiment several number of times and then counting the relative number $f(x)$ for each outcome $x$. According to the *statistical* interpretation of probability, the relative number or frequency $f(x)$ approaches $P(x)$ in the limit of an indefinitely large number of experiments.

### A stochastic trajectory

Every stochastic variable can be viewed as a function of two variables: $t$ and $\omega$. One single realization of a stochastic process is called a *trajectory*. A given trajectory is denoted as $\omega = (x_t)_{0 \leq t \leq \mathcal{T}}$. If $x_0$ is the initial state of the system, then we denote by $d\mathcal{P}_{x_0}(\omega)$ the probability density for the system to follow the trajectory $\omega$ over time $\mathcal{T}$. The expected value of a random variable or any observable which is a function of the trajectory is defined as an average all possible trajectories(which are all possible paths or manifestations of a system starting from the same initial condition). It is written mathematically as follows:

$$\langle g(\omega) \rangle_{x_0} = \int d\mathcal{P}_{x_0}(\omega) g(\omega) \tag{2.1}$$

where one integrates(or sums depending on the nature of time) over all possible trajectories starting from $x_0$ at time zero. For more general description of trajectories and their properties I refer you to their discussion in [126, 90].

## 2.4    Markov process

### 2.4.1    Introduction

The efforts of probabilists of the first half of the 20th century had been mostly dedicated(the problem of foundations aside), to the study of independence: sums of independent random variables. After independent variables, the simplest type of random evolution is Markovian dependence(named after A.A. Markov, 1906). Andrey Markov, a Russian mathematician produced the first results [98] (1906) for these processes, purely theoretically with the aim to extend the law of large numbers to dependent events. A generalization to

countably infinite state spaces was given by Kolmogorov (1936) [79]. In 1913, Markov applied his findings for the first time to the first 20,000 letters of Pushkin's Eugene Onegin [110].

As an example of a Markov process, consider the successive states of a deck of cards that is being shuffled. For predicting the order of cards after shuffling, all useful information is included in (complete) knowledge of the current state of the deck; if this is known, knowledge of previous states does not bring more information about the accuracy of the prediction. Most examples of random evolution given by nature are Markovian, or become Markovian by a suitable interpretation of the words "current state" and "complete knowledge".

The theory of Markov processes divides into sub-theories, processes where the time increment is discrete is called a Markov chain. Processes which update on continuous time but the state space is discrete are called continuous time Markov processes (e.g. Random Walk on a lattice).

Diffusion is a continuous time Random Walk where a continuum limit is taken for the lattice spacing ( e.g. Brownian motion).

The stochastic process $\{X_t\}_{t \in \mathcal{T}}$ takes values in a set $S$ - the state space. Usually, $S$ will be either $\mathbb{N}$ (as in the case of branching processes) or $\mathbb{Z}$ (random walks). Sometimes, a more general, but still countable, state space $\Omega$ will be needed for e.g. the configurations of a molecule while it goes through a cycle(this example will be discussed in much detail in Chapter 3.2). A generic element of $S$ will be denoted by $i$ or $j$.

Markov state models and their extensions are important tools for modeling thermodynamic processes of open systems [75] and they find numerous applications in chemical kinetics [107, 46, 20] and in bio-chemistry [82].

## 2.4.2 Markov process - Continuous time

In this section we shall go through the basic definitions and properties of a continuous time Markov process.

### The Markov Property

Simply put, a stochastic process has the Markov property if its future evolution depends only on its current position, not on how it got there. Here is a more precise mathematical definition.

**Definition** A stochastic process $\{X_t\}_{t \in \mathbb{R}}$ taking values in a countable state space $S$ is called a Markov process (or said to have the Markov property) if

$$P[X(t_n) = i_n | X(t_{n-1}) = i_{n-1}; X(t_{n-2}) = i_{n-2}; \ldots ; X(t_0) = i_0] =$$

$$P[X(t_n) = i_n | X(t_{n-1}) = i_{n-1}] \tag{2.2}$$

for all $t_n > t_{n-1} > \cdots > t_0 \in \mathbb{R}$, all $i_0, i_1, \ldots, i_n \in S$, whenever the two conditional probabilities are well defined, i.e., when

$$P[X(t_n) = i_n | \ldots ; X(t_1) = i_1; X(t_0) = i_0] > 0$$

Given the state of the system at time $t$ is $i$, the probability that between time $[t, t + \mathrm{d}t]$ it will jump to state $i'$ is given by

$$P(i'|i, t)\mathrm{d}t = w_t(i, i')\mathrm{d}t + \mathrm{O}(\mathrm{d}t)^2$$

$w_t(i, i')$ is the *transition rate* for the jump. We assume that the probability of more than one jump in the time interval $[t, t + \mathrm{d}t]$ is of $\mathrm{O}(\mathrm{d}t)^2$ and is therefore negligible.

The probability to not jump within this time interval is then given by

$$P(i|i, t)\mathrm{d}t = 1 - \sum_{i' \neq i} w_t(i, i')\mathrm{d}t + \mathrm{O}(\mathrm{d}t)^2$$

$\lambda_t(i) = \sum_{i' \neq i} w_t(i, i')$ is the *escape rate* associated with each state $i \in S$ at time $t$.

Given the transition rate $w_t$ and the escape rate $\lambda_t$, we can now write down the finite time probability that the system stays in state $i$ for time $t_2 - t_1$ and would jump in the time interval $[t_2 + \mathrm{d}t_2]$ from state $i$ to $i'$. For this we divide the time interval $t_2 - t_1$ into $n$ parts each of size $k = (t_2 - t_1)/n$, then we write down the finite time probability as the product of probabilities that the system does not make a jump from state $i$ in any of the $n$ time intervals from $t_1$ to $t_2$ and the probability that the system jumps in the time interval $[t_2, t_2 + \mathrm{d}t_2]$ to state $i'$. In the limit of large $n$, the length of each interval $k$ becomes very small, so that we can assume that the escape rate in each sub interval is constant.

$$P(i', t_2|i, t_1)\mathrm{d}t_2 = w_{t_2}(i, i')\mathrm{d}t_2 \prod_{r=0}^{n}[1 - \lambda_{t_1 + rk}(i)k] \tag{2.3}$$

We can rewrite the right hand side with the help of the following equation, for very small $k$

$$\exp \left( \sum_{r=0}^{n} \log \left[ 1 - \lambda_{t_1+rk}(i)k \right] \right) = \exp \left( \sum_{r=0}^{n} -\lambda_{t_1+rk}(i)k \right)$$

Rewriting (2.3), we get

$$P(i', t_2|i, t_1)\mathrm{d}t_2 = w_{t_2}(i, i')\mathrm{d}t_2 \exp \left( -\int_{t_1}^{t_2} \lambda_u(i)\mathrm{d}u \right) \tag{2.4}$$

Hence the finite time probability that the system remains in state $i$ for a time $t_2 - t_1$ after which it jumps out of state $i$ is

$$P(t_2|i, t_1)\mathrm{d}t_2 = \lambda_{t_2}(i)\exp \left( -\int_{t_1}^{t_2} \lambda_u(i)\mathrm{d}u \right) \mathrm{d}t_2 \tag{2.5}$$

This is the probability distribution of the waiting time in state $i$.

The probability of transition from $i$ to $i'$ is given by

$$p_{t_2}(i, i') = \frac{P(i', t_2|i, t_1)}{P(t_2|i, t_1)} \tag{2.6}$$

$$= \frac{w_{t_2}(i, i') \exp \left( -\int_{t_1}^{t_2} \lambda_u(i)\mathrm{d}u \right) \mathrm{d}t_2}{\lambda_{t_2}(i) \exp \left( -\int_{t_1}^{t_2} \lambda_u(i)\mathrm{d}u \right) \mathrm{d}t_2}$$

$$= \frac{w_{t_2}(i, i')}{\lambda_{t_2}(i)}$$

$$\sum_{j \in S} p_{ij} = 1; \ p_{ii} = 0$$
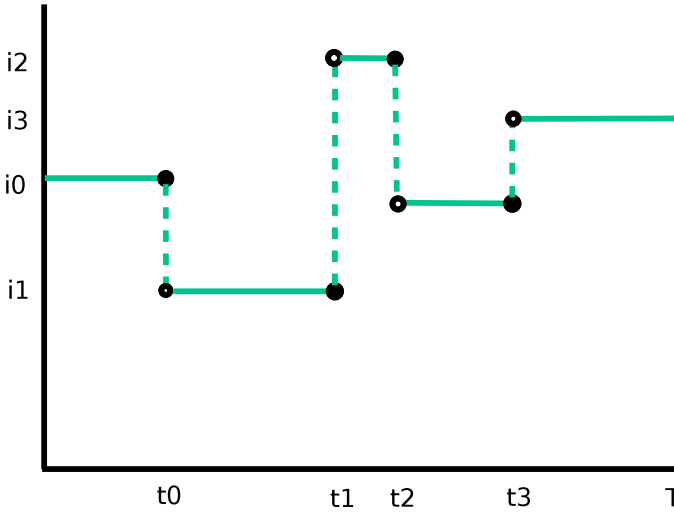
Figure 2.1: Representation of a continuous-time Markov process

## Probability of a stochastic trajectory

The figure 2.1 illustrates an example of a continuous-time stochastic process. A random process $X(t)$ starts in an initial state $i_0$ at time $t = 0$ and stays in this state until some time $t_0$. In the interval $[t_0 + \mathrm{d}t_0]$ it makes a transition to a different state $i_1$. It stays in this state for time $t_1 - t_0$ after which it jumps to a state $i_2$. The trajectory $\omega = (X(t), t \geq 0)$ of the state of the system which is undergoing a continuous-time Markov jump process is assumed to be piecewise constant.

The jump times $(t_0, t_1, t_2, \cdots, t_n)$ and the corresponding sequence of states $(i_0, i_1, i_2, \cdots, i_n)$ are sufficient to completely specify the trajectory of the state of the system.

The initial probability density from which the initial state of the system is sampled is

$$\mu(0) = \{\mu_i(0) = P(X(0) = i) : i \in S\}$$

Using the finite-time probabilities (2.4) and the transition rates and transition probabilities, one can write down the probability of a given trajectory $\omega$ between $0 \leq t \leq T$ as

$$\mathrm{d}\mathcal{P}_{\mu_0}(\omega) = \mu_0(i_0) \prod_{r=0}^{n-1} \left[ w_{t_{r+1}}(i_r, i_{r+1}) \exp\left( -\int_{t_r}^{t_{r+1}} \lambda_u(i_r)\mathrm{d}u \right) \mathrm{d}t_{r+1} \right]$$

$$\times \exp\left( -\int_{t_n}^{T} \lambda_u(i_n)\mathrm{d}u \right) \tag{2.7}$$

A stochastic process is called *time-homogeneous* when,

$$P(i', t+\tau; i, t) = P(i', \tau; i, 0) \text{ for all } i', i, \tau, t$$

which from now on can be written as $P(i', i; \tau)$

On the other hand, a process is called *time-inhomogeneous*, if the transition probability $P(i', t+\tau; i, t)$ depends on both times $t$ and $t+\tau$ and not just on the time interval $\tau$.

A time inhomogeneous process is also called a *time-dependent Markov process*. In further sections, we are going to focus our attention mainly on time-dependent Markov processes and discuss the various known properties of Markov systems for time-dependent dynamics i.e., the transition probability and escape probability density depend on time.
Time-dependence can be assumed when parameters governing the dynamics depend on time. The rates of chemical reaction depending on the concentration of reactants or Brownian motors which are governed by time-varying external parameters are examples of time-dependent dynamics.

## 2.4.3   Generator of a Continuous-Time Markov process

So far and in the sections below, we discussed the continuous-time Markov process in the more intuitive language of trajectories and probabilities of trajectories. Here we would like to make a small excursion into a different formalism to treat Markov processes.

There exists a more algebraic way to treat Markov processes which is done in terms of matrices and generators. The transition probability $P(X_{t_1+t_2} = i'|X_{t_1} = i)$ is represented by a matrix $P_{t_1+t_2}^{t_1}$. Each entry in the matrix is the transition probability $P_{t_1+t_2}^{t_1}(i, i')$. For a time-homogeneous process the

transition matrix depends only on the difference between the initial and the final times. Thus, $P(i, i')_{t_1+t_2}^{t_1} = P_{t_2}(i, i')$. From here we can reach the property of a semi group

$$P_{t_1+t_2} = P_{t_1} P_{t_2}$$

## The generator

The generator is defined as the infinitesimal transition matrix

$$L^\dagger = \lim_{s \to 0} \frac{[P_s - I]}{s} \tag{2.8}$$

where $I$ is the identity.

The time-evolution of the transition matrix is hence given by

$$\frac{dP_t}{dt} = \lim_{s \to 0} \frac{P_{t+s} - P_t}{s}$$

and using the semi-group property of the transition matrices and definition (2.8) one is able to write down the forward Kolmogorov equation

$$\frac{dP_t}{dt} = L^\dagger P_t \tag{2.9}$$

which leads us to the result

$$P_t = e^{L^\dagger t}$$

If the probability distribution on space $S$ is denoted by $\mu_t$, then its finite time-evolution is given by the equation

$$\frac{d\mu_t}{dt} = L^\dagger \mu_t \tag{2.10}$$

and

$$\mu(t) = L^\dagger \mu(0)$$

Equation (2.10) is the equivalent of the Master equation discussed in section 2.4.5.

$$L^\dagger \mu_t(i) = \sum_{i'} [w(i', i)\mu(i') - w(i, i')\mu(i)]$$

**The backward generator** is defined as follows

$$\sum_i g(i) L^\dagger f(i) = \sum_i f(i) Lg(i) \qquad (2.11)$$

where $f$ and $g$ are arbitrary functions defined on $S$. The backward generator acts on a function $f$ in the following manner

$$Lf(i) = \sum_{i'} w_{i,i'} [f(i') - f(i)]$$

The right hand side of this equation is the change in the value of function $f$ times the rate of that change. Hence, the backward generator governs the time evolution of function $f$ as follows

$$\frac{d}{dt} \langle f(i_t) \rangle_{\mu_0} = \langle Lf(i_t) \rangle_{\mu_0} \qquad (2.12)$$

whose solution is

$$\langle f(i_t) \rangle_{\mu_0} = \sum_i \mu_0(i) e^{tL} f(i)$$

### 2.4.4 Embedded Markov chain

Consider a continuous time Markov process $X(t)$ defined on the state space $S$, whose dynamics is governed by the escape rates $\lambda(t)$ and the transition probability $p_{ij}$. If $t_n$ denotes the time of the last transition, we define $Y_n := X(t_n^+)$ as the state right after the $n^{\text{th}}$ transition. The set $Y = \{Y_n\}$ is called the Embedded Markov chain corresponding to the Markov process $X(t)$.

For every state $Y_m = i$, the probability of transition to an arbitrary state $j \in S$ is $p_{ij}$. The waiting times do not play a role in the dynamics of the $Y$ process.

The process $Y(t)$ is again a Markov process, since the probability of jump at any time is governed only by the current state of the system.

Governed by the transition probability $p_{ij}$, there exists a probability density $\mu_i(t)$ of every state $i \in S$ such that:

$$\sum_i p_{ij}(t)\mu_i(t) = \mu_j(t)$$

## Periodic Markov process

The Markov process $X(t)$ is a *periodic* if $\exists\ \mathcal{T} \in \mathbb{R}$:

the conditional probability of transition

$$\wp_{ij}(t + \tau, t) = P(X_{t+\tau} = j | X_t = i)$$

is periodic.

$$\wp_{ij}(t + \tau, t) = \wp_{ij}(t + \mathcal{T} + \tau, t + \mathcal{T}),\ \forall\ i, j \in S,\ \forall\ t, \tau \qquad (2.13)$$

This implies that the escape rate $\lambda_i(t)$ and the transition probability $p_{ij}(t)$ are periodic as well.

$$\wp_{ij}(t + \mathcal{T} + \tau, t + \mathcal{T}) = \wp_{ij}(t + \tau, t),\ \forall\ i, j \in S,\ \forall\ t, \tau$$

$$\lambda_i(t + \mathcal{T} + \tau, t + \mathcal{T}) p_{ij}(t + \mathcal{T} + \tau) = \lambda_i(t + \tau, t) p_{ij}(t + \tau)$$

$$\Rightarrow$$

$$\lambda_i(t + \mathcal{T} + \tau, t + \mathcal{T}) = \lambda_i(t + \tau, t);\ p_{ij}(t + \mathcal{T} + \tau) = p_{ij}(t + \tau)\ \forall\ i, j \in S,\ \forall\ t, \tau$$
$$(2.14)$$

**For a Periodic Markov process, the corresponding Embedded Markov chain is homogeneous**

We construct the Embedded Markov chain

$$Y = \{X_t = i, X_{t+\mathcal{T}} = j, X_{t+2\mathcal{T}} = k, \ldots\}$$

The probability of transition for this process is $p_{ij}(t)$, which we have shown in (2.14) is periodic.

$$p_{ij}(t) = p_{ij}(t + \mathcal{T})$$

It follows from this equation that the Embedded Markov chain $Y$ is homogeneous.

### 2.4.5   The Master equation

The master equation describes the time evolution of the single-time probability $\mu_i(t) = \sum_j p_{ji}(t)\mu_j(0)$ to occupy a state $i$. We choose the time interval of transition $\Delta t$ small enough so that the Markov jump process can make utmost one transition in this time interval. $w_{kj}\Delta t$ is the probability that the process moves from $k$ to $j$ in the time interval $\Delta t$. The conditional probability is then

$$\mu_i(t+\Delta t) \approx \left(1 - \sum_k w_{ik}(t)\Delta t\right)\mu_i(t) + \sum_k w_{ki}(t)\mu_k(t)\Delta t + o(\Delta t)^2 \quad (2.15)$$

for small $\Delta t$. The term in the parentheses is the probability that if the system is in state $i$ at time $t$ then it remains there through the time interval $\Delta t$. There is an unrestricted summation over $k$ since $w_{ii}(t) = 0$. The second term is the probability to jump in time interval $\Delta t$ from $k$ to $i$.

Expanding the left hand side of this equation to first order in $\Delta t$ and eventually taking the limit $\Delta t \to 0$, we find that $\mu_i(t)$ is evolving according to the Master equation

$$\frac{d}{dt}\mu_i(t) = \sum_k [\mu_k(t)w_{ki}(t) - \mu_i(t)w_{ik}(t)] \quad (2.16)$$

The first term on the left hand side is the gain in probability from transitions into state $i$ while the second term is the loss in probability from transitions from state $i$ to other states. This equation is also called the *forward equation.*

## Probability current

The above equation can be rewritten in form of a continuity equation for probability density. The left hand side is the time rate of change of the probability density for the system to be in state $i$. The right hand side is the net probability in unit time that the system makes a jump into state $i$. The quantity

$$[\mu_i(t)w_{ik}(t) - \mu_k(t)w_{ki}(t)] = j_{ik}(t)$$

is the probability current. And the equation (2.16) is rewritten as

$$\frac{d}{dt}\mu_i(t) + \sum_{k \neq i} j_{ik}(t) = 0 \quad (2.17)$$

## 2.4.6   Stationarity & Detailed Balance dynamics

**Definition:** A Markov process is called *stationary or steady state*, if the single-time probability density $\mu_j(t)$ is time-independent. A system can initially start in a non-stationary density and evolve over time to stationarity such that the probability density of each state in space becomes a constant. Under the assumption that every configuration can be reached from every other configuration, the dynamics is ergodic and has a unique stationary solution,

$$\mu^{\text{st}} \equiv \lim_{t \to \infty} \mu(t)$$

A time-dependent Markov process does not reach a stationary state asymptotically. In other words, $\exists$ no $\mu_i(t)$ which satisfies the equation

$$\frac{d}{dt}\mu_i(t) = 0$$

On the other hand, there exist processes which are time dependent but whose dynamics is detailed balance.

**Detailed Balance dynamics**

Let us assume that the time-dependence of the rates $w_{ij}(t)$ lies entirely in parameter $\alpha(t)$, which could be an external constraint like temperature $\beta(t)$, or a time-dependent potential $U(t)$.

A time dependent Markov process whose transition probability is governed by rates $w_{ij}(t)$ as defined above and on which no other sources of non-equilibrium such as non-gradient forces (time dependent or time independent) act, we say obeys a detailed balance dynamics.

At any time $t$, the probability distribution for this process is the Gibbs distribution parametrized by the value of the parameter at time $t$, $\alpha(t) = \alpha$.

$$\mu_i^\alpha = \frac{e^{-\beta E_i^\alpha}}{Z_\alpha}$$

The distribution $\mu_i^\alpha(t)$ satisfies detailed balance at each possible value that $\alpha(t)$ assumes.

$$\mu_i^\alpha w_{ik}^\alpha = \mu_k^\alpha w_{ki}^\alpha \tag{2.18}$$

$\forall\, i,j \in S$

## 2.4.7    Arrhenius rate law

To end this chapter we look at the most frequently used form for the transition rates. The Arrhenius law was introduced by Swedish scientist Svante Arrhenius in 1884. It is an empirical law used to model the temperature dependence of transition rates. Historically it has been most used to model rates of chemical reactions and was motivated by the observation that most reaction rates at room temperature double with every 10℃ rise in temperature. The Arrhenius rate law is given as follows

$$k_\beta(i,j) = \mathcal{A}(i,j)e^{-\beta E_a(i,j)} \tag{2.19}$$

In terms of chemical reactions, $k$ is the total number of transitions from $i$ to $j$ which occur in unit time. $\mathcal{A}(i,j)$, the pre-exponential factor called *frequency factor*, is the number of collisions that occur in unit time between the reactant molecules which could lead to a reaction (depending e.g. on the right orientation of the molecules). Only those collisions would lead to a transition which would also have energy greater than a critical energy. The *activation energy* labeled as $E_a(i,j)$ is the minimum energy required for a transition $i$ to $j$ to occur. The activation energy can be externally controlled. In case of chemical reactions it is usually lowered by the introduction of a catalyst. The exponential factor denotes the probability that a given collision would lead to a transition. This probability rises with increase in temperature for a postie activation energy.

The frequency factor $\mathcal{A}(i,j) = \mathcal{A}(j,i)$ is assumed to be symmetric for a forward and reverse reaction, since the number of collisions would depend on the concentration of reactants and temperature, which are the same for reactions in both directions. The activation energy on the other hand is asymmetric and changes according to the direction in which the reaction proceeds.

To be illustrative, let us imagine the system to be a point in an energy landscape as seen in (Fig 1.1). The troughs are the energies $(E_i, E_j)$ of the stable configurations $(i,j)$ and the crests are the potential barriers $(\Delta(ij))$ through which the system has to go through to reach the next stable configuration. The activation energy for the transition $i$ to $j$ is given by $E_a(i,j) = \Delta(ij) - E_i$ and the transition rates are given by,

$$k_\beta(i,j) = \mathcal{A}(i,j)e^{\beta(\Delta(ij)-E_i)}$$

The activation energy can be positive, negative or zero. A negative activation has been observed by Stiller and Müller in [67] and is displayed by systems
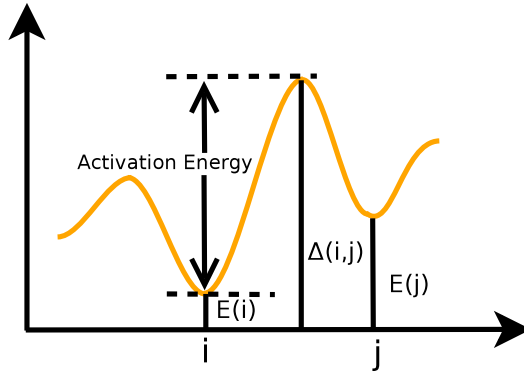
Figure 2.2: Free energy landscape depicting activation energy

where the probability of reaction falls with the increase in temperature. It is mostly seen in chemical reactions where a molecule needs to be trapped in a potential well before it combines with another molecule, with an increase in temperature it gets harder to trap the molecule and hence the reaction rate reduces.

To make a comparison with the Markovian transition rates $w_{ij}$, we again look at the ratio of the forward and reverse rates given from local detailed balance as

$$\frac{w_{ij}}{w_{ji}} = e^{-\beta(U(j)-U(i))}$$

From the above equation, one conclude that the transition rates have the form

$$w_{jk} = \mathbb{A}e^{-\frac{\beta}{2}(U(j)-U(i))} \tag{2.20}$$

where $\mathbb{A}$, a symmetric function, is a proportionality constant which would depend on the nature of the particles and the dynamics of the system.

If the frequency factor $\mathcal{A} := \mathbb{A}e^{-\frac{\beta}{2}(U(i)+U(j))}$, the transition rates (2.20) can be rewritten in the Arrehenius form:

$$w_{ij} = \mathcal{A}_{ij}e^{\beta U(i)} \tag{2.21}$$

This form is more useful since as opposed to transition probabilities and escape rates, activation energy is an experimentally measurable quantity and can be controlled externally.

# Chapter 3

# Molecular machines & the No-go Theorem

## 3.1 Molecular motors: An introduction

Much of all cell behavior and architecture depends on the directed transport of macromolecules. Molecular motors are little machines which are responsible for much of the biological functions such as muscle contraction, cell movement, transport of intracellular cargo and extracellular motion such as bacterial cilia and flagella, certain signal transduction pathways, cell division (mitosis and meiosis) [15, 77, 116, 21, 22]

Though, these molecular motors work on very different mechanisms and have very different purposes, the process by which they convert energy from stored adenosine triphosphate into motion (kinetic energy) follows a common structure. Molecular motors, in response to either external or internal stimuli, convert the energy stored in the cell into useful work, where **work** is defined as a displacement (change in position), rotation or change in configuration such that after a full cycle, when the motor comes back to its original state, the task performed is not undone [125, 24]. The study of the design and function of molecular motors is essential in not only understanding the cell structure and function but is also primary in the development of artificial nanostructures that can act as molecular machines. These nanaostructures are

essential towards the construction of sensors, transporters and smart materials [62, 63, 127, 12, 2]. Richard Feynman, in his 1959 lecture, ***There's plenty of room at the bottom***, at the California Institute of Technology, had envisioned of machines of nanodimensions which could be controlled externally [50, 49]

Artificial molecular machines fueled either photo &/or electrochemically [76, 52, 86, 61], have already been tried out experimentally. Experiments performed by Leigh et. al show a slow rotary molecular motor in which a full 360° unidirectional movement around a central axis is observed.

### 3.1.1  The Experiment

Here, we will elaborate into the workings of one of these artificial motors, to have a better idea on how they actually function. This would also lead to simplicity in visualizing the mathematical model which we aim to build around molecular machines, discussed in Section 3.2.1.

We look here at the experiments performed by Leigh et al. [86], with an artificial molecular rotor, which is a molecule undergoing unidirectional 120° intramolecular rotation around a single bond is studied.

A [2]catenane [1] in which one ring moves around 3 different binding sites, as shown schematically in Fig 3.1 is considered. Through a series of chemical reactions, the binding energy $K_a$ of two sites A and B can be altered, such that at any given point in the cycle, the ring preferentially binds to one of the 3 sites. In practice this is done by applying an external time dependent stimulus. The periodic change in the binding energy, creates a time dependent global minimum of energy for the smaller ring, which follows this change in minimum with time. Over a course of several cycles, it was observed that although the ring changes its position in response to the external stimulus in discrete steps, the route it takes to get there is not directionally biased. Over a complete sequence an equal number of times it goes from A through C in one direction and the opposite. Hence the time averaged current through several sequences in zero.

On the other hand, when the same experiment is performed with a [3]catenane see figure 3.2, which has two instead of one interlocking ring, a non-zero time averaged current in the anti-clockwise direction was observed. The affinities of the two rings and the external stimulus are chosen in such a fashion that each ring is able to block the motion of the other in a particular direction, but

---

1. A mechanically interlocked molecular architecture consisting of two or more interlocked cyclic macromolecules
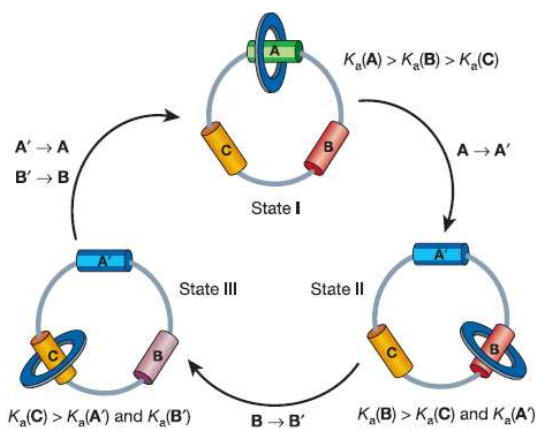
Figure 3.1: Stimuli induced sequential motion of a macrocycle between 3 different binding sites in a [2]catenane. Figure has been reproduced from [86].

only transiently to allow 360° rotation around the macrocycle. The presence of such time dependent barriers prevents net motion in both directions.

In case of the [2]catenane, the time dependent external stimulus was changing the energy minima alone, without introducing a time dependent barrier against motion in any direction and no time averaged current was observed. In the experiment with [3]catenane, by using 2 rings, a time dependent barrier was introduced together with the time dependent change in energy minima and a net current in a particular direction was observed.

## *The principle*

behind this experiment and others concerning artificial motors is the following: The motion in molecular machines is brought about by external (often time dependent) stimuli. The time dependent stimuli work to keep the global minimum in the state space of the molecular machine varying. Thus the molecule constantly finds itself in energetically unfavorable conformations from which it escapes due to the thermal fluctuations in the bath around it. The molecule, thus in response to the external stimuli is driven along the macrostates to a new global minimum, in the kinetically most accessible direction. It is thus relevant, in attempts to synthesize and control artificial molecular motors, to understand the relation between external pumping and creation of systematic flows.
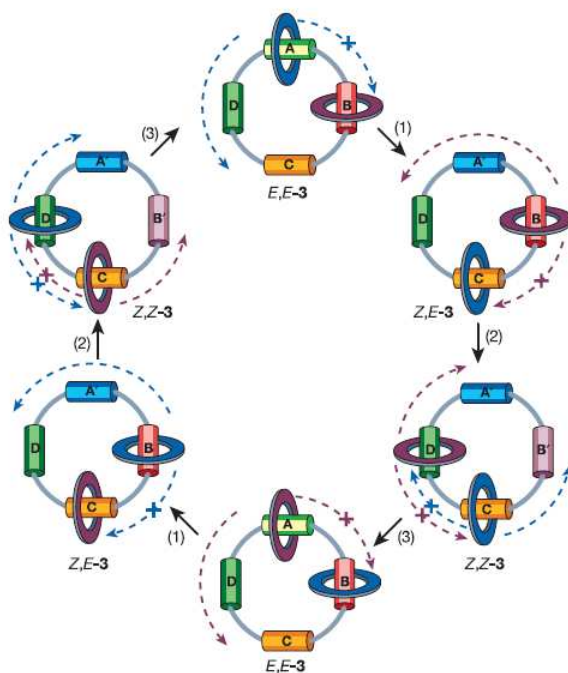
Figure 3.2: Stimuli induced unidirectional rotation in a 4 state [3]catenane. Figure has been reproduced from [86].

Thouless created a mathematical model [123], for electronic pumping. Astumian and Derényi [10] studied charge transfer from a lower to a higher chemical potential by varying the gate and portal energies. Astumian also analyzed the adiabatic regime of ion pumping in externally driven protein structures [8] and in a molecular motor based on a three-ring catenane [9]. A general theory of adiabatic pumps in terms of geometrical phase was proposed by Sinitsyn and Nemenman [121]. Chernyak and Sinitsyn [28] have discovered that the adiabatic pumping currents become quantized at low temperatures. Generalizations beyond adiabatic regimes are so far limited to Markov models. The derivations and results which follow are taken from our work in [92].

## 3.2   The No-go theorem

We model the dynamics here as a Markov state system for which the transitions between states $i$ and $j$ have an Arrhenius-type time-dependence (2.4.7)

$$w_t(i,j) = \mathcal{A}(i,j)e^{\beta G_t(i)}, \ \mathcal{A}(i,j) = \mathcal{A}(j,i) \tag{3.1}$$

with periodic time-dependent energy wells $G_t(i)$ and the constant energy barriers as represented by the symmetric factors $\mathcal{A}(i,j)$.

**The No-go theorem** states that for rates defined in this manner, the time-averaged current $J(i,j)$ along every transition $i \to j$ is zero. As a result, no net work can be done with such protocol.

Rahav, Horowitz and Jarzynski [111] were the first to give a no-go theorem for jump processes with non-adiabatic pumping and generalization to diffusion processes [64]. This was further studied and systematized by Chernyak and Sinitsyn [27]. We present here the shortest general proof of this result (Section 3.2.2), which at the same time also applies to classes of non-Markov models (Section 3.3). At the end we put the result into a broader context by showing that the time-dependent protocol under consideration, in arbitrary (in general nonequilibrium) systems, modifies all currents by a global multiplicative factor (Section 3.5). We start with the general set-up in terms of a Markov jump process.

### 3.2.1   The Model

The various chemo-mechanical configurations that the motor can exist in are labeled as $i, j, \ldots$ and constitute a finite state space $\Omega$. These long-lived or metastable states locally minimize a given free-energy landscape $G_\alpha(i)$ under equilibrium. They can be regarded as nodes of a stochastic network and an allowed transition is denoted by an edge $(ij)$. The index $\alpha$ is a parameter which can be externally manipulated and which varies the depth of the local free-energy minimum $G(i)$. In general, it quantifies the time-dependence of the dynamics. We assume that the dynamics is detailed balance. This means that for a fixed value of the external parameter $\alpha$, the system evolves, over time, to the global minimum of the free-energy landscape $G_\alpha(i)$.

*This is in contrast with a non-detailed balance dynamics where even for fixed external parameters, the system can never relax to equilibrium. An example of non-detailed balance dynamics is a metal rod held between two heat baths at*

*different temperatures. The temperature difference between the heat baths held
fixed, there is a constant, non-zero current across the metal bar.*

The existence of a detailed balance dynamics implies that the rates satisfy the
condition

$$e^{-\beta G_\alpha(i)} w_\alpha(i,j) = e^{-\beta G_\alpha(j)} w_\alpha(j,i) \tag{3.2}$$

The transition rate in general is given as

$$w_t(i,j) = \mathcal{A}(i,j) e^{G_{\alpha(t)}(i)}, \ \ \mathcal{A}(i,j) = e^{-\Delta(i,j)} \tag{3.3}$$

$\beta$ is assumed to be unity.

The effective barrier height $\Delta(i,j) = \Delta(j,i)$, defines the Arrhenius prefactor.
We can see that given our definitions of the free-energy minima $G_{\alpha(t)}$ and
the barrier heights $\Delta(i,j)$, the activation energy for the transition $i \to j$ is
$E_{\alpha(t)}(i,j) = -G_{\alpha(t)}(i) + \Delta(i,j)$. We assume that the heights of the barriers and
the energy minima can be independently manipulated. Fig 3.3 illustrates the
energy wells and barriers which are time dependent and can be independently
manipulated.

If $\rho_t$ is the instantaneous distribution function and $j_t(i,j)$, the instantaneous
current between states $i$ and $j$, then they satisfy the Master equation

$$\frac{d}{dt}\rho_t(i) = -\sum_j j_t(i,j) \tag{3.4}$$

$$j_t(i,j) = \rho_t(i)w_t(i,j) - \rho_t(j)w_t(j,i) \tag{3.5}$$

When the protocol $\alpha(t)$ is periodic in time, we expect to find that $\rho_t$ itself
becomes periodic in time, at least for sufficiently large times $t$. In any event,
we can define the time-averaged current

$$J(i,j) = \lim_{T\to\infty} \frac{1}{T} \int_0^T j_t(i,j)\mathrm{d}t \tag{3.6}$$

### 3.2.2   The proof of No-go theorem

The No-go theorem states that for *some specific types* of time-dependence — in
general for those considered in (3.3), where the energy wells are time-dependent

but the energy barriers are time-independent, the long-time average of current (3.6) equals zero for all pairs of states $i, j$.

Thinking of independent particles hopping on the network over $i \to j$ with rate $w_t(i, j)$, the no-go refers to having no net time-averaged flow of particles between any two nodes $i$ and $j$, i.e. $J(i, j) = 0$ for all pairs $i, j \in \Omega$.

We now come to our formulation of the no-go theorem. Consider the class of Markov jump processes with states $i, j, \ldots$ as in Section 3.2.1. For all bonds $(ij)$ in our stochastic network that are part of a loop in the network we require that the time-dependence in the transition rates is of the form

$$w_t(i, j) = \lambda_t(i)p(i, j) \tag{3.7}$$

where $\lambda_t(i) = \sum_j w_t(i, j)$ is the time-dependent escape rate and $p(i, j)$ is a time-independent transition probability; $p(i, j) \geq 0, \sum_j p(i, j) = 1$. We assume that the matrix $[p(i, j)]$ is irreducible so that there is a unique left eigenvector $\rho$ for eigenvalue 1: $\sum_i \rho(i)p(i, j) = \rho(j)$. (That is automatically so when the network of states is connected via $p(i, j) > 0$ - Perron-Frobenius theorem.)

We also assume that the corresponding embedded Markov chain (as described in Section 2.4.4, whose transition rates are just transition probabilities $p(i, j)$) is detailed balance, i.e., for some potential $V$ ,

$$e^{-V(i)}p(i, j) = e^{-V(j)}p(j, i) \tag{3.8}$$

so that in fact $\rho(i) \propto e^{-V(i)}$. Finally, we suppose that the limit

$$\varpi(i) := \lim_{T \to \infty} \frac{1}{T} \int_0^T \rho_t(i)\lambda_t(i)\mathrm{d}t \tag{3.9}$$

exists. That is automatically satisfied (shown below) when the time-dependence is periodic but, clearly that is not strictly necessary.

When the time-dependence is periodic with a period $\mathcal{T}$: $\rho_t = \rho_{t+\mathcal{T}}$; $\lambda_t = \lambda_{t+\mathcal{T}}$, $\forall\, t$, we can rewrite time $T = n\mathcal{T} + s$, where the limit $T \to \infty$ translates to $n \to \infty$. Hence

$$\varpi(i) = \lim_{n \to \infty} \frac{1}{n\mathcal{T} + s} \int_0^{n\mathcal{T}+s} \rho_t(i)\lambda_t(i)\mathrm{dt}$$

$$= \lim_{n \to \infty} \frac{n}{n\mathcal{T} + s} \int_0^{\mathcal{T}} \rho_t(i)\lambda_t(i)\mathrm{dt} + \lim_{n \to \infty} \frac{1}{n\mathcal{T} + s} \int_{n\mathcal{T}}^{n\mathcal{T}+s} \rho_t(i)\lambda_t(i)\mathrm{dt}$$

$$(3.10)$$

In the second integral, making a change of variables $t' = t - n\mathcal{T}$ we arrive at

$$\lim_{n \to \infty} \frac{1}{n\mathcal{T} + s} \left[ \int_{n\mathcal{T}}^{n\mathcal{T}+s} \rho_t(i)\lambda_t(i)\mathrm{dt} = \int_0^s \rho_{t'}(i)\lambda_{t'}(i)\mathrm{dt'} \right]$$

The integral

$$\int_0^s \rho_{t'}(i)\lambda_{t'}(i)\mathrm{dt'}$$

is finite, hence the limit $n \to \infty$ of the right hand term is zero.

Hence,

$$\varpi(i) = \lim_{n \to \infty} \frac{n}{n\mathcal{T} + s} \int_0^{\mathcal{T}} \rho_t(i)\lambda_t(i)\mathrm{dt}$$

which in the $n$ going to infinity limit is finite.

$$\varpi(i) = \frac{1}{\mathcal{T}} \int_0^{\mathcal{T}} \rho_t(x)\lambda_t(x)\mathrm{dt}$$

The no-go theorem is now easily proven as follows. The full time evolution is obtained by solving (3.4) & (3.5). The time integral of the former gives

$$\lim_T \frac{1}{T} \int_0^T \frac{d\rho_t}{dt} = -\sum_j J(i,j) = 0 \tag{3.11}$$
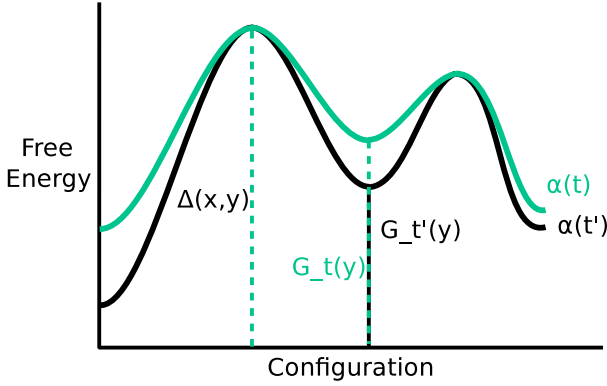
Figure 3.3: The free energy landscape; at two times $t$ and $t'$

and

$$J(i,j) = \varpi(i)p(i,j) - \varpi(j)p(j,i) \tag{3.12}$$

where we have inserted condition (3.7) and definition (3.9). Using (3.11) in (3.12)

$$\sum_j \varpi(j)p(j,i) = \varpi(i)$$

which is the stationary Master equation for a time-independent Markov chain with (unnormalized) distribution $\varpi$ and current $J$. By irreducibility and by detailed balance of the embedded Markov chain (3.8), the equations (3.11) and (3.12) have the unique solution

$$\varpi(i) \propto e^{-V(i)}, \ J(i,j) = 0 \ \text{(all pairs)} \tag{3.13}$$

as was to be proven.

The conditions (3.7), (3.8) are just equivalent to (3.2), (3.3) and hence the above theorem can immediately be applied to this situation. Specifically, for a system with free energy wells $G_\alpha(i)$ and effective energy barriers $\Delta(i,j) = \Delta(j,i)$ as in (3.3), we consider an arbitrary cyclic path $\alpha(t) = \alpha(t+T)$ with some period $\mathcal{T}$. Keeping the energy barriers constant, the condition (3.7) is verified with time-dependent escape rates

$$\lambda_t(i) = e^{G_\alpha(t)(i)} \sum_j e^{-\Delta(i,j)}$$

and time-independent transition probabilities

$$p(i,j) = \frac{e^{-\Delta(i,j)}}{\sum_j e^{-\Delta(i,j)}}$$

satisfying detailed balance (3.8) for $V(i) = -\log\left(\sum_j e^{-\Delta(i,j)}\right)$.

In conclusion, the essential ingredients are two-fold. First, the original time-dependent jump process is detailed balanced for each fixed $t$ and secondly, the transition rates can be decomposed into a product of time-dependent escape rates $\lambda_t(i)$ and time-independent transition probabilities $p(i,j)$. The idea of the proof above, at least for a periodic time-dependence, is that the time-averaged current in the original system (3.3) exactly coincides with the stationary current in a temporally coarse-grained system with transition probabilities $p(i,j)$. As the original process is detailed balanced for each fixed time, the stationary coarse-grained process is time-reversal symmetric and therefore the net current in the original process vanishes.

As a final comment, it is important to realize that the vanishing of the net (i.e., time-averaged) current, $J(i,j) = 0$, does not imply that $j_t(i,j) = 0$ at each time, unless the process runs in the quasistatic regime. Related to that, the overall dissipation does remain nonzero in general. For this it suffices to look at the time-averaged entropy flux (discussed in [93])

$$\frac{1}{T}\int_0^T \sigma_t dt = \frac{1}{2T}\sum_{i,j}\int_0^T j_t(i,j)\log\left(\frac{w_{\alpha(t)}(i,j)}{w_{\alpha(t)}(j,i)}\right)dt \geq 0$$

where the equality holds in the quasistatic or the adiabatic limit, when the external parameter $\alpha(t)$ is varied very slowly with time, such that $\rho(i) \propto e^{-\beta G_{\alpha(t)}(i)}$.

## 3.3   Non-Markov generalization

We would like to extend the proof of the No-go theorem to systems whose dynamics is non-Markovian. In Section (2.4.2), we had defined Markov

processes as those processes for which the waiting times was exponentially distributed. The exponential distribution of waiting times imply that the escape rate $\lambda_t$ depends only on the present configuration of the system. And there is no dependence on the path which the system took since the start of the experiment. But many biophysical and biochemical processes are believed to be essentially non-Markovian for a natural choice of states [57] and hence the extension of the No-go theorem to non-Markovian dynamics is essential to the understanding of such processes.

The memory of a non-Markovian dynamics can go from the last occupied state: "*short*" to the last several occupied states: "*long*". Here, we consider a jump process for which the main change with respect to the Markov case consists in its dependence on the time $t_0$ of the previous jump. In that way, given that the system is in state $x$ at time $t$ since its last jump to $i$ at $t_0$, the probability that the next jump occurs within the time-interval $[t, t + dt]$ is given by $\lambda(i; t_0, t)dt$. (The Markov case corresponds to $\lambda(i; t_0, t) = \lambda_t(i)$). The probability rate that the next jump goes to $j$ is then

$$w(i, t_0; j, t) = \lambda(i; t_0, t)p(i, j) \tag{3.14}$$

generalizing the time-dependent Markov transition rates (3.7). We keep the same assumptions on the transition matrix $[p(i, j)]$, with its most important property being the condition of detailed balance (3.8). The $p(i, j)$ define what is often called the embedded Markov chain. The complication of the memory present in the escape rates $\lambda(i; t_0, t)$ turns out to be irrelevant for our proof of the no-go, as we now show.

The probability density that at time $t$ the system is found in state $i$ and that the last jump before $t$ occurred within $[t_0, t_0 + dt_0]$ is denoted by $\rho(i; t_0, t)dt_0$ - it relates to the standard single-time distribution as

$$\rho_t(i) = \int_0^t \rho(i; t_0, t)dt_0 \tag{3.15}$$

The mean current $j(i, t_0; j, t)dt_0$ counts the expected rate of (directed) jumps $i \to j$ at time $t$ when the previous jump occurred in $[t_0, t_0 + dt_0]$:

$$j(i, t_0; j, t) = \rho(i; t_0, t)w(i, t_0; j, t) - \rho(j; t_0, t)w(j, t_0; i, t) \tag{3.16}$$

It is related to the standard mean current as

$$j_t(i, j) = \int_0^t j(i, t_0; j, t)dt_0 \tag{3.17}$$

Differentiating (3.15) with respect to $t$ and using the relation (3.16), the single-time quantities $\rho_t$ and $j_t$ satisfy the balance equation

$$\frac{d\rho_t(i)}{dt} + \sum_j j_t(i,j) = 0 \tag{3.18}$$

We proceed analogously as in the Markov case. We assume that the limiting quantities

$$\varpi(i) = \lim_T \frac{1}{T} \int_0^T \sum_0^t \rho(i; t_0, t) \lambda(i; t_0, t) \mathrm{dt_0 dt} \tag{3.19}$$

$$J(i,j) = \lim_T \frac{1}{T} \int_0^T j_t(i,j) \mathrm{dt} \tag{3.20}$$

are well defined. Then again,

$$J(i,j) = \varpi(i)p(i,j) - \varpi(j)p(j,i) \tag{3.21}$$

and from integrating (3.18),

$$\sum_j J(i,j) = 0 \tag{3.22}$$

By detailed balance (3.8) we reach the conclusion $J(i,j) = 0$ which ends the proof. As before, *time-homogeneity and detailed balance of the embedded Markov chain imply that the net flux through any pair $(ij)$ asymptotically goes to zero.*

To end this proof we would like to point out two important features of the No-go theorem.

## 3.4 Flashing ratchet & Geometry of Network

The No-go theorem is only valid for some specific types of time-dependence - in general for those considered in (3.3). Though the rates are satisfying the condition of detailed balance (3.2) for each fixed value of the parameter $\alpha$, there is no a priori reason why there could not arise a net current $J(i,j)$ in the

process with time-dependent $\alpha(t)$. In fact, that is exactly what happens in so called flashing (and other) ratchets where the change in the potential landscape produces a net flow of particles [112]. For example, a system (like a ratchet) with transition rates

$$\tilde{w}_t(i,j) = \mathcal{A}(i,j)e^{-\frac{1}{2}[G_t(j)-G_t(i)]}, \ \mathcal{A}(i,j) = \mathcal{A}(j,i) \tag{3.23}$$

also satisfies detailed balance (3.2) for each fixed time $t$ and can be written analogous to (3.3) as

$$\tilde{w}_t(i,j) = e^{G_t(i)-\Delta_t(i,j)} \tag{3.24}$$

but the effective barriers $\Delta_t(i,j) = [G_t(i) + G_t(j)]/2 - \log\mathcal{A}(i,j)$ have become *time-dependent*. See figure 3.4
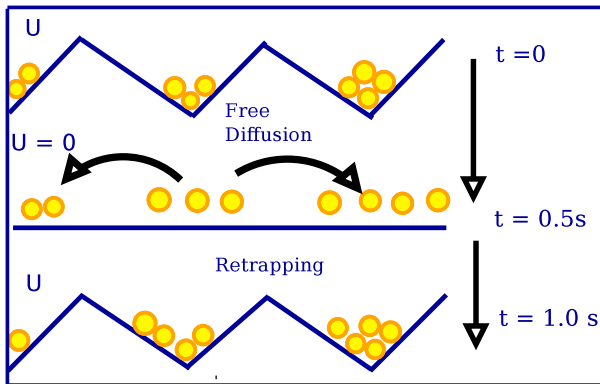


Figure 3.4: Flashing ratchet: Both the energy wells and barriers are time-dependent

Within the framework of the no-go theorem there is absolutely no reason now that the net currents would be identically zero (unless further symmetries are imposed).

Secondly, the geometry of the stochastic network is certainly relevant for the possible generation of a current. In fact, the net current $\int_0^T j_t(i,j)dt$ over any edge $(ij)$ connecting two otherwise disconnected subgraphs is a total time-difference of the form $N_T(i,j) - N_0(i,j)$ and hence automatically approaches zero when time-averaged as in (3.6). Thus $w_t(i,j)$ can be arbitrary ($=$ no restriction) over such a "bridge". The restricted form of time-dependence as in
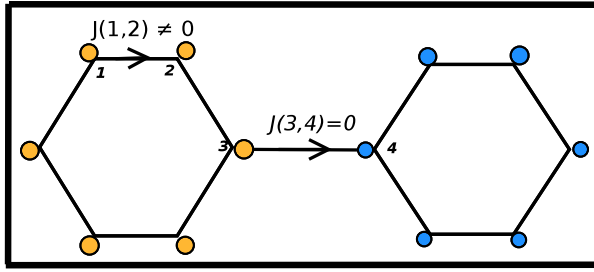
Figure 3.5: Time averaged current between states 3 and 4 is zero.

(3.3) is only required over those edges $(ij)$ which belong to a loop. See figure 3.5.

## 3.5 Non-equilibrium generalization

A natural question arises how the long-time characteristics of a general nonequilibrium system with steady currents already present, modify when an extra time-dependence affecting only the energy wells or escape rates like in (3.7) is applied. We answer here that question by generalizing the above argument, restricting ourselves to the case of jump processes. This will throw more light into the nature and robustness of no-go theorems.

As before in (3.3) we start from transition rates

$$w_t(i,j) = w(i,j)e^{G_t(i)} \tag{3.25}$$

with time-dependent energy function $G_t(i) = G_{\alpha(t)}(i)$. The time-independent rates $w(i,j)$ are no longer detailed balance. We can assume a time-homogeneous non-equilibrium process with the reference stationary state $\rho^s(i)$ and the steady state current

$$j^s(i,j) = \rho^s(i)w(i,j) - \rho^s(j)w(j,i), \quad \sum_j j^s(i,j) = 0 \tag{3.26}$$

The long-time averaged current of the time-dependent process is

$$
\begin{aligned}
J(i,j) &= \lim_T \frac{1}{T} \int_0^T j_t(i,j)\mathrm{dt} \\
&= \varpi(i)w(i,j) - \varpi(j)w(j,i)
\end{aligned}
$$

with

$$
\varpi(i) = \lim_T \frac{1}{T} \int_0^T \rho_t(i)e^{G_t(i)}\mathrm{dt} \tag{3.27}
$$

and satisfying the stationarity condition in all nodes:

$$
\sum_j J(i,j) = 0 \tag{3.28}
$$

By the assumed irreducibility of the equations (3.27) & (3.28) have a unique solution in the form

$$
\varpi(i) = \rho^s(i), \ \ J(i,j) = j^s(i,j) \tag{3.29}
$$

with the normalization

$$
\Omega = \lim_T \frac{1}{T} \sum_i \int_0^T \rho_t(i)e^{G_t(i)}dt \tag{3.30}
$$

Hence, we have arrived at an important conclusion: For the time-dependent protocols under consideration, the time averaged current (3.27) is merely a *global multiplicative factor* of the reference steady current. If the latter is zero, there is also no resulting pumped current and we recover the original results.

# Chapter 4

# Large Deviation Theory: Entropy, Free Energy & Statistical force

*The probable is what usually happens. - Aristotle*

*When you have eliminated the impossible, whatever remains, however improbable, must be the truth.*

*- Sherlock Holmes in The Sign of the Four*

## 4.1 Introductory examples

The theory of large deviations refers to fluctuations of a macroscopic quantity, related to a stochastic process, from its typical value. This could be deviation of an empirical average taken over some distribution from its theoretical expectation or the deviation of an empirical trajectory (or empirical vector, in case of discrete time) $\omega_{0 \leq t \leq \tau}$ over time from the most probable one or the deviation of an empirical probability distribution over states from its typical distribution.

We start with a few examples to illustrate the meaning and significance of LDT. The first example is a heuristic one.

**Example 4.1.1: Uniform Sample Mean**   Assume that a dice is thrown 6 times resulting in the following result: $(4, 4, 2, 1, 5, 6)$. Then, the empirical average is given by

$$\frac{1}{6}(4 + 4 + 2 + 1 + 5 + 6) = 4.16$$

and the empirical distribution is given by

$$\left(\frac{1}{6}, \frac{1}{6}, 0, \frac{2}{6}, \frac{1}{6}, \frac{1}{6}\right)$$

The theoretical distribution for a dice on the other hand is

$$\frac{1}{6}, \frac{1}{6}, \frac{1}{6}, \frac{1}{6}, \frac{1}{6}, \frac{1}{6}$$

and the theoretical mean being 3.5. The deviation of the empirical mean from the theoretical value is non zero for a small number of trials. And the probability of deviations from the theoretical distribution and mean becomes small with the system size or increase in the number of trials.

*How fast the probability of deviations from the typical outcomes disappears is the subject matter of Large Deviation Theory, which shows that many (but not all) systems show an exponential decay in the probability of large deviations with system size.*

In equilibrium statistical physics, the rate of decay has been related to the entropy, relative entropy or free energy of the system.

The next example indicates the function and meaning of these rate functions in case of identically distributed Gaussian variables. The theory of Large Deviations discussed in this chapter is heavily based on a brilliant review on the subject by Touchette [124].

**Example 4.1.2: Gaussian Sample Mean**   The random variable $X_i$ takes values $x \in \mathbb{R}$ from a distribution (4.1), which is Gaussian with mean $\mu$ and standard deviation $\sigma$ . We ask the question, what is the probability that the

empirical mean of the $n$ random variables will deviate from their theoretical mean $\mu$.

$$p(x)\mathrm{dx} = \frac{1}{\sqrt{2\pi\sigma^2}}e^{-(x-\mu)^2/2\sigma^2}\,\mathrm{dx} \tag{4.1}$$

Let us denote the sample mean after $n$ trials by

$$S_n = \frac{1}{n}\sum_{i=1}^{n}X_i$$

The probability density of $S_n$ can be written as an integral:

$$p(S_n = s) = \int_{\mathbb{R}^n} \delta(S_n(x) - s)p(x)dx \tag{4.2}$$

$x = (x_1, x_2, \ldots, x_n)$ is a random vector in $\mathbb{R}^n$, and

$p(x) = p(x_1, x_2, \ldots, x_n) = p(x_1)p(x_2)\ldots p(x_n)$ is the joint probability density.

Replacing the expression for $p(x_i)$ from (4.1) into the above equation (4.2). The probability density of the empirical mean is given by:

$$p(S_n = s) = \sqrt{\frac{n}{2\pi\sigma^2}}e^{-n(s-\mu)^2/2\sigma^2} \tag{4.3}$$

For a large deviation approximation ($n \to \infty$), the multiplicative factor of $\sqrt{n}$ which grows much slower than the exponential decay, is ignored, thereby obtaining the large deviation result,

$$p(S_n = s) \approx e^{-nJ(s)}, \ J(s) = \frac{(s-\mu)^2}{2\sigma^2} \tag{4.4}$$

$J(s)$ the rate factor gives a detailed description of the fluctuations of $S_n$ around its typical value. It displays some features which are generally true. $J(s)$ is convex and has a single minimum and zero at $\mu$ the theoretical mean. As the value of $n$ rises the system converges probabilistically to the mean value $\mu$ and we can say that $S_n$ obeys the *Law of Large numbers*,

$$\lim_{n\to\infty} P(S_n \in [\mu - \delta, \mu + \delta]) = 1, \ \forall \ \delta > 0$$

The third example deals with large deviations in probability distributions.

**Example 4.1.3:** Consider a sequence of IID random variables, $X = (x_1, x_2, \ldots, x_n)$, drawn from a state space $\Lambda = (1, 2, \ldots, q)$ with a probability distribution $P(x_i = j) = \rho_j$. For a given experiment of $n$ trials, the empirical distribution of states is given by:

$$l_j = \frac{1}{n} \sum_{i=1}^{n} \delta_{x_i, j} \tag{4.5}$$

Hence, there exists a normalized vector of size $q$ giving relative frequencies:

$$L_n(X) = (L_{n,1}(X), L_{n,2}(X), \ldots, L_{n,q}(X)), \;\; \sum_{j \in \Lambda} L_{n,j}(X) = 1$$

for all $X \in \Lambda^n$

The empirical vector $L_n$ is distributed according to the distribution

$$P(L_n = l) = \frac{n!}{\prod\limits_{j=1}^{q} (nl_j)!} \prod_{j=1}^{q} (\rho_j)^{nl_j} \tag{4.6}$$

$l = (l_1, l_2, \ldots, l_q)$

Using Stirling's approximation we can extract a large deviation approximation:

$$\log(P(L_n = l)) \approx \left( n\log(n) - n - \sum_{j=1}^{q} (nl_j)\log(nl_j) - nl_j \right) + \sum_{j=1}^{q} nl_j \log(\rho_j)$$

Using the normalization condition $\sum\limits_{j=1}^{q} l_j = 1$, we reach

$$P(L_n = l) \approx e^{-nI_\rho(l)}, \;\; I_\rho = \sum_{j=1}^{q} l_j \log\frac{l_j}{\rho_j} \tag{4.7}$$

The rate function $I_\rho$ is called the *relative entropy* or the *Kullback-Leibler distance* between the probability vectors $\rho$ and $l$. Next we illustrate that the

rate function is convex, positive and has its minimum and zero at $l = \rho$. This implies that as the system size increases, the most probable value of the random variable $l$ is $\rho$, and the probability of any other fluctuating configurations decay exponentially to zero.

We will be proving some of these properties below for this particular example. Before we lay down the proofs, here are a few definitions and known results which we will employ in our proofs.

- **A function $f(x)$ is convex** if for any real numbers $x_1 < x_2$, each point on the line segment joining $(x_1, f(x_1))$ and $(x_2, f(x_2))$ lies either above or on the curve $f$. Algebraically, this implies the following:

$$f(\lambda x_1 + (1 - \lambda)x_2) \leq \lambda f(x_1) + (1 - \lambda)f(x_2), \ \lambda \in [0, 1]$$
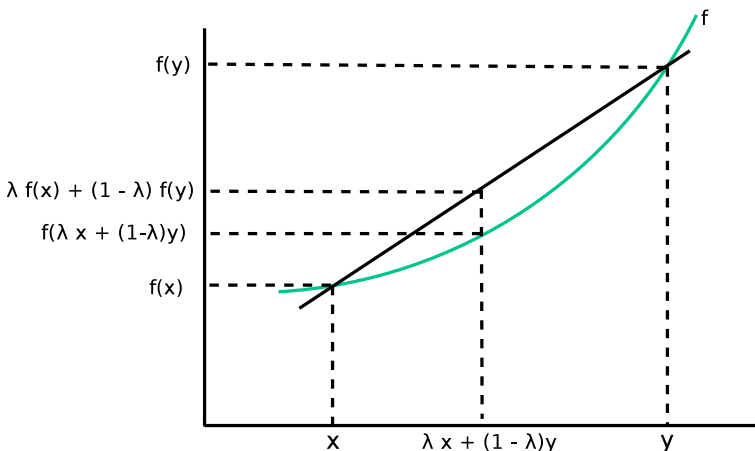


Figure 4.1: Convex function $f(x)$

- ***Jensen's Inequality***

  In the context of probability theory it is generally stated as follows: If $X$ is a random variable and $f(X)$ is a convex function:

$$f(\langle X \rangle) \leq \langle f(X) \rangle,$$

  $\langle \rangle$ denotes expectation value with respect to some distribution. For a concave function Jensen's Inequality reverses itself.

- ### *Log-Sum Inequality*

  For non-negative numbers $(a_1, a_2, \ldots, a_n)$ and $(b_1, b_2, \ldots, b_n)$,

  $$\sum_{i=1}^{n} a_i \log\left(\frac{a_i}{b_i}\right) \geq \left(\sum_{i=1}^{n} a_i\right) \log\left(\frac{\sum_{i=1}^{n} a_i}{\sum_{i=1}^{n} b_i}\right)$$

  with equality holding iff, $\frac{a_i}{b_i}$ is a constant.

  **Proof:** The function $f(x) = x \log(x)$ is a convex function. Hence, applying Jensen's inequality on this function:

  $$\sum_i \alpha_i f(x_i) \geq f\left(\sum_i \alpha_i x_i\right), \ \alpha_i > 0, \ \sum_i \alpha_i = 1$$

  Assume that $a_i, b_i > 0$, then setting $\alpha_i = b_i / \sum_i b_i$ and $x_i = a_i / b_i$, we obtain the log-sum inequality.

We next present, with proof some general features of the rate function $I$.

- ### *Relative Entropy is non-negative*

  Using the log-sum inequality, with $a_j = l_j$ and $b_j = \rho_j$

  $$
  \begin{aligned}
  I_\rho(l) &= \sum_{j \in \Lambda} l_j \log\left(\frac{l_j}{\rho_j}\right) \\[2ex]
  &\geq \left(\sum_{j \in \Lambda} l_j\right) \log\left(\frac{\sum_{j \in \Lambda} l_j}{\sum_{j \in \Lambda} \rho_j}\right) \quad \text{using log-sum inequality} \\[2ex]
  &= 0, \ \text{ Since } \sum_{j \in \Lambda} l_j = \sum_{j \in \Lambda} \rho_j = 1
  \end{aligned}
  \tag{4.8}
  $$

## • *Relative Entropy is convex*

To show the convexity of the relative entropy we employ two probability mass functions $l_1$ and $l_2$ and need to show that

$$I_\rho(\lambda l_1 + (1 - \lambda)l_2) \leq \lambda I_\rho(l_1) + (1 - \lambda)I_\rho(l_2) \text{ i.e.}$$

$$\sum_{j=1}^{q}(\lambda l_{j1} + (1 - \lambda)l_{j2}) \log\left(\frac{\lambda l_{j1} + (1 - \lambda)l_{j2}}{\rho_j}\right) \leq \lambda \sum_{j=1}^{q} l_{j1} \log \frac{l_{j1}}{\rho_j}$$

$$+ (1 - \lambda) \sum_{j=1}^{q} \log \frac{l_{j2}}{\rho_j} \quad (4.9)$$

Using the log-sum inequality with $a_1 = \lambda l_{j1}$, $a_2 = (1 - \lambda)l_{j2}$, $b_1 = \lambda \rho_j$, $b_2 = (1 - \lambda)\rho_j$, then

$$(\lambda l_{j1} + (1 - \lambda)l_{j2}) \log\left(\frac{\lambda l_{j1} + (1 - \lambda)l_{j2}}{\rho_j}\right) \leq \lambda l_{j1} \log \frac{\lambda l_{j1}}{\lambda \rho_j}$$

$$+ (1 - \lambda)l_{j2} \log \frac{(1 - \lambda)l_{j2}}{(1 - \lambda)\rho_j}$$

Summing the two sides of the inequality over all $j$ we reach the desired result. Given the non-negativity of the relative entropy and its strictly convex nature, one can safely say that the zero of $I_\rho(l)$ at $l = \rho$ is its unique minimum.

After having demonstrated the meaning and function of the LDT through these simple examples, we can proceed to formally introduce the LDT, with some general results.

## 4.2  The Large Deviation principle

In this section we present a formal definition of the *principle of large deviation* and state some general theorems with examples.

We have established with the few examples above that for several systems the deviation of macroscopic variables from their typical configuration decays exponentially in the limit of large system size or large number of trials. Formally, this limit can be spoken of as follows. Let $X_n$ be a random variable with $n$ denoting the system size which eventually is taken to infinity, then we talk about $P(X_n \in G)$, the probability that $X_n$ takes on a value in set $G$. This probability is said to satisfy a *large deviation principle* if the limit,

$$\lim_{n \to \infty} -\frac{1}{n}\log P(X_n \in G) = I_G \tag{4.10}$$

exists. Or in other words $P(X_n \in G) \approx e^{-nI_G}$ is the dominant behavior of $P(X_n \in G)$ in the $n$ large limit. $I_G$ is a positive constant which depends on the system parameters and constraints.

In case of a continuous state space, we use probability density and the principle takes the following form:

$$P(X_n \in [x, x + \mathrm{dx}]) \approx \mathrm{e}^{-\mathrm{nI(x)}}\mathrm{dx}, \text{ to be written as } \mathrm{P(X_n \in dx)} \asymp \mathrm{e}^{-\mathrm{nI(x)}}\mathrm{dx}$$

The relation $a_n \asymp b_n$ denotes that $a_n$ and $b_n$ are equal upto first order in their exponents.

$$\lim_{n \to \infty} \frac{1}{n}\log a_n = \lim_{n \to \infty} \frac{1}{n}\log b_n$$

To establish that a large deviation principle exists and from there to calculate the rate function can be achieved if one can calculate the probability distribution of the random variable. And then applying a Stirling's kind of approximation leads us to the asymptotic behavior of the probability density. But to be able to write down the probability distribution for a general stochastic process or to be able to apply a Stirling's kind of approximation is not always possible, like in case of continuous variables or for random variables which are non-IID. Here, we present a fundamental result of the large deviation theory, which serves as a general criterion to find if the large deviation principle is satisfied and to derive the rate function.

## 4.2.1  Gärtner-Ellis theorem

For a real random variable $X_n$, we define a scaled cumulant generating function by the limit

$$\lambda(k) = \lim_{n\to\infty} \frac{1}{n} \log \langle e^{nkX_n}\rangle, \ k \in \mathbb{R} \tag{4.11}$$

$$\langle e^{nkX_n}\rangle = \int_{\mathbb{R}} e^{nkX_n} P(X_n \in \mathrm{dx}) \tag{4.12}$$

The Gärtner-Ellis theorem states that if $\lambda(k)$ exists and is differentiable for all $k \in \mathbb{R}$, then $X_n$ satisfies a large deviation principle,

$$P(X_n \in dx) \asymp e^{-nI(x)}\mathrm{dx}$$

with $I(x)$ given by

$$I(x) = \sup_{k\in\mathbb{R}}[kx - \lambda(k)] \tag{4.13}$$

The symbol "sup" stands for "supremum of", which for all practical purposes takes the same meaning as "maximum of" here. The transform defined by (4.13) is called the *Legendre-Fenchel transform* of $\lambda(k)$.

Once we assume that the existence of $\lambda(k)$ guarantees a large deviation principle, we can substitute the asymptotic form of the probability density into the expectation expression (4.12). Next, the integral can be approximated with the maximum of $kx - I(x)$. This is called the *saddle point approximation*. Therefore,

$$\langle e^{nkX_n}\rangle \asymp \exp\{n \sup_{x\in\mathbb{R}}[kx - I(x)]\}$$

This relation when used in (4.11) renders,

$$\lambda(k) = \sup_{x\in\mathbb{R}}[kx - I(x)]$$

Legendre-Fenchel transform can be inverted when $\lambda(k)$ is everywhere differentiable, giving us the result (4.13).

We state here without proving that $\lambda(k)$ is always convex. And for a differentiable and convex generating function, the Legendre-Fenchel transform reduces to the better known, Legendre transform.

Also, noteworthy are the following properties:

1. $\lambda(0) = 0$

2. $\lambda'(0) = \lim_{n \to \infty} \frac{\langle X_n e^{nkX_n} \rangle}{\langle e^{nkX_n} \rangle}|_{k=0} = \lim_{n \to \infty} \langle X_n \rangle$,
   which for IID sample mean reduces to $\langle X \rangle$

3. Similarly, $\lambda''(0) = \lim_{n \to \infty} n[\langle X_n^2 \rangle - \langle X_n \rangle^2]$
   which for IID sample mean reduces to $\text{var}(X)$.

We will now illustrate the power of the Gärtner-Ellis theorem using two examples which we visited in the last section.

**Example 4.2.1:** *__The Gaussian Sample Mean:__* Consider again, the sample mean $S_n$ of random variables $X_i$ which are randomly picked from a Gaussian distribution. The cumulant generating function

$$\lambda(k) = \lim_{n \to \infty} \frac{1}{n} \log \langle \exp \left( k \sum_{i=1}^{n} X_i \right) \rangle = \lim_{n \to \infty} \frac{1}{n} \log \prod_{i=1}^{n} \langle e^{kX_i} \rangle = \frac{1}{n} \log \left( \langle e^{kX} \rangle \right)^n$$

since $X_i$ are independent IIDs

For a Gaussian distribution the expectation value

$$\log \langle e^{kX} \rangle = \mu k + \frac{1}{2} \sigma^2 k^2 = \lambda(k)$$

Since, $\lambda$ is everywhere differentiable, the rate function $I(s)$ is calculated by ordinary calculus. The maximum is reached at $k = (s - \mu)/\sigma^2$. Hence the rate function

$$I(s) = k(s)s - \lambda(k(s)) = \frac{(s - \mu)^2}{2\sigma^2}, \ s \in \mathbb{R}$$

The sample mean of Gaussian distributed random variables $X_n$ asymptotically equals $\mu$, for a large sample size.

Our second application of the Gärtner-Ellis theorem is on random variables which are vectors defined in $\mathbb{R}^d, d > 1$. These results on vector random variables are put under the name *__Sanov's theorem__*

**Example 4.2.2:** Recall example 4.1.2 of a sequence of n IID random variables $X = (x_1, x_2, \ldots, x_n)$ in a finite set $\Lambda$ distributed as $P(x = j) = \rho_j$, $j \in \Lambda$. We had calculated the probability distribution $P(L_n = l)$ associated with the empirical vector $L_n$ defined as

$$L_{n,j}(x) = \frac{1}{n} \sum_{i=1}^{n} \delta_{x_i, j}, \ j \in \Lambda$$

The vector $L_n$ has $|\Lambda| = q$ components and is a set of probability distributions on $\Lambda$.

To find the large deviations of $L_n$, we consider the extension to vector space of the Gärtner-Ellis theorem. This is done by replacing the product $kX_n$ by a dot product $\mathbf{k} \cdot L_n$, where $\mathbf{k}$ is now a vector in $\mathbb{R}^d$.

Using the Gärtner-Ellis theorem, the expression for $\lambda(k)$ is given below

$$\lambda(\mathbf{k}) = \lim_{n \to \infty} \frac{1}{n} \log \left\langle \exp \left( n \sum_{j=1}^{d} k_j L_{nj} \right) \right\rangle$$

$$= \lim_{n \to \infty} \frac{1}{n} \log \left\langle \exp \left( n \sum_{j \in \Lambda} k_j \frac{1}{n} \sum_{i=1}^{n} \delta_{x_i, j} \right) \right\rangle$$

$$= \lim_{n \to \infty} \frac{1}{n} \log \left\langle \exp \left( \sum_{j \in \Lambda} k_j (\delta_{x_1, j} + \delta_{x_2, j} \cdots + \delta_{x_n, j}) \right) \right\rangle$$

$$= \lim_{n \to \infty} \frac{1}{n} \log \left( \left\langle \exp \left( \sum_{j \in \Lambda} k_j (\delta_{x, j}) \right) \right\rangle \right)^n \text{, since } x_i \text{ are IID random variables}$$

$$= \log \left( \sum_{j \in \Lambda} \rho_j e^{k_j} \right) \tag{4.14}$$

Given that $\lambda$ is analytic in $\mathbf{k}$, using the Gärtner-Ellis theorem we conclude that a large deviation principle holds for $L_n$ with the rate function given by

$$I(\mathbf{l}) = \sup_{\mathbf{k}} [\mathbf{k} \cdot \mathbf{l} - \lambda(\mathbf{k})] = \mathbf{k}(\mathbf{l}) \cdot \mathbf{l} - \lambda(\mathbf{k}(\mathbf{l}))$$

where $\mathbf{k(l)}$ is the unique root of the equation $\nabla\lambda(\mathbf{k}) = \mathbf{l}$ thus yielding the rate functions

$$I(\mathbf{l}) = \sum_{j \in \Lambda} l_j \, \log \frac{l_j}{\rho_j}$$

the *relative entropy* of the system.

Next we would study the application of LDT on another class of stochastic processes which are instrumental in the study of dynamical processes in statistical mechanics.

## *Markov processes*

**Example 4.2.3:** Large deviation Theory as known today was formulated by Donsker and Varadhan [36, 34, 35] for Markov processes. We start of with a simple example. Consider a sequence of bits $x = (x_1, x_2, \ldots, x_n)$; $x_i \in \{0, 1\}$ which form a Markov chain defined by

$$P(x) = P(x_1, x_2, \ldots, x_n) = \rho(x_1) \prod_{i=1}^{n} \pi(x_i | x_{i-1})$$

Here $\rho(x_1)$ is the probability distribution of the initial state $x_1$, and $\pi(x_i | x_{i-1})$ is the conditional probability of state $x_i$ given the current state is $x_{i-1}$. The transition matrix $\Pi$ is defined as

$$\Pi = \begin{pmatrix} \pi(0|0) & \pi(0|1) \\ \pi(1|0) & \pi(1|1) \end{pmatrix} = \begin{pmatrix} 1 - \alpha & \alpha \\ \alpha & 1 - \alpha \end{pmatrix}$$

with $\alpha \in (0, 1)$

The Large Deviation principle for the sample mean $S_n = \frac{1}{n} \sum_{i=1}^{n} x_i$ can be arrived at by applying the Gärtner-Ellis theorem.

$$\langle e^{nkS_n} \rangle \;=\; \sum_{x_1, x_2, \ldots x_n \in \{0,1\}} P(x_1, x_2, \ldots x_n) \exp\left( k \sum_{i=1}^{n} x_i \right)$$

$$=\; \sum_{x_1, x_2, \ldots x_n} \pi(x_n|x_{n-1}) e^{kx_n} \ldots \pi(x_2|x_1) e^{kx_2} \rho(x_1) e^{kx_1}$$

$$=\; \sum_{j \in \{0,1\}} (\Pi_k^{n-1} \rho_k)_j \qquad\qquad (4.15)$$

where $(\Pi_k)_{ji} = \Pi(j|i) e^{kj}$ and $\rho_k(i) = \rho(i) e^{ki}$

Since, $\Pi_k^{n-1}$ is a positive real matrix, using the Perron-Frobenius theory, its largest eigenvalue is a unique positive number. Hence,

$$\lambda(k) = \lim_{n \to \infty} \frac{1}{n} \log \left( \sum_{j \in \{0,1\}} (\Pi_k^{n-1} \rho_k)_j \right)$$

can be extracted from this expression. For $\Pi$ being irreducible and aperiodic, there exists a unique stationary probability distribution $\rho_{\mathrm{st}}$ and $\Pi_k$ has a unique dominant eigenvalue $\xi_k$. It follows from here,

$$\langle e^{nk \cdot S_n} \rangle \asymp \xi_k^{n-1}, \text{ and hence } \lambda(k) = \log \xi_k$$

which is analytic in $k$. Hence, $S_n$ satisfies a LDT principle. The rate function is then easily given by

$$I(s) = \sup{}_k [ks - \log \xi_k]$$

For our simple example of two bits $\{0, 1\}$,

$$\Pi_k = \begin{pmatrix} 1 - \alpha & \alpha \\ \alpha e^k & (1 - \alpha) e^k \end{pmatrix}$$

The largest eigenvalue of which can be easily determined and is a function of $k$ and $\alpha$. For $\alpha = 1/2$ we return to IID variables.

## 4.3    Large Deviation Theory in statistical mechanics

### *Heuristic Motivation*

Statistical mechanics is the study of a physical process across different scales of description. We start from the microscopic level of particle positions, momenta and spins and scale out into a description in terms of magnetization or total angular momentum. Statistical physics aims to describe the global or coarse grained levels by taking an average of more detailed levels. A system which can be segregated into a numerous number (also called the thermodynamic limit $n \to \infty$) of identical subsystems is shown to obey the Law of Large Numbers which states that the values assumed by the macroscopic observables are reproducible (inspite of the ever changing microscopic landscape) and the fluctuations around these most probable values behave in accordance with the Central Limit theorem.

The Large Deviation Theory was put into use to study physical systems by Ruelle [115], Lanford [83], Ellis [45, 43, 44] and later many links between the two branches were forged by Pfister, Lewis and Sullivan [88]. LDT tells us that whenever the Law of Large Numbers holds, variational principles exist which lead to the most probable values of the macroscopic variables. In statistical mechanics, we are aware of variational principles such as the *maximum entropy principle* and the *minimum free energy principle.*These can be derived using LDT. The study of most probable states is reduced to the corresponding rate functions in the LDT. We will see ahead that thermodynamic variables such as *entropy* and *free energy* are rate functions of LDT. It also gives us the probability of the macroscopic variable to deviate from its most probable value.

The aim of this section is not to be an exhaustive discussion of LDT in statistical mechanics, but to be an introduction into connections between a few important concepts of statistical mechanics and of LDT. We would, with the help of a few examples, especially like to illustrate how free energies and through these statistical forces can be derived in equilibrium.

For a general system with $(n)$ degrees of freedom, which can exist in several microstates, denoted in general by a vector $\mathbf{x} = \{x_1, \ldots, x_n\}$. Each microstate has a corresponding energy $E(\mathbf{x})$ associated with it. For example, a system of particles suspended under the gravitational force, the state of the $ith$ particle is given by $x_i = (p_i, h_i)$, where $p_i$ is the momentum and $h_i$ is its height. The energy of such a microstate is

$$E(\mathbf{x}) = \sum_{i=1}^{n} \left( \frac{\|p_i\|^2}{2m} + mgh_i \right)$$

$m$ is the mass of each particle and $g$ is the constant of gravitation.

Each state is distributed according to the probability density

$$P(\mathbf{x}) = \frac{e^{-\beta E(\mathbf{x})}}{Z(\beta)} \tag{4.16}$$

where $Z(\beta) = \int_{\mathbf{x}} e^{-\beta E(\mathbf{x})} d\mathbf{x}$ is the normalization constant.

We will start with a LDT for the average energy per particle $u$, such that the total energy $E(\mathbf{x}) = nu$. The entropy per particle

$$s(u) = k_B \lim_{n \to \infty} \frac{\log \Omega(u)}{n} \tag{4.17}$$

where $\Omega(u)$ is the number of microstates with energy $E(\mathbf{x}) = nu$ and $k_B$ is the Boltzmann's constant. Hence, the probability to observe the energy per particle between $[u, u + du]$ is given by

$$
\begin{aligned}
P(u \in du) &= \int_{\mathbf{x}:u(\mathbf{x}) \in du} P(\mathbf{x}) dx \\
&= \frac{\Omega(u) e^{-\beta nu} du}{Z(\beta)}
\end{aligned}
\tag{4.18}
$$

We know from thermodynamics that $Z(\beta)$ is not just a normalization constant. Observables such as the Helmholtz free energy per particle

$$\mathcal{F} = -\frac{1}{n\beta} \log(Z(\beta)) \tag{4.19}$$

other quantities like the average energy and the specific heat can be derived using the normalization constant.

The asymptotic probability, in terms of the Helmholtz free energy is thus given as follows:

$$P(u \in du) \asymp e^{-n[\beta u - \frac{s(u)}{k_B} - \beta \mathcal{F}]} \tag{4.20}$$

where equations (4.16), (4.17), (4.19) are used.

In equilibrium the rate function $I(u) = \beta u - \frac{s(u)}{k_B} - \beta \mathcal{F}$ is minimized and zero, thus we arrive at the *minimum free energy principle*

$$\mathcal{F}(\beta) \asymp \min_u [u - Ts(u)]$$

Let $u_\beta$ be the energy which minimizes the expression, then the Helmholtz free energy per-particle in the thermodynamic limit

$$\mathcal{F}(\beta) \asymp [u_\beta - Ts(u_\beta)] \tag{4.21}$$

renders the usual thermodynamic relation between the free energy and entropy as Legendre transforms of each other.

The next section consists of a statistical system in equilibrium where, with the help of LDT we derive equilibrium state and the corresponding potentials. We also introduce the notion of *statistical forces* in fluctuating systems.

## 4.4   Entropic Spring

Consider a one-dimensional array of $N$ springs arranged along a straight line. Each spring in this coupled system can assume either length 0 or $\lambda$ independently. Both states are equally probable. The state of the *ith* element is labeled by $x_i \in \{0, \lambda\}$. This system is placed in a heat bath with inverse temperature $\beta$, such that the fluctuations of the bath lead the spring to explore the whole phase space. This system of springs is attached to a classical spring with spring constant $k$ and equilibrium length $x_0$. The complete system is confined between two walls at a distance $L$ from each other.

**Our aim is to calculate the statistical reaction force acted on the classical spring by the entropic spring, using LDT.**

To calculate the force due to a spring, we should first determine the probability of a given extension in the equilibrium length of the entropic spring. Let $l = n\lambda$ be the total length of the entropic spring, where $n$ is the number of springs with length $\lambda$. If $x$ is the extension or contraction in the classical spring, then the two systems are coupled by the following relation

$$L = l + x_0 - x$$
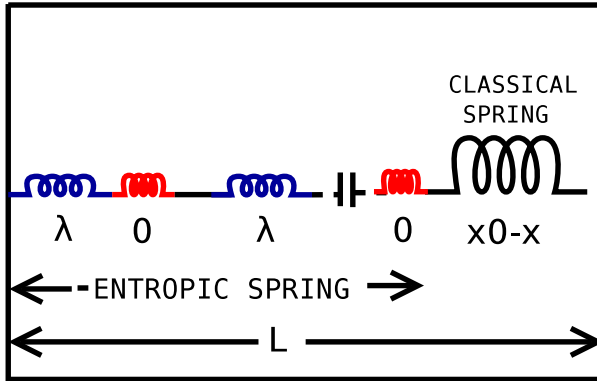
Figure 4.2: Entropic Spring coupled to a Classical spring
The color blue denotes length $\lambda$ and red denoted length 0

For the macroscopic variable $l$, we wish to calculate the probability $P(l/N = X)$ that the average length of each spring is $0 < X < \lambda$.

The total number of configurations the spring could take are $2^N$. Each microstate is equally probable with a probability $P(\eta) = 2^{-N}$. Hence, the probability of a configuration with length $NX$ is

$$P(l/N = X) = 2^{-N} \begin{pmatrix} N \\ NX/\lambda \end{pmatrix} \tag{4.22}$$

For a large system size $N \to \infty$, we apply the Stirling's approximation and assuming that the LDT principle holds, with the rate function $j(X)$,

$$\log[P(l/N = X)] \asymp -\beta N j(X) = -N[\log 2 + \frac{X}{\lambda}\log\left(\frac{X}{\lambda}\right) + (1 - \frac{X}{\lambda})\log(1 - \frac{X}{\lambda})] \tag{4.23}$$

Since there is an energy exchange between the entropic spring and its environment at inverse temperature $\beta$, the rate function $j(X)$ is a free energy per spring $f(X)$.

Free energy being an extensive quantity, the total free energy of the spring of length $l$ is

$$\mathcal{F}(l) = Nf(X)$$

We also notice that the minimum and zero of the rate function lies at $X = \lambda/2$, which implies that the most probable macro-state is the one for which $l = \lambda N/2$ as expected from the symmetry of the spring. The free energy of the spring around this equilibrium point, $l_0$ is hence

$$\mathcal{F}(l) \approx \frac{1}{2}\mathcal{F}''(l_0)(l - l_0)^2 = \frac{1}{l_0\lambda\beta}(l - l_0)^2$$

Given the free energy of the entropic spring around its equilibrium configuration, the total energy of the spring system is

$$E(x) = \frac{1}{l_0\lambda\beta}(l - l_0)^2 + \frac{1}{2}kx^2$$

Using the constraint equation $L = l + x_0 - x$, the energy in terms of the extension $x$ of the classical spring is

$$E(x) = A + B[x - C]^2 \tag{4.24}$$

where $A = \frac{(L - x_0 - l_0)^2}{\lambda\beta l_0}$, $B = (\frac{1}{\lambda\beta l_0} + \frac{1}{2}k)$ and $C = \frac{(x_0 + l_0 - L)}{\frac{\lambda\beta l_0 k}{2} + 1}$.

The total energy must be minimized around the equilibrium configuration of the system,

$$-\frac{d}{dx}E(x) = -2B[x - C] = 0$$

Hence, when the extension of the classical spring $x_{\text{eq}} = C$, the system is in equilibrium. The *statistical force* acting acting on the classical spring due to the fluctuations in the entropic spring is hence,

$$F_{\text{Stat}} = -kx_{\text{eq}} = -k\frac{(x_0 + l_0 - L)}{\frac{\lambda\beta l_0 k}{2} + 1} \tag{4.25}$$

This force pushes the entire system towards a minimum free energy configuration. Using this analysis we would try to lay down the meaning and few characteristics of *Statistical or Entropic forces* on which we would elaborate further in chapters ahead.

$F_{\text{Stat}}$ is called a Statistical or Entropic force. It has the following features which would be accepted in this text, as the defining features of a Statistical force.

1. The force is a **macroscopic force**, i.e. it acts *only* on a macroscopic scale and depends on the coupling between the micro and macro variables.

2. It essentially arises, because a system with numerous degrees of freedom (microstate) transitions between those microstates in such a way that the long-time behavior of the observables representing the system would tend to the macrostate with the most number of microstates corresponding to it. Hence, it seems that there is a force which pushes the system to macrostates with larger micro support. *In equilibrium, this force is hence proportional to the entropy gradient or the free-energy gradient.*

3. It can be attractive e.g. the elastic force in a polymer under stress or repulsive e.g. the repulsive forces between colloids in a **dense** bath of small particles.

If we consider the classical spring as a probe which is coupled to the entropic system, we can say something about the variance $\lambda$ in the length of each entropic spring. The statistical force is inversely proportional to the variance, since less is the variance, the less the system wishes to move away from its mean value.

The present model is an example of ***passive coupling*** between the entropic spring and the probe. As seen above, the equilibrium configuration of the entropic spring and probability of any configuration is independent of the extension of the probe $x$ coupled to it. Hence the probe is passive and does not influence the system. Reverse is not true. The equilibrium configuration of the probe, depends heavily on the configuration of the entropic spring.

# Chapter 5

# Entropic Forces

*To see a world in a grain of sand and a heaven in a wild flower, hold infinity in the palm of your hand and eternity in an hour.*

*- William Blake, Auguries of Innocence*

## 5.1 Introduction

**At sea on a windless day, in a strong swell free floating ships will roll heavily. It was believed in the days of the clipper ships that under those circumstances, two vessels at close distance will attract each other.**

Do they ? asked S. Boersma in A maritime analogy of the Casimir effect [17]. In a passage in The Mariner's Album, a handbook published in 1836, French nautical guru P.C. Causseé observed the following:

When two ships lie in close proximity on a rolling sea with little wind, then " une certaine force attractive " pulls the ships together causing them to collide. Treating the two ships as two Casimir plates in a fluctuating environment, Boersma concluded that this attractive force was very real and gave a closed expression for this force.

The crashing of ships is a dramatic manifestation of a force which in general

is coined as the *"Entropic force", "Statistical force" or "fluctuation-induced force".*[1]

There exist in nature several examples of fluctuation-induced forces and in the most diverse and unrelated areas. We discuss below few of them.

## 5.1.1 Granular matter: Depletion forces

Entropic force between macromolecules ($\mu m$ sized) in suspension is often produced by the addition of smaller particles to the background solvent. The binary mixture is of such nature that the difference in **size** or **shape** (spherical, rod shaped particles ) of the constituent particles, under the influence of thermal fluctuations, is a cause for the emergence of an entropically favored state of the system. This results in a net aggregation (attractive force) or repulsion of one of the species in the mixture.

### *Depletion model: Asakura & Oosawa (1954)*

For low concentrations of the smaller species in the mixture, Asakura and Oosawa, in 1954 proposed an *ideal gas approximation* [7] for particles. This model assumes a bidisperse hard core interaction between the large particles. The model predicts an effective attractive interaction between the larger particles in the mix, with the range of the force given by the smaller species diameter and the magnitude of the force of the order of the *osmotic pressure* of the solution of smaller species. The attractive force was shown to be stronger in solutions of chain shaped molecules or dissymmetrical molecules.

Around every large particle of radius $R$, there exists a *depletion region or excluded volume* which is slightly larger than its own volume and denotes a space within which the center of the smaller particles cannot lie. The free energy of the system decreases with the increase in volume fraction $\Delta V / V$ of the smaller particles. When two large particles come close to each other, a part of their excluded volumes merge, decreasing the net excluded volume of the system. The system evolves such that the small particles "push" two close enough large colloidal particles towards each other, to decrease the depletion region between them and in turn increasing their volume fraction.

The entropy $S$ of the mixture increases with the increase in the overlap volume $\Delta V$, hence decreasing the net free energy $\mathcal{F}$.

---

1. Physicist Fabrizio Pinto in an article in Nature argues that the whole story of attraction between ships is nothing more than the fact that "Physicists love lore about their own science," http://www.nature.com/news/2006/060501/full/news060501-7.html
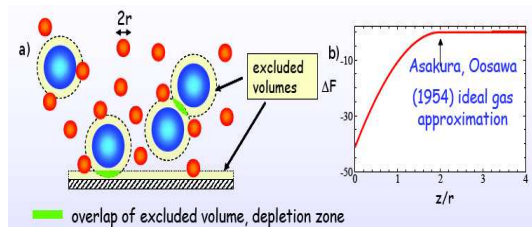
Figure 5.1: **a)** Two species red and blue separated by the excluded volumes (yellow) **b)** When the distance between the large particles is of the order of the radius of the small particles $r$, they experience an attractive force between each other. For distances much larger than $r$ the large particles are non-interacting. Figure reproduced from [13].

$$\Delta \mathcal{F} = \Delta U - T\Delta S = -Nk_B T\log(1 + \Delta V/V)$$

*Entropy leads to an effective attractive force between large particles, though all pair interactions are repulsive hard core.*

**Experiment:** In a direct experimental measurement of the entropic force between two colloidal particles in a suspension of smaller particles, Crocker et al. [29] immersed an isolated pair of PMMA spheres ($1100 \pm 15$nm diameter) in a background of 83nm of polystyrene beads. To this mixture was added some salt solution and surfactant to prevent colloidal aggregation. The only pair-wise interaction between the particles is a screened electrostatic repulsion, with a screening distance of $3nm$, which makes this interaction as good as hard sphere like.

The two PMMS spheres were threaded to each other with a *rod of light*. Optical tweezers were used to constrain the motion of the spheres along the line joining them. The motion is essentially confined to one-dimensions. Probability distribution of the relative distance between the two spheres $r$ was empirically obtained. This distribution was fitted to the Boltzmann's distribution:

$$P(r) \propto \mathrm{e}^{-\beta \mathcal{F}(r)}$$

$\mathcal{F}(r)$ is the free energy of the system when the distance between the large particles is $r$. The experiment was re conducted with different volume fractions of the small particles.
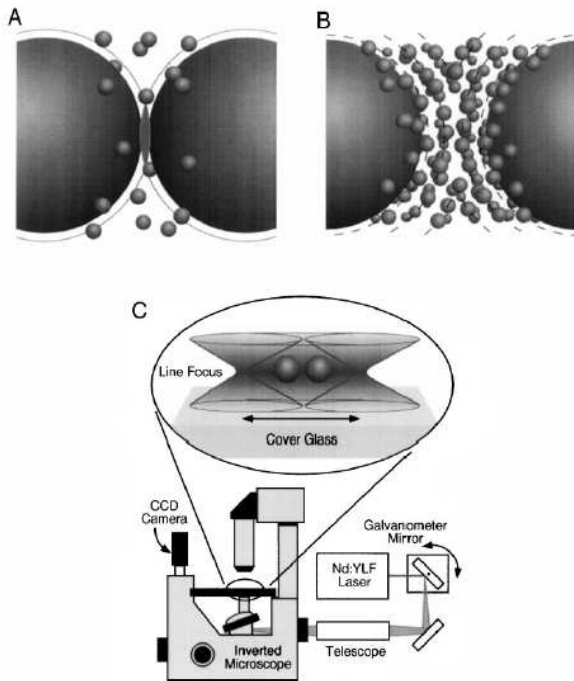
Figure 5.2: **A)** Each large sphere is surrounded by a depletion zone. **B)** At higher volume fractions, the small spheres form shells around the large spheres, analogous to the fluid layering near a flat wall. **C)** The threading of two large spheres using optical tweezers. The figure is reproduced from [29]

*Observations:* As displayed in plot 5.3

- A **strong attractive force**, in agreement with the A & O theory, was observed at short range and at low concentrations of the small particles.
- For volume fractions $\phi_s > 0.1$ of the small particles, a **repulsive force** at a distance of one small sphere diameter was observed. A very heuristic interpretation being that at high concentration of small particles, they squeeze between the colloidal particles and form a first level layer between them, if the gap between the spheres is commensurate with the layers, the free energy is lower (hence causing a repulsion); when the gap is incommensurate the free energy is higher.
- For volume fractions $\phi_s > 0.25$, the free energy $F(r)$ is oscillatory. The oscillation wavelength being inversely proportional to the volume fraction.
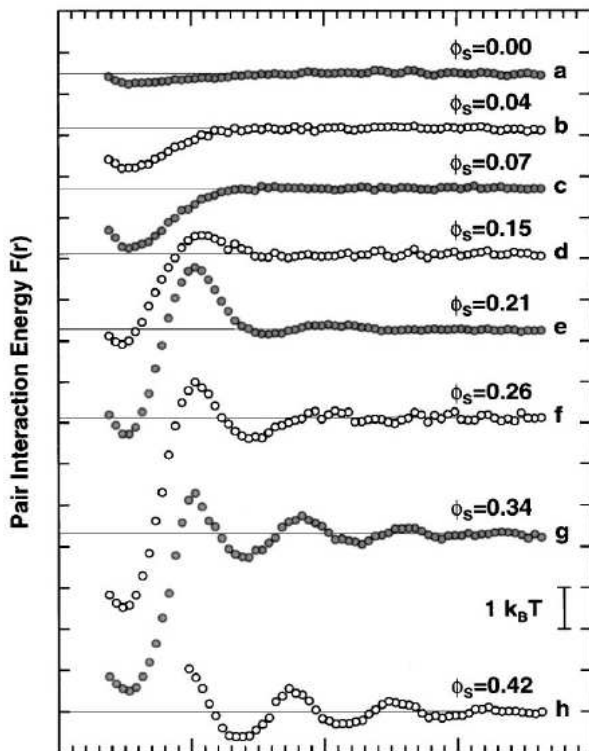
Figure 5.3: The entropic interaction potentials measured for small sphere volume fractions from 0 to 0.42. Curves b) and c) potential is monotonically attractive, according to the the Depletion Layer theory. Curves d) and e) a repulsive barrier forms. Curve f) onwards the potential becomes oscillatory. The figure is reproduced from [29].

## Applications of Depletion forces

The entropic depletion forces have several applications of scientific as well as industrial interest. Protein crystallization is exactly what it sounds like. It is a process in which supersaturated solution of biological macromolecules like protein, are prompted to form crystals. In presence of a certain seed protein, the molecules align themselves in a repeating series of unit cells with a consistent orientation. The protein crystals are used as a basis for X-ray crystallography of proteins, wherein an X-ray diffraction pattern is used to determine the three-dimensional tertiary structure of the protein. Entropic forces also slow down the reaction rates in concentrated macromolecular solutions and introduce many

metastable states in the depletion-induced colloidal crystals.

In industry, entropic forces can be used to reverse aggregate suspensions. and entropically stabilize colloidal which would otherwise aggregate.

## 5.2   A Generalized formalism

In the present section we propose a mathematical set-up through which one could derive statistical forces in some generality. We would especially like to discuss the nature of statistical forces, when the microscopic variables have a nonequilibrium dynamics. The present work displays some explorations into nonequilibrium statistical forces using some toy models alone. We display, using these toy models, the dependencies of the vector potential associated with the statistical forces on dynamical activity. There still remain several limitations in the present understanding of forces in general.

Another important aspect worth paying some attention to, is the **separation of time scales**. A significant point of difference between the microscopic or bath degrees of freedom and the macroscopic or probe degree of freedom is the difference in the time scale of their dynamics. The bath being the "fast" variables and the probe being the "slow" variable. On one end of the spectrum lies the infinitely separated time-scale of the bath and the probe. The other end of the spectrum is indeed when the bath and the probe have the same time scale. We would quantify the difference in time scale through a parameter $\gamma \gg 1$ or $\epsilon \ll 1$. Through tuning this parameter, we are able to display the influence of various scales of separation on statistical forces.

In the formalism presented below we focus our attention on processes in discrete state space evolving in continuous time. Hence, putting into use the machinery for Markov jump processes from Chapter 2.

### 5.2.1   Parameterization

We consider $H_t$, a jump process moving in a finite dimensional state space. This process is in general driven, which means that the dynamics does not satisfy detailed balance. The dynamics is itself open and coupled to reservoirs, which make a fluctuating environment. Very generally speaking, the effect of the fluctuating environment is incorporated in the following transition rates of

the process

$$k_\alpha(\eta, \eta') = \psi_\alpha(\eta, \eta') e^{s_\alpha(\eta, \eta')/2} \tag{5.1}$$

Here, $\psi(\eta, \eta') = \psi(\eta', \eta)$ is the symmetric prefactor, which in general is temperature dependent. $s(\eta, \eta') = -s(\eta', \eta)$ is an anti-symmetric function which in general is interpreted as the change in entropy of the environment as the system transitions from state $\eta$ to $\eta'$. We would refer to $\alpha$ as an "external", possibly time-dependent parameter which can be present in either or both the prefactor $\psi$ and the entropy change $s$. The real meaning of this parameter would become clear further.

In case of detailed balance, for the system in contact with one thermal bath at inverse temperature $\beta$, the change in entropy is related to the system energy $U_\alpha$ in the following manner

$$s_\alpha(\eta, \eta') = \beta[U_\alpha(\eta) - U_\alpha(\eta')]$$

Hence, the resulting detailed balance rates are

$$k_\alpha^{\mathrm{eq}}(\eta, \eta') = \psi(\eta, \eta') e^{-\frac{\beta}{2}[U_\alpha(\eta') - U_\alpha(\eta)]} \tag{5.2}$$

$$= e^{a\beta\Delta_\alpha(\eta, \eta') + b\beta U_\alpha(\eta)} \tag{5.3}$$

We have rewritten the transition rates above in form of the Arrehenius rates discussed in Chapter 2. Jumps are occurring between metastable states $\eta$ and $\eta'$, well separated by energy barriers $\Delta_\alpha(\eta, \eta') = \Delta_\alpha(\eta', \eta)$. Factors $a$ and $b$ in the exponential are parameters which signify the relative strength and coupling between various intensive variables.

In case when the microscopic dynamics is driven by a non-conservative force there is an additional entropy flux $F(\eta, \eta') = -F(\eta', \eta)$. A useful parametrization becomes,

$$k_\alpha(\eta, \eta') = e^{a\beta\Delta_\alpha(\eta, \eta') + b\beta U_\alpha(\eta) + \beta c F(\eta, \eta')/2} \tag{5.4}$$

Once we have established the transition rates for the process, a point of interest is the information we can extract from here regarding the macroscopic

variables and observables. Statistical forces have been argued to be macroscopic forces and hence to understand their origins in general one has to study the connections between statistical physics and thermodynamics. In equilibrium statistical physics, these connections are well established. We have also displayed in the previous chapters aspects of the large deviation rate functions, their origin in fluctuations of microscopic variables and their interpretation in terms of thermodynamic variables such as free energy and relative entropy. We reveal further more of such connections which would later be instrumental in extending our understanding into driven systems.

## 5.3 Adding the probe

To the microscopic dynamics thus defined by the $H-$ process, we introduce a probing system with its own dynamics. At first we would call "the probe" all those degrees of freedom which are coupled to the $H-$ process and the environment. Later we ask whether we can reconstruct (aspects of the ) $H-$ process from its action on other variables. It would of course be overly ambitious to try to recover the entire bath dynamics, say to the level of the transition rates of the individual jumps. And of course, depending on what we want to know, different probes could be used.

The probe here is a process $X_t$ again to be modeled as a jump process which is influenced by the $H-$ process.

### Active-Passive probes

The coupling between the system and the probe is essentially of two kinds: **Active or Passive**. An active coupling is such that the probe is influenced by and in turn influences the $H-$ process. In other words, there exists a feedback from the probe $(X-)$ process to the bath $(H-)$ process.

Here, the coupling between the probe and the bath is defined exactly via parameter $\alpha$. The transition rates for the probe are

$$r_\alpha(x, x') = z_\alpha(x, x') e^{\frac{\beta}{2}[h(\eta,x) - h(\eta,x')]} \tag{5.5}$$

for the transition from $x$ to $x'$ with symmetric pre-factor $z_\alpha(x, x') = z_\alpha(x', x)$ and joint potential $h(\eta, x)$ mediated at inverse temperature $\beta$. A natural choice is then to assume that $\alpha$ in the $H-$ process takes the same value as the $X$, or

$$U_\alpha(\eta) = h(\eta, x), \ \alpha = x$$

In other words, for an active probe, we really have a joint Markov process $(H_t, X_t)$ with jump rates

$$k_x(\eta, \eta') = e^{a\beta\Delta_x(\eta,\eta')+b\beta h(\eta,x)+c\beta F(\eta,\eta')/2}, \ r_\eta(x, x') = z(x, x')e^{\frac{\beta}{2}[h(\eta,x)-h(\eta,x')]}$$

(5.6)

A passive probe would on other hand be such that the bath dynamics does not depend on the state of the probe.

$$h(\eta, x) - h(\eta', x) = \tilde{h}(\eta) - \tilde{h}(\eta') \text{ and } \Delta_x(\eta, \eta') = \Delta(\eta, \eta')$$

## 5.3.1 Scaling of the microscopic dynamics

We are interested in the effective dynamics of the probe, where the bath dynamics is averaged out. Mostly this is done by assuming that the bath degrees of freedom evolve much faster than the probe degree of freedom, e.g. the probe is much heavier than the bath particles. In these cases we speak of systems with separation of time scales of fast $\eta$ and slow $x$ degrees of freedom. In this section we present some formal techniques to understand the time separation in a systematic manner. We restrict ourselves to the Markovian systems and we will examine the effective dynamics of slow degrees of freedom using the projection operators. This work is a result of collaboration with J. Pešek, and K. Netočný.

The joint probability density which defines the coupled system is $\mu_t(\eta, x)$. We describe the time evolution of our system by the forward generator $L_\epsilon^\dagger$.

$$\partial_t \mu_t(x, \eta) = L_\epsilon^\dagger[\mu_t](x, \eta)$$

(5.7)

For a Markov jump process, where the symmetric part of the jump rates of the fast degrees of freedom are scaled by $\epsilon^{-1}$, i.e.

$$k[(\eta, x); (\eta', x)] = \frac{1}{\epsilon}k(\eta; \eta'); \ r[(\eta, x); (\eta, x')] = r(x, x')$$

For the joint generator of such a process, we choose the following scaling:

$$L_\epsilon^\dagger = L_S^\dagger + \frac{1}{\epsilon}L_F^\dagger \tag{5.8}$$

where $L_S^\dagger$ acts only upon slow degrees of freedom and $L_F^\dagger$ acts only upon fast degrees of freedom.

Our goal is to find an evolution equation for reduced density for slow variables

$$\nu_t(x) = \sum_\eta \mu_t(\eta, x). \tag{5.9}$$

We further assume that there exists a unique stationary distribution of fast degrees of freedom conditioned on the slow ones $\rho_F(\eta)$ to which the fast degrees of freedoms tends to converge, i.e. we fix the slow degrees of freedom and we are searching for stationary density of overall generator $L_\epsilon^\dagger$ restricted only on the fast variables as $\epsilon \to 0^+$. Under this assumption we can define the projection operator $\mathcal{P}$ as follows:

$$\mathcal{P}\left[\mu\right](\eta, x) = \rho_F(\eta) \sum_\eta \mu(\eta, x) \tag{5.10}$$

The condition of the existence of unique stationary state $\rho_F$ for fast degrees of freedom with respect to slow degrees of freedom fixed at some value reduces to the condition of existence of unique solution of equation

$$L_F^\dagger[\rho_F] = 0.$$

The properties of the generator acting upon fast degrees of freedom can be then summarized as

$$\mathcal{P}^2 = \mathcal{P}, \tag{5.11a}$$

$$L_F^\dagger \mathcal{P} = 0, \tag{5.11b}$$

$$\mathcal{P} L_F^\dagger = 0. \tag{5.11c}$$

These properties can very easily be verified by applying the definitions of the projection operator and the action of the generator $L_F^\dagger$.

We use (5.10) to split the time evolution (5.7) to the time evolution of projected density $\mathcal{P}[\mu_t]$ and the rest $(1 - \mathcal{P})[\mu_t]$

$$\partial_t \mathcal{P}[\mu_t] = \mathcal{P} L_\epsilon^\dagger \mathcal{P}[\mu_t] + \mathcal{P} L_\epsilon^\dagger (1 - \mathcal{P})[\mu_t], \tag{5.12}$$

$$\partial_t (1 - \mathcal{P})[\mu_t] = (1 - \mathcal{P}) L_\epsilon^\dagger (1 - \mathcal{P})[\mu_t] + (1 - \mathcal{P}) L_\epsilon^\dagger \mathcal{P}[\mu_t].$$

We formally solve the later equation

$$(1 - \mathcal{P})[\mu_t] = \int_0^t \mathrm{d}t' \, \mathrm{e}^{(t-t')(1-\mathcal{P})L_\epsilon^\dagger(1-\mathcal{P})}(1 - \mathcal{P}) L_\epsilon^\dagger \mathcal{P}[\mu_{t'}]$$

$$+ \, \mathrm{e}^{t(1-\mathcal{P})L_\epsilon^\dagger(1-\mathcal{P})}(1 - \mathcal{P})[\mu_0], \tag{5.13}$$

and insert the solution in equation (5.12). Integrating over the fast degrees of freedom, assuming that the initial state of the system was uncorrelated (i.e. $\mu_0(\eta, x) = \nu_0(x)\rho_F(\eta)$), we obtain an effective time evolution for the slow degrees of freedom

$$\partial_t \nu_t(x) = \sum_\eta L_\epsilon^\dagger [\nu_t \rho_F] + \int_0^t \mathrm{d}t' \sum_\eta L_\epsilon^\dagger \mathrm{e}^{(t-t')(1-\mathcal{P})L_\epsilon^\dagger(1-\mathcal{P})}(1 - \mathcal{P}) L_\epsilon^\dagger [\nu_{t'} \rho_F]$$

$$\tag{5.14}$$

Now we would like to do an expansion in $\epsilon$ as $\epsilon \to 0^+$ up to lowest order and derive what will be later defined as the fluid limit of the bath.

Inserting the total generator (5.8) together with the properties (5.11b), (5.11c) to the effective evolution equation (5.14) we obtain

$$\partial_t \nu_t(x) = \sum_\eta L_S^\dagger [\nu_t \rho_F] + \int_0^t \mathrm{d}t' \sum_\eta L_S^\dagger e^{(t-t')\left[\frac{1}{\epsilon}L_F^\dagger + (1-\mathcal{P})L_S^\dagger(1-\mathcal{P})\right]}(1-\mathcal{P})L_S^\dagger [\nu_{t'} \rho_F]$$

(5.15)

which can be expanded in $\epsilon$ using Laplace transform. Upto first order in $\epsilon$ we present the result for the effective generator for slow degrees of freedom:

$$\partial_t \nu_t(x) = \sum_\eta L_S^\dagger [\nu_t \rho_F] - \epsilon \sum_\eta L_S^\dagger \frac{1}{L_F^\dagger} L_S^\dagger [\nu_{t'} \rho_F] + O(\epsilon^2),$$

(5.16)

The memory in the lowest order of $\epsilon$ is only present in the time integration over all time, hidden in pseudo-inverse [19] defined as

$$\frac{1}{L_F^\dagger} = \int_0^\infty \mathrm{d}t \left[\mathcal{P} - e^{tL_F^\dagger}\right],$$

For the purposes of the results which we pursue in the fluid limit, the results upto zeroth order in $\epsilon$ are sufficient. We do not elaborate here on the first order correction but merely state the result for future use.

In the fluid limit ($\epsilon \to 0$) an effective generator, $L_{\text{eff}}^\dagger$ governing the effective slow dynamics of $x$, once all the fast degrees of freedom have been integrated out, is defined as

$$\partial_t \nu_t(x) = \sum_\eta L_S^\dagger [\nu_t \rho_F]$$

(5.17)

$$:= L_{\text{eff}}^\dagger [\nu_t(x)]$$

(5.18)

### 5.3.2 Effective dynamics of the probe

**Effective rates**

In order to derive an effective dynamics of the probe, we start with the fluid limit assumption. The action of the effective generator $L_{\text{eff}}^\dagger$ is presented below

$$L_{\text{eff}}^{\dagger}[\nu(x)] \;\; = \;\; \sum_{\eta} \left[ \sum_{x'} [\nu(x')r_{\eta}(x',x) - \nu(x)r_{\eta}(x,x')]\rho_F(\eta) \right]$$

$$= \;\; \sum_{x'} \left[ \nu(x') \sum_{\eta} r_{\eta}(x',x)\rho_F(\eta) - \nu(x) \sum_{\eta} r_{\eta}(x,x')\rho_F(\eta) \right]$$

$$= \;\; \sum_{x'} [\nu(x')\chi(x',x) - \nu(x)\chi(x,x')] \qquad (5.19)$$

where

$$\chi(x,x') := \sum_{\eta} \rho_F(\eta)r_{\eta}(x,x')$$

are the effective rates governing the dynamics of the probe in the fluid limit.

Other aspects of the bath dynamics, which carry over information into the effective motion of the probe are the so called large deviation rate functions, called short fluctuation functionals. With the help of examples, we will show that some of them like the **Information potential** or **Stationary potential**

$$\varphi(\eta,x) := -\log\left(\rho_F(\eta)\right)$$

do not appear in the effective dynamics in equilibrium. $\rho_F(\eta)$ is the stationary state of the bath process for a fixed state of the probe $x$. We wish to explore, whether this fluctuation functional plays any role in the effective dynamics, in case of nonequilibrium.

On the other hand, as shown below, the slow dynamics in detailed balance evolves along the gradient of the **Generalized free energy**.

$$\mathcal{F}(x) := \sum_{\eta} \rho_F(\eta|x) \left[ h(\eta,x) - \frac{1}{\beta}\varphi(\eta,x) \right] \qquad (5.20)$$

Again, we would like to explore the role of $\mathcal{F}$ out of equilibrium.

**Stationary escape rate**

For dynamical fluctuations such as current fluctuations we do not have sufficient structure in the generally defined $H-$ process, though current fluctuations are

related to aspects of dynamical activity. One important such aspect is the stationary escape rate

$$e(x) := \sum_{\eta, \eta'} \rho_F(\eta|x) k(\eta, \eta') \tag{5.21}$$

It features prominently in the Donsker-Varadhan fluctuation functionals for the occupation times

$$P_x \left( \frac{1}{T} \int_0^T dt \, \delta_{H_t, \eta} = \pi(\eta) \; \forall \eta \right) \asymp e^{-T\mathcal{D}_x(\pi)}$$

in the sense of large deviations for $T \gg 1$. $H_t$ is the state of the fast variable at time $t$.

The functional $\mathcal{D}_x$ is the difference between expected rates

$$\mathcal{D}_x(\pi) = \sum_{\eta} \pi(\eta)[\xi_x(\eta) - \xi_x^V(\eta)], \; \xi_x(\eta) := \sum_{\eta'} k_x(\eta, \eta')$$

More precisely,

$$\xi_x^V(\eta) := \sum_{\eta'} k_x^V(\eta, \eta'), \; k_x^V(\eta, \eta') := k_x(\eta, \eta') e^{[V(\eta) - V(\eta')]/2}$$

with the potential $V$ depending on $\pi$ such that $\pi$ is the stationary distribution for the process with rates $k_x^V(\eta, \eta')$, see e.g. [31].

Obviously, the parameters $a, b, c$ enter the aspects $\varphi(\eta, x)$ and $\xi_x$ or $\mathcal{F}(x)$ and $e(x)$. These parameters will thus help in understanding the general dependencies.

### 5.3.3  Reconstruction in case of equilibrium

Given the above set-up we reiterate our original aim: to reconstruct aspects of the bath by observing the effective behavior of the probe, to study the nature of the statistical force on the probe and its dependence on bath dynamics. We would like to begin the analysis in the case when the bath dynamics is detailed balance. To this effect we assign the parameter $c = 0$.

In equilibrium the effective rates reduce to

$$\chi(x, x') = \frac{1}{Z_\beta(x)} \omega(x, x')$$

where the symmetric function $\omega(x, x') = \sum_{\eta \in \Gamma} z_\eta(x, x') \mathrm{e}^{-\beta[U(\eta,x)+U(\eta,x')]/2}$.

The ratio between the forward and reverse rates is hence

$$\frac{\chi(x, x')}{\chi(x', x)} = \frac{Z(x')}{Z(x)}$$

The equilibrium distribution $\rho_F(\eta|x)$ reduces to a canonical Gibbs distribution.

$$\rho_F(\eta|x) = \frac{\mathrm{e}^{-\beta h(\eta, x)}}{Z_\beta(x)}$$

where $Z_\beta(x) = \sum_\eta \mathrm{e}^{-\beta h(\eta, x)}$ is the partition function.

The **generalized free energy** $\mathcal{F}$ defined in equation (5.20), in equilibrium thus reduces to

$$\mathcal{F}^{\mathrm{eq}}(x) = -\frac{1}{\beta} \log Z_\beta(x) \tag{5.22}$$

Deriving inspiration from thermodynamics, **the statistical force** $F_{\mathrm{Stat}}$ on the probe, is defined as a change in the conservative potential:

$$
\begin{aligned}
F_{\mathrm{Stat}}(x, x') &= -[V(x') - V(x)] \\
&= -[\mathcal{F}^{\mathrm{eq}}(x') - \mathcal{F}^{\mathrm{eq}}(x)] \tag{5.23} \\
&= \frac{1}{\beta} \log \left[ \frac{Z(x')}{Z(x)} \right] \tag{5.24}
\end{aligned}
$$

On the other hand, from local detailed balance, the ratio of the effective rates

$$\frac{\chi(x, x')}{\chi(x', x)} = e^{s(x, x')} \tag{5.25}$$

where $s(x, x')$ is the total entropy flux into the environment, which in equilibrium is simply equal to the change in the free energy of the system.

Hence in general, the **statistical force** on the probe is defined as follows:

$$F_{\text{Stat}}(x, x') := \frac{1}{\beta} \log \left[ \frac{\chi(x, x')}{\chi(x', x)} \right] \tag{5.26}$$

This definition would hold, also when the bath dynamics is not detailed balance, though we would see in this case that the statistical force would no longer be defined only terms of a scalar potential $V$. An additional vector potential would enter the picture.

## 5.3.4 Extension into nonequilibrium

When detailed balance in the bath dynamics is broken, in general it is expected that the effective dynamics of the probe would also lose its detailed balance, unless there exist some hidden symmetries in the dynamics which uphold detailed balance in the dynamics of the probe. Otherwise, the statistical force would no longer remain conservative. The non conservative or rotational component of the force would result in a non-zero current in the probe state space. We are interested to see what factors govern the strength and direction of the statistical force. Also, by observing the nature of the current can we extrapolate the nature of the nonequilibrium forcing in the bath ? What is the role of the dynamical fluctuation functionals in the nature of this force ?

To start with, we lift the constraint $c = 0$, which makes the $H-$ process non-detailed balance. The statistical force from (5.26) is:

$$F_{\text{Stat}} := \frac{1}{\beta} \log \left[ \frac{\chi(x, x')}{\chi(x', x)} \right]$$

Using, the stationary distribution $\rho_F(\eta)$, the effective rates $\chi(x, x')$ can be calculated.

The statistical force can be decomposed as a sum of gradient and non-gradient parts:

$$F_{\text{Stat}}(x, x') = V(x) - V(x') + \mathcal{A}(x, x')$$

where the antisymmetric function $\mathcal{A}(x, x') = -\mathcal{A}(x', x)$ is the rotational part of the force.

The conservative potential $V(x)$ is only defined upto a constant $C$. Hence we can impose an additional constraint to completely specify its value.

$$\sum_{x \in \Gamma'} V(x) = 0$$

This fixes the constant as $C = -\sum_{x \in \Gamma'} V(x)/3$. Since $V(x) - V(x')$ is the conservative part of the force, the work done by this force over a complete cycle is zero.

This naturally implies that the statistical force summed over a whole cycle is

$$\sum_{x, x' \in \Gamma'} F_{\text{Stat}}(x, x') = \sum_{x, x' \in \Gamma'} \mathcal{A}(x, x')$$

Again, since the vector potential defining this non-gradient force is determined only uptil the gradient of a scalar $\nabla\lambda$. We demand that norm of the non-gradient force

$$\|\mathcal{A}(x, x')\|^2 = \sum_{x, x' \in \Gamma'} \mathcal{A}(x, x')^2$$

is minimized.

With the help of these constraints we obtain the gradient and non-gradient parts of the force uniquely.

$$V(x) \quad = \quad \frac{1}{2n} \sum_{x \neq x'} [F_{\text{Stat}}(x, x') - F_{\text{Stat}}(x', x)] \tag{5.27}$$

$$\mathcal{A}(x, x') \quad = \quad F_{\text{Stat}}(x, x') - [V(x) - V(x')] \tag{5.28}$$

where $n$ is the number of states is the state space of the probe.

Using these expressions we derive the conservative and non-conservative parts of the force.

Given that now we have some general expressions in equilibrium and nonequilibrium, we can construct a toy model to explore the nature of these forces and potentials like the generalized free energy and the stationary escape rate.

## 5.3.5   Example: A three-state discrete model

To illustrate and further understand such ideas as discussed above, we introduce a simple Markov jump process with two coupled systems. Both processes $H$ and $X$ are defined on the discrete state space $\Gamma, \Gamma' : \{-1, 0, 1\}$. We use the parametrization already set in place in Section 5.2.1. The symbols used correspond to the definitions in that section.

The dynamics of the bath is governed by the potential $U(\eta, x) = x\eta$, which gives rise to a force on the bath and the probe which depends on the state of the probe and the bath respectively. On top an external non-conservative force $f(\eta, \eta')$ is applied on the bath. A constant force is non-conservative when the state space being acted upon is a circle since it cannot be written as a gradient of a potential [19].

The transition rates for the bath dynamics are

$$k_x(\eta, \eta') = \gamma \mathrm{e}^{-\frac{a}{2}[bx(\eta+\eta')]+b\eta x+\frac{c}{2}f(\eta,\eta')} \tag{5.29}$$

The inverse temperature $\beta$ is assumed to be 1. $\gamma \gg 1$ is the parameter which makes the bath dynamics much faster than the probe dynamics. The force $f(\eta, \eta')$ drives the bath in a cyclic fashion $1 \to 0 \to -1$ (named clockwise) with a constant driving $f$ and in the anti-clockwise direction with driving $-f$.

The probe $X$ is **active**. Its dynamics is detailed balance and is governed by the rates

$$r_\eta(x, x') = z_\eta(x, x')\mathrm{e}^{\eta(x-x')/2} \tag{5.30}$$

The symmetric pre-factor $z_\eta(x, x')$ re-enforces the coupling between the bath and the probe.

$$
\begin{aligned}
z_\eta(x, x') &= 1; \ \eta = 1, 0 \\
&= 0; \ \eta = -1
\end{aligned}
\tag{5.31}
$$

**In Equilibrium**

Given this setup we first analyse the situation when the $H$ dynamics is detailed balance. To this effect we select parameter $c = 0$ and show how to determine the free energy of the $H-$process from monitoring the dynamics of the probe.

The detailed balance solution of the Master equation for the $X$ dynamics with rates $k_x(\eta, \eta')$ is

$$
\rho_F^{\text{eq}}(1) = \frac{1}{1 + e^{bx} + e^{2bx}}; \ \rho_F^{\text{eq}}(-1) = \frac{e^{2bx}}{1 + e^{bx} + e^{2bx}} \ ; \rho_F^{\text{eq}}(0) = \frac{e^{bx}}{1 + e^{bx} + e^{2bx}}
$$

As can be seen, the equilibrium state for $x = -1$ is at $\eta = 1$ and for $x = 1$ is at $\eta = -1$. For $x = 0$ all states are equally probable.

Using (5.23), the ratio of the effective rates for the integrated out dynamics of the probe is given by

$$
\frac{\chi(x, x')}{\chi(x', x)} = \frac{1 + 2 \cosh[bx']}{1 + 2 \cosh[bx]}
\tag{5.32}
$$

We use the effective dynamics, to calculate the statistical force $F_{\text{Stat}}(x, x')$ on the probe, (5.26). This force can be written down as a difference

$$
\begin{aligned}
F_{\text{Stat}}(x, x') &= -\log\left(\frac{1 + 2 \cosh[bx]}{1 + 2 \cosh[bx']}\right) \\
&= -[V(x') - V(x)]
\end{aligned}
\tag{5.33}
$$

The statistical force, in equilibrium, moves the system along the gradient of the free energy landscape. The free energy or the generalized free energy (since this is an effective dynamics) of the $H-$ process is hence

$$
\mathcal{F}^{\text{eq}}(x) = V(x) = -\log(1 + 2 \cosh[bx])
\tag{5.34}
$$

In equilibrium, the effective dynamics depends on the terms which constitute the anti-symmetric part of the rate function, $h(\eta, x) - h(\eta', x)$. This is evident by the presence of variable $b$ alone. There is no influence of the symmetric escape rates, $\Delta_x(\eta, \eta')$, which are flagged by variable $a$.

## Breaking detailed balance

To continue we wish to go further into more interesting and richer realm of non-equilibrium. By measuring the current in the probe state space, we can have an ambition to predict the nature of non-equilibrium forces in the "sea" itself. To take this model into non-equilibrium we lift the constraint that $c = 0$ from the $H$ dynamics, which makes it non-detailed balance.

In non-equilibrium, the stationary solution of the Master equation for the $H$ dynamics renders

$$Z_x = e^{cf} + e^{2cf} \left[ e^{ax} + e^{bx} \right] + e^{ax/2} + e^{2bx} + e^{(a+b)x} + e^{cf+ax/2+bx} \left( 1 + e^{cf+bx} + e^{ax/2+bx} \right)$$

$$\rho_x(1) = \frac{e^{cf} + e^{(ax)/2} + e^{2cf+ax}}{Z_x}$$

$$\rho_x(-1) = \frac{e^{2bx}(1 + e^{2cf+(ax)/2} + e^{cf+ax})}{Z_x}$$

$$\rho_x(0) = \frac{e^{bx}(e^{2cf} + e^{ax} + e^{cf+(ax)/2})}{Z_x}$$

Before we move on, one interesting point which is to be noted is that unlike in diffusion where with increasing driving the stationary distribution of a particle on a ring tends to the uniform distribution, for the jump processes the stationary distribution, at very large driving, is not uniform anymore, nor is it independent of the conservative potential. In diffusion the influence of the

potential becomes smaller and smaller as the non gradient force increases and the probability to stay in any part of the ring becomes the same. For jump processes on the hand, since the transition rates depend on the exponential of the potential, even as $f$ becomes large, the dynamics continues to depend on the potential as well. This fact is illustrated in the plot 5.4.
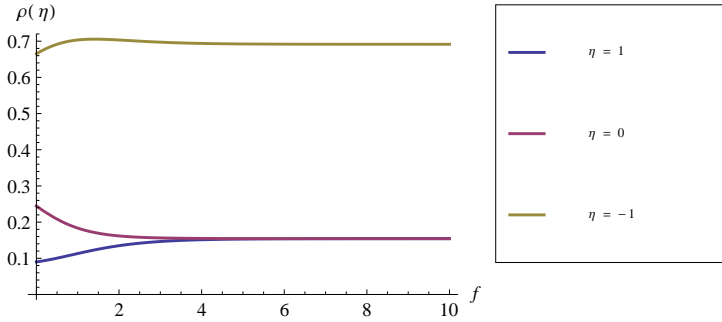


Figure 5.4: Stationary distribution $\rho(\eta)$ vs $f$.
Parameter values $a = b = c = x = 1$

As f goes to infinity, for $c = 1$, the stationary distributions are:

$$\lim_{f \to \infty} \rho_x(1) = \frac{e^{ax}}{\left(e^{ax} + e^{bx} + e^{1/2(a+4b)x}\right)}$$

$$\lim_{f \to \infty} \rho_x(-1) = \frac{e^{1/2(a+4b)x}}{\left(e^{ax} + e^{bx} + e^{1/2(a+4b)x}\right)}$$

$$\lim_{f \to \infty} \rho_x(0) = \frac{e^{bx}}{\left(e^{ax} + e^{bx} + e^{1/2(a+4b)x}\right)}$$

## Average stationary potential

Moving on, we illustrate the various dependencies of the average stationary potential $\varphi_{\text{avg}} = \sum_{\eta=-1}^{1} \rho_x(\eta)\varphi(\eta)$ and the generalized free energy in nonequilibrium on parameters $a$, $b$, $c$. We show the variation of $\varphi_{\text{avg}}$ with the nonequilibrium driving, plot 5.5 and it is seen that as $f$ increases $\varphi_{\text{avg}}$ tends to the same value as in equilibrium, for $a = 1$. Dependence of $\varphi_{\text{avg}}$ on $a$ is studied in plot 5.6
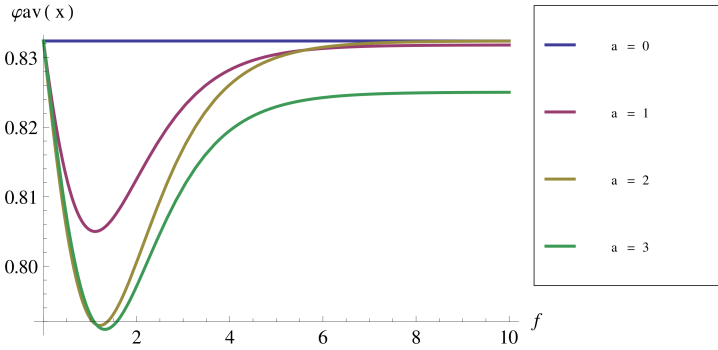


Figure 5.5: The average of stationary potential vs $f$.
Parameter values $b = c = x = 1$
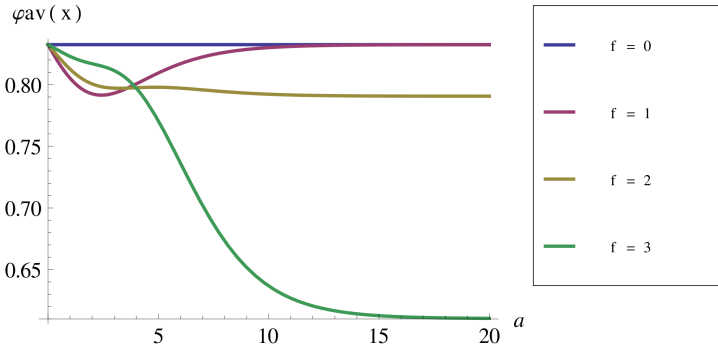


Figure 5.6: The average of stationary potential vs $a$.
Parameter values $b = c = x = 1$

## Stationary escape rate

The stationary escape rate $e(x) = \sum\limits_{\eta=-1}^{1} \rho_x(\eta)\xi(\eta)$, where $\xi(\eta)$ is the escape rate of the fast dynamics, upto linear order in $f$ is:

$$
\begin{aligned}
e(x) &= \frac{\gamma \left(1 + 2 \, \cosh\left[\frac{ax}{2}\right]\right)^2}{1 + 2 \, \cosh[bx]} \\[2mm]
&\quad - \frac{ce^{(-a+b)x}e^{ax/2} \left(1 + 2 \, \cosh\left[\frac{ax}{2}\right]\right) \left(1 - 3e^{\frac{ax}{2}} + 3e^{ax} + 3e^{bx} - e^{2bx}\right) \gamma f}{2e^{2bx} \left(1 + 2 \, \cosh[bx]\right)^2} \\[2mm]
&\quad - \frac{c \left(1 + 2 \, \cosh\left[\frac{ax}{2}\right]\right) \left(e^{\frac{ax}{2}} + e^{\left(\frac{a}{2}+b\right)x} + e^{bx} - 1\right) \gamma f}{2 \left(1 + 2 \, \cosh[bx]\right)^2} \\[2mm]
&\quad + O[f]^2
\end{aligned}
\tag{5.35}
$$

Its variation with $f$ is shown in plot 5.7



Figure 5.7: Stationary escape rate, a factor governing the dynamical fluctuations vs $f$. Parameter values $b = c = x = 1$

## Stationary distribution of the effective dynamics

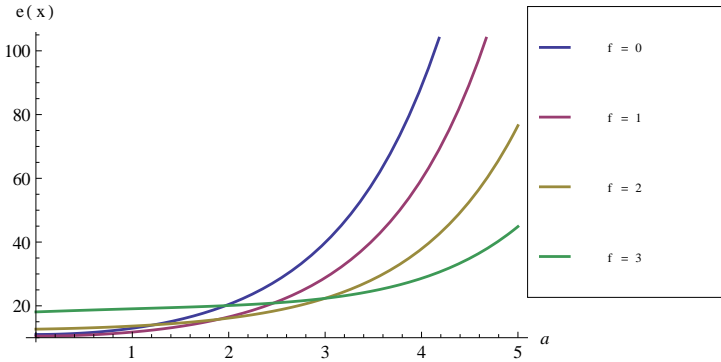The stationary distribution $\nu(x)$ of the probe is plotted above. The stationary distribution is of course different from its equilibrium form. What is interesting to see is that the state of maximal occupation changes with $f$ and $a$. In equilibrium there is a degeneracy between states $x = \pm 1$, which were both equally maximally occupied. This degeneracy is lifted in nonequilibrium. In the plots 5.8, 5.9, 5.10 we see that the distribution function varies as a function of $f$ for small $f$. For all three states, above $f = 4$, the distribution saturates (to different values for different $a$). We will see below in the analysis of the effective forces, the reason behind this saturation.



Figure 5.8: Stationary distribution of the effective slow d.o.f, $\nu(x)$ vs $a$, the part of the rates governing kinetics. Parameter values $b = c = f = 1$
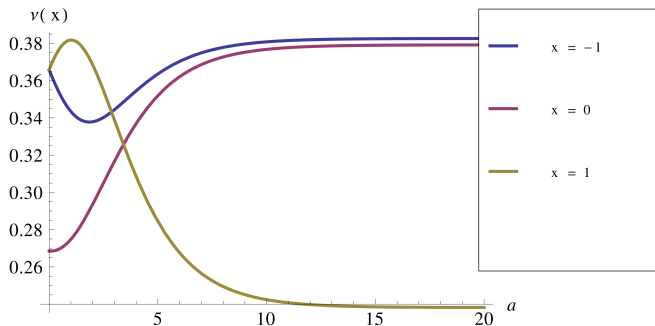


Figure 5.9: Stationary distribution of the effective slow d.o.f, $\nu(x)$ vs $a$, the part of the rates governing kinetics. Parameter values $b = c = 1$, $f = 2$
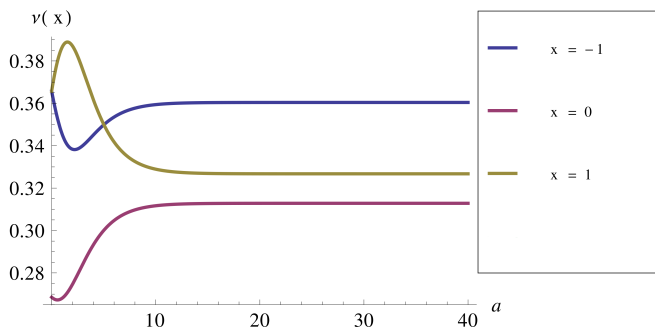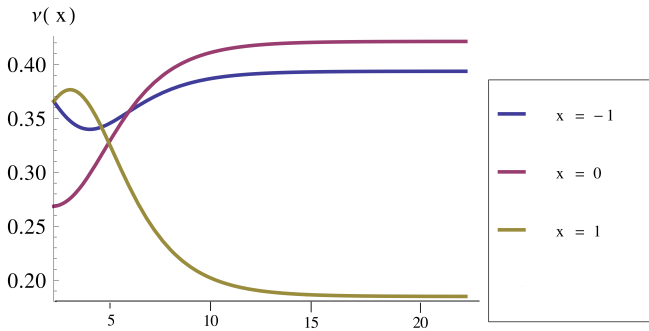
Figure 5.10: Stationary distribution of the effective slow d.o.f, $\nu(x)$ vs $a$, the part of the rates governing kinetics. Parameter values $b = c = 1$, $f = 3$

## The nature and direction of the statistical force

The Statistical force $F_{\text{Stat}}(x, x')$ is calculated using (5.26). The direction of this force can be determined by determining the sign of a quantity called the Netforce, NetF:

$$\text{NetF} = F_{\text{Stat}}[1, 0] + F_{\text{Stat}}[0, -1] + F_{\text{Stat}}[-1, 1] - F_{\text{Stat}}[1, -1] - F_{\text{Stat}}[-1, 0] - F_{\text{Stat}}[0, 1]$$

This quantity is basically the difference between the non-gradient force $A(x, x')$ in the clockwise and anti-clockwise directions. Upto linear order in $f$ it is given as:

$$\text{NetF} = -\frac{4\left(c \sinh\left[\frac{a}{4}\right]^2 \tanh\left[\frac{b}{4}\right]\right) f}{1 + 2\cosh\left[\frac{a}{2}\right]} + \text{O}[f]^2$$

For $cf > 0$, this force acts in the anti-clockwise direction.

We use (5.27) to arrive at the expressions for the gradient and the non-gradient parts of the force themselves. The non-gradient forcing upto second order in $f$ is given by
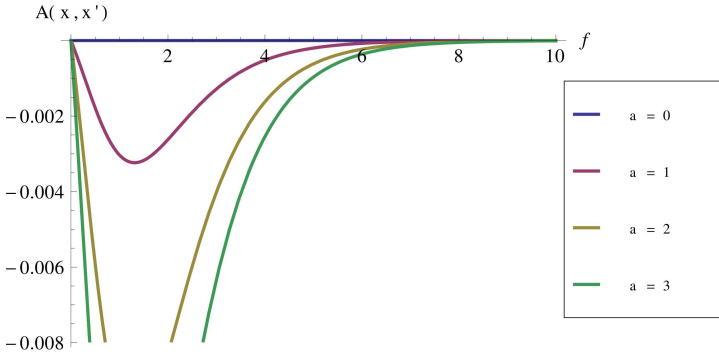
Figure 5.11: Statistical non-gradient force $A(1,0)$ vs $f$.
Parameter values $b = c = x = 1$, $x' = 0$

$$A(1,0) = -\frac{2\left(-1+\sqrt{e}\right)\,\sinh\left[\frac{a}{4}\right]^2 f}{3\left(1+\sqrt{e}\right)\left(1+2\,\cosh\left[\frac{a}{2}\right]\right)} \tag{5.36}$$

$$-\frac{\sinh\left[\frac{a}{4}\right]^2\left(-1+e+\left(-1+\sqrt{e}\right)^2\,\sinh\left[\frac{a}{2}\right]\right)f^2}{\left(1+\sqrt{e}\right)^2\left(1+2\,\cosh\left[\frac{a}{2}\right]\right)^2}+\mathrm{O}[f]^3$$

Its behavior is plotted in 5.11

It is clear seen as $f$ goes to infinity, the nonconservative force goes to 0. With increasing values of escape rates, the non-conservative force rises, which is understandable since, if the $H$ system escapes easily from its current state then the magnitude of the nonequilibrium current would also rise and hence the net force on the probe as well.

The gradient part of the force for $x = 1$, $V(x)$ (upto linear order in $f$) is shown in Fig 5.12.
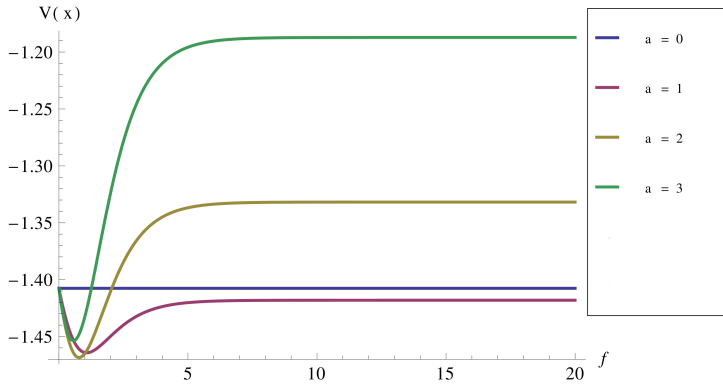
Figure 5.12: Statistical gradient force $V(1)$ vs $f$.
Parameter values $b = c = x = 1$

$$V(1) = \frac{1}{6}\left(2 + \ \log[9] - 2\ \log\left[1 + e + e^2\right]\right) \tag{5.37}$$

$$- \frac{2\ \sinh\left[\frac{a}{4}\right]\left(3 + 6\sqrt{e} - 6e - 3e^{3/2} + 3e^2 + 6e^{5/2}\right)\ \cosh\left[\frac{a}{4}\right]f}{3\left(1 + \sqrt{e}\right)\left(1 + e + e^2\right)\left(1 + 2\ \cosh\left[\frac{a}{2}\right]\right)}$$

$$+ \frac{2\ \sinh\left[\frac{a}{4}\right]\left(-2 - 3\sqrt{e} + e + 4e^2 + 3e^{5/2}\right)\ \sinh\left[\frac{a}{4}\right]f}{3\left(1 + \sqrt{e}\right)\left(1 + e + e^2\right)\left(1 + 2\ \cosh\left[\frac{a}{2}\right]\right)} + O[f]^2$$

The parameters $b$ and $c$ are fixed to one here as the expressions were get very cumbersome otherwise.

Its behavior is plotted in 5.12

The conservative force on the other hand, saturates for large values of $f$ and as $a$ rises the saturation potential rises as well. For $a = 1$ it seems to saturate to the equilibrium level but not so for higher values of $a$.

## Relation with generalized free energy

In the previous section we had found a relation between the generalized free energy in equilibrium and the potential $V(x)$ which was as follows:

$$\mathcal{F}^{\text{eq}}(x) = V(x)$$

The question we ask now is whether in non-equilibrium this relation still holds. The expression for $V(y)$ is shown above (5.37) upto first order in $f$. The correction in change in free energy $\mathcal{F}(x, x')$ upto first order in $f$ is found to be zero, which leads us to conclude and even close to equilibrium, the above equality is no longer true. This is also illustrated in plot 5.13. We also compared the two in the $f \to \infty$ limit, taking cue from the observations above that as $f$ becomes very large the system goes back to detailed balance (statistical non-gradient force becomes zero). The plot 5.13 below shows the variation of the limiting values of Free energy and $V(1)$ as a function of $f$. It is clear that they are not the same functions even in this limit.
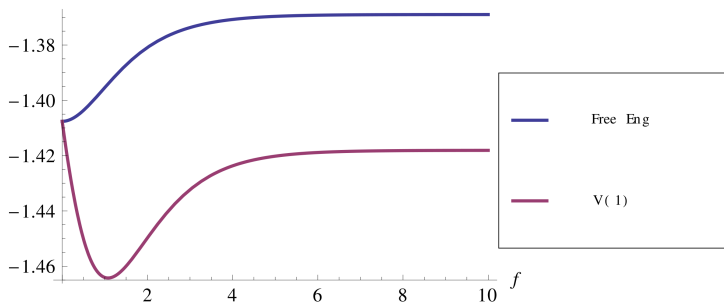


Figure 5.13: Comparison with generalized free energy of the conservative potential, $\mathcal{F}$ and $V(1)$ . On the $x$ axis is plotted the non-conservative force $f$. System returns to equilibrium for large values $f$. This equilibrium is different from the one in which the system started with. Parameter values $a = b = c = 1$

## 5.4 Archimedes' principle: Buoyancy in granular matter

For the remaining of chapter, we would like to present the action of entropic forces in granular matter. This section is mainly derived from our work in [95].

Size segregation phenomena like the Brazil nut effect, where a binary mixture of macroparticles segregate on shaking or vibration and the larger particles

raise to the top of the mix have been extensively observed and discussed in the literature. There are many factors which seem to play a role in the effect, like friction with the walls of the container causing convection currents, or void formation effects, when vibration-induced convection currents cause large particles move up through the middle of the container and small particles move down along the edges. The large particles cannot slip back down along the edges since the gap is too narrow for them to do so and are hence are stuck at the top of the mixture.

Another phenomenon which reminds us of something similar is the *Archimedes' law* and the *Law of Floatation.* Proposed by Archimedes of Syracuse in his work **On Floating Bodies** [39], which is supposed to have been written in 250 BCE.

The Archimedes' principle states that:

**Any body wholly or partially immersed in a fluid experiences an upward force (buoyancy) equal to the weight of the fluid displaced.**

and the Law of Flotation states that:

**Any floating object displaces its own weight of fluid.**

We present in the following work variations of Archimedes' law which have been observed in granular media and propose a mathematical model which explains some of the observed phenomena. We also propose *buoyancy* as an entropic force and derive the well known Archimedes' law by taking the fluid limit of the granular medium.

A main characteristic of granular media is that their behavior varies between being more fluid- and being more solid-like. Initializing flow via shaking or stirring fluidizes granular baths. That has been observed in various experiments and simulations, in particular by verifying Archimedes' law, [66, 102, 119]. Also phenomenological arguments have been added to the understanding of the buoyancy force in granular media, e.g. from using the Enskog hydrodynamic equations [1]. Nevertheless numerous controversies have remained and various corrections must be considered. In the present work we take up a simple excluded volume model to study the origin and the corrections to Archimedes' law around the fluid limit.

Fluid-like behavior of a granular material should obviously include hydrostatic and hydrodynamic effects. A natural way to study the origin of granular hydrostatics and their possible corrections is via flow induction, i.e., stirring

or shaking the system. That causes energy transfer to the grains which is dissipated again in the collisions between the moving grains. Further simplifications can help to understand the essence of what happens. In that spirit we consider the asymmetric exclusion process to simulate the dynamics of the grains (monomers) with one large particle (rod) immersed in them. The condition of detailed balance enables us to identify the buoyancy force on the rod, as function of its size and of its relative weight, and locally as function of the height. We recover Archimedes' law in the fluid limit and we create a theoretical framework for a detailed study of possible corrections.

Corrections arise from various effects such as from the discrete nature of the lattice where the lattice spacing measures the size of the grains. Corrections also arise from thermal effects especially when the grains are themselves immersed in a heat bath (e.g. hot air), and as studied here, from finite shaking rates. Other possible corrections arise from convection currents in the granular medium, to which we turn briefly in Section 5.5.

To the extent that our modeling via the asymmetric exclusion process is relevant for the experimental conditions of granular media under shaking, Archimedes'-like behavior was already predicted in [48]. Five years later Archimedes' law was confirmed experimentally [66] in a granular medium, and some corrections were explored before the fluid limit. In the mean time further experimental work and simulations which show an explicit Archimedes' like behavior have been added, including [102, 119]. We come back to the basic set-up.

### 5.4.1 Phenomenon & Experiment

In an experiment by Huerta et al. [66] in 2005, a bidisperse bath of beads sized 3 and 4 mm were placed in a box, which was shaken at the wall, giving horizontal, periodic impulses, given in general as $x(t), y(t) = \text{A} \sin(\omega t + \phi_{1,2})$. Here $x(t)$ is the impulse given in the $x$ direction and $y(t)$ is the impulse given in the $y$ direction. ($\phi_1 = -\phi_2$). The maximum amplitude of the walls is $\Gamma = A\omega^2/g = 10$, where $g$ is the acceleration due to gravity. Since, the impulse to the grains is given in the horizontal plain, there is no vertical kinetic energy transferred into the system and $g$ is used only as a reference. The net friction between the walls and the beads is also kept very low, so all effects due to convention can be ruled out. At high values of oscillation amplitude the medium is fluidized and effects such as buoyancy can be studied.
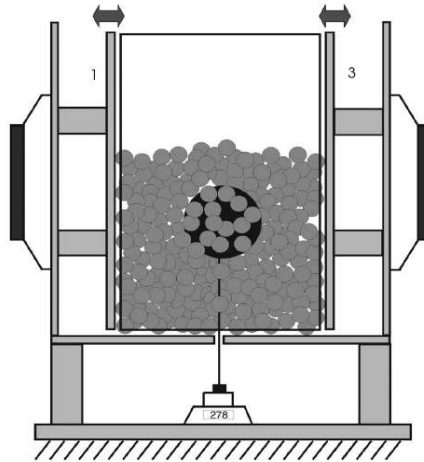
Figure 5.14: Experimental set-up. $500W$ loud speakers are firmly mounted on the lateral walls of an external and rigid box. This figure has been reproduced from [66].

A large, low density polystyrene ball is placed in the box and one end of it is tied to a dynamometer (to measure the tension in the string attaching the two). As the bath is fluidized, the ball starts rising through the fluidized medium , until the string is completely stretched. The buoyant force on the polystyrene sphere balances its weight and the tension in the string. Archimedes' law was verified in the system as a plot between the measured buoyancy force for different volumes of the sphere was found to be a straight line, see plot 5.15. The slope of the line gave the effective density of the fluidized bidisperse bath. The ratio between the effective density of the fluidized bath and the density of the glass beads gave the volume fraction of the bath as $0.63 \pm 0.03$, which came quite closed to the measured volume fraction of the bi-dispersion used in the experiment 0.64.

A more interesting observation was the dependence of the buoyant force on the oscillation amplitude $\Gamma$. It was observed that, above a certain cut off value of the amplitude, the observed buoyant force was independent of $\Gamma$ and equaled the theoretical buoyant force to be expected if the bath was a fluid. Below that cut-off though, the buoyant force decreases monotonically with $\Gamma$, see plot 5.16. This behavior separates the fluidized granular bath from a real fluid bath. The fact that the granular medium is a dissipative medium, which is never thermalized to an equilibrium state plays a role. Also, there are long-time and space correlations which exist in a granular bath which certainly modify its

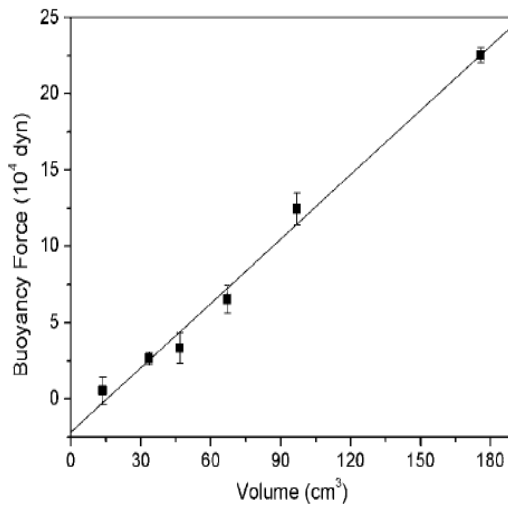Figure 5.15: Buoyancy forces for spheres of polystyrene (density 0.24 gm/cc) plotted as a function of their volume $\Gamma = 9.5$. The figure has been reproduced from [66].



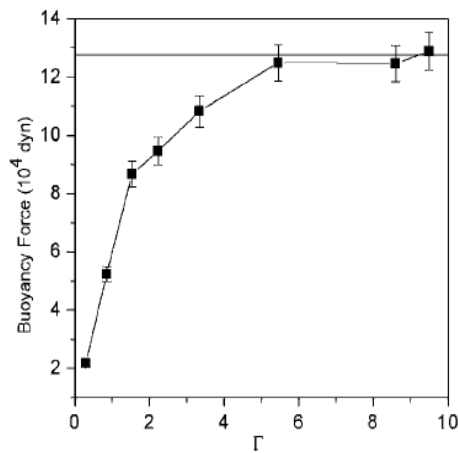Figure 5.16: Buoyancy force vs $\Gamma$ for a 92 cm$^3$ sphere. The horizontal part of the curve corresponds to the force as given by the Archimedes' principle.
At around $\Gamma \leq 5$, buoyancy force drops. The figure has been reproduced from [66].

behavior.

Using our model we derive that a correction to the Archimedes' law in fluids to granular media can be written in terms of a drag force (memory) in the system. Several experiments have studied the behavior of this drag force [66, 102, 128, 25] and [59]. Most agree that in the fluidized and low density limit the drag force is observed to be proportional to the velocity. Moreover the coefficient of viscosity is seen to vary exponentially with the shaking amplitude [66, 128], or, in [102], observed inversely proportional to the shaking amplitude. For denser media the drag force was seen to be varying logarithmic with velocity [25]. In our model we discuss the nature of drag force and corrections to it in Section 5.4.6.

## 5.4.2   The Model: A rod in a lattice

We introduce a coarse grained model of the granular medium with a large "intruder" immersed in it, originally proposed in [48]. The medium is composed of single particles called "monomers" ($\eta$) which exist on a two-dimensional lattice. The intruder on the other hand is a long rod ($Y$), which exists on this lattice and whose size extends to several lattice points. The coarse graining is done in such a way that the only interaction between the monomers and the rod is a simple exclusion. The monomers themselves behave as an ideal gas, with simple exclusion. There exist no hydrodynamic or long range interactions in the system. The only external force is the force of gravitation, which is uniform throughout the system. Hence, the system is an example of an equilibrium dynamics [2]. The boundaries are assumed to be far and are assumed to not have any influence on the system dynamics or steady state. Hence, phenomena like convection currents or friction from the walls and energy dissipation are not a consideration of this model. The whole system is maintained at a constant inverse temperature $\beta$.

### *The Fluid limit*

As far as the dynamics of the system goes it is a Markovian reduced dynamics for the rod. The rod is considered as the *slow variable* which navigates through the bath which is considered as the *fast variable*. Between any two moves of the rod, the monomer configuration has time to relax to a stationary measure

---

2. It has to be clarified here that this model does not take into account the dissipative collisions between the granular bath particles which leads to non-conservation of energy. Forgetting about this non-conservative effect, we call the dynamics of the granular bath equilibrium.

conditioned on the position of the rod and the external force. We call this the **fluid limit**. This is quite representative of a non-viscous, low density fluid, whose configuration at any moment is subject to the intruder configuration at that moment and is independent of the history of the intruder dynamics.

| | Entropic spring | Lattice model | Coarse graining |
|---|---|---|---|
| Probe | Classical spring | Intruder rod | Slow variable |
| Bath | Entropic spring | Monomer bath | Fast variable |
| Feed back | Passive:<br>No influence on the bath dynamics due to the intruder | In the fluid limit :<br>Minimally Active (only the stationary state of the bath is conditioned on the probe position)<br><br>Away from the fluid limit:<br>Active (the intruder influences both the dynamics and the stationary state of the bath) | Bath dynamics is infinitely faster than the probe<br><br><br>Bath dynamics is comparable to the probe |

Figure 5.17

In further sections, we would be lifting this constraint and study the system as it becomes responsive to longer history of the intruder. There are of course, several levels of feedback possible. In this study we concern ourselves with the influence of the last jump of the intruder on the bath dynamics and hence the feedback it has on the current intruder dynamics and more particularly on the *Archimedes' law*. This is an example of a *non-Markovian dynamics*.

We build in table 5.17 some correspondences and analogies with the *Entropic Spring model* which we considered in the last chapter.

## *Model*

All motion takes place on the square lattice $\mathbb{Z}^2$ where the mesh size, taken unity here, gives the size of the grains. These grains (also called, monomers) can occupy sites $i = (x, y)$ having "vertical" coordinate $y$ and "horizontal" coordinate $x$. There can be at most one grain per site. There is one big particle or intruder, called rod and we only follow its vertical position. The vertical position of the rod at time $t$ is denoted by $Y_t$ taking values in $\mathbb{Z}$. The

rod occupies $\mathbf{N} \in \{2, 3, ...\}$ lattice sites in the horizontal direction, i.e., the region

$$A_N(y) = \{(0, y), (1, y), ..., (N - 1, y)\} \tag{5.38}$$

is forbidden for the monomers when $Y_t = y$.
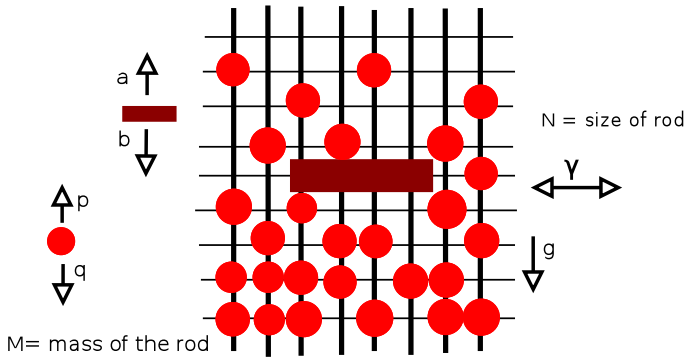


Figure 5.18: The red points denote the granular particles and the brown rod is the large intruder in the granular bath. The size of the lattice is unity. The bath is maintained at constant temperature $\beta$ and horizontal shaking at the boundary is replaced by a bulk horizontal jump rate $\gamma$

The horizontal jumps of the monomers are symmetric at rate $\gamma$. Increasing the rate $\gamma$ speeds up the monomer dynamics in the horizontal direction (orthogonal to the motion of the rod). The vertical jumps of the monomers and the rod are asymmetric; modeling a gravitational field. Note that the vertical motion is not speeded up, but of course it is influenced by $\gamma$ as well.

More formally, the microscopic dynamics looks as follows (Fig. 5.18) : The monomer configuration is denoted by $\eta \in \{0, 1\}^{\mathbb{Z}^2}$; $\eta_t(i) = 0$ means there is no monomer at site $i$ at time $t$ and $\eta_t(i) = 1$ if there is a monomer at site $i$ at time $t$. The dynamics is of exclusion- type because all motion is via jumping to vacant sites and rod and monomers never overlap. A monomer moves horizontally to a vacant nearest neighbor site, symmetrically with rate $\gamma$. It moves vertically up with rate $p$ and down with rate $q$.

The rod only moves vertically, up with rate $a$ and down with rate $b$. We choose $p/q, a/b < 1$ to represent the gravitational field, e.g. via

$$p/q = \exp(-\beta m g), a/b = \exp(-\beta M g)$$

where $M, m$ denote the mass of the rod, respectively of the monomers; $1/\beta = k_B T$ is a typical unit of thermal energy at temperature $T$ which plays little role in what follows, except for allowing fluctuations. The temperature could also refer to an additional heat bath that makes contact with the grains. Yet, granular media are typically a-thermal in which case we think of $Mg, mg >> k_B T$. The lattice unit is not indicated; it is taken to be one and should be thought of as the size of the grains. All that motion gets summarized in the formal generator

$$Lf(\eta, y) \equiv aI[\eta(i) = 0, \forall i \in A_N(y+1)][f(\eta, y+1) - f(\eta, y)]$$

$$+ bI[\eta(i) = 0, \forall i \in A_N(y-1)][f(\eta, y-1) - f(\eta, y)]+$$

$$\sum_{i=(i_1, i_2)} \{p\eta(i)(1 - \eta(i_1, i_2+1))I[(i_1, i_2+1) \notin A_N(y)]$$

$$\times [f(\eta^{i,(i_1,i_2+1)}, y) - f(\eta, y)]$$

$$+ q\eta(i)(1 - \eta(i_1, i_2-1))I[(i_1, i_2-1) \notin A_N(y)]$$

$$\times [f(\eta^{i,(i_1,i_2-1)}, y) - f(\eta, y)]\}$$

$$+ \gamma \sum_{\langle ij\rangle i:i_2=j_2} I[\langle ij\rangle \cap A_N(y) = \emptyset][f(\eta^{i,j}, y) - f(\eta, y)] \qquad (5.39)$$

where $I[\cdot]$ is the indicator function of the event in the brackets, giving one or zero depending on the event being realized, and $\eta^{i,j}$ is the grain configuration $\eta$ after switching the occupations in sites $i$ and $j$. The last term represents the horizontal shaking in which the occupations of (horizontal) nearest neighbor pairs $\langle ij\rangle$ get exchanged. Observe that there is always both horizontal and vertical motion, subject to the exclusion rule, which, besides from the shaking, can arise from an extra heat bath in which the grains are moving and with which energy can be exchanged. We need (5.39) for writing down the kinetic equations that are all of the form

$$\frac{d}{dt}\langle f(\eta_t, Y_t)\rangle = \langle Lf(\eta_t, Y_t)\rangle$$

Here and from now on, brackets $\langle i \rangle$ are with respect to the stochastic dynamics and over the following initial conditions. At starting time $t = 0$ we put $Y_{t=0} = 0$ so that the rod starts from the center of the lattice, but that is really arbitrary. For the initial distribution on monomer occupations we take density

$$d(x, y) = d(y) = \frac{\kappa(p/q)^y}{1 + \kappa(p/q)^y} \tag{5.40}$$

for parameter $\kappa > 0$. This formula satisfies

$$pd(y)(1 - d(y + 1)) = qd(y + 1)(1 - d(y))$$

which is a detailed balance relation for the motion of the grains. The density varies between zero (at the top) to one (at the bottom). The height where $d(y) = 1/2$ scales like $y \sim \log \kappa$. The derivative of the density at that height (where the transition is made between higher and lower density) is proportional to $\beta mg$. Therefore, choosing $\kappa \simeq 1$ and large $\beta mg$ corresponds to a more constant density as in a liquid or as in a granular medium in a container filled from the bottom to around $y = 0$; on the other hand, looking at positive $y$, for $\kappa = 1$ and for smaller $\beta mg$ corresponds to a gas condition where (5.40) simulates a barometric formula. Low density granular media under heavy shaking would also fall in that category which in our modeling is most typical. The density is constant in the horizontal direction $(x)$, but always conditioned on having $\eta(i) = 0$ for all $i$ covered by the rod, i.e., for all $i \in A_N(Y)$. More precisely, we let $\nu_d$ denote the product measure on $\{0, 1\}^{\mathbb{Z}^2}$ with density

$$\text{Prob}[\eta(x, y) = 1] = d(y) \tag{5.41}$$

defined by (5.40). The conditional probability

$$\nu_d^0 = \nu^d(\cdot \,|\eta(i) = 0, \forall i \in A_N(0)) \tag{5.42}$$

is then the initial distribution on the monomers. The dynamics such as defined above gives rise to the Markov process $(\eta_t, Y_t)$.

## 5.4.3  The Fluid limit

In the limit $\gamma \to \infty$, the motion of the rod decouples from the monomer dynamics. Then, the reduced dynamics of the rod becomes that of a random walker with rates directly given in terms of the equilibrium fluid density:

the rod moves up $y \to y + 1$ with new rate $a[1 - d(y+1)]^N$ and goes down $y \to y - 1$ with new rate $b[1 - d(y-1)]^N$. The factors $[1 - d(y \pm 1)]^N$ of course express the plausibility of having space for the rod to move from height $y$ to $y \pm 1$; there must be a hole of size $N$. Hence, in the limit of excessive horizontal shaking, the rod is doing a continuous time random walk on $\mathbb{Z}$ with backward generator

$$L^{\mathrm{RW}} f(y) = a[1 - d(y+1)]^N [f(y+1) - f(y)] + b[1 - d(y-1)]^N [f(y-1) - f(y)] \tag{5.43}$$

The density profile $d(y)$ is obtained from (5.40).

We call this limit $\gamma \to \infty$ the fluid limit. The reason of the decoupling is that the monomers relax to their stationary reversible density in between any two moves of the rod. The resulting motion (5.43) is itself satisfying the condition of detailed balance for a potential $V$, which can be interpreted as giving rise to a conservative force $F$ given by the logarithmic ratio of up *versus* down rates

$$F(y) = -V(y) + V(y-1) \quad = \quad -k_B T \log \frac{b[1 - d(y-1)]^N}{a[1 - d(y)]^N} \tag{5.44}$$

$$= \quad -Mg - NkT \log\left[1 + \frac{d(y) - d(y-1)}{1 - d(y)}\right]$$

To go to a continuum description (at least in the vertical direction) we introduce a lattice mesh of size $\epsilon > 0$, under which $\log(a/b) = -\beta M g \epsilon$, $\log(p/q) = -\beta m g \epsilon$. This imagines that the grains are of vertical size $\epsilon$. We compute the force $F_\epsilon$ as $\epsilon \downarrow 0$:

$$F_\epsilon(y) = \frac{-V(y) + V(y - \epsilon)}{\epsilon} = -Mg - \frac{k_B T N}{\epsilon} \log\left[1 + \epsilon \frac{d'(y)}{1 - d(y)}\right] \tag{5.45}$$

where the density $d(y)$ is now on $\mathbb{R}$ and, similar to (5.40), verifies

$$d'(y) = -d(y)(1 - d(y))\beta m g \tag{5.46}$$

Hence, (5.44) becomes $F_\epsilon \to F$ for

$$F(y) = -Mg + d(y)mgN \qquad (5.47)$$

which is Archimedes' law for the total upward force on a body of volume $N$ and mass $M$ replacing a weight equal to $mgd(y)N$ of fluid. In short, we call this the buoyancy force. The rod will thus move to a height where the fluid density is proportional to $1/N$. That is the equilibrium position, consistent with Archimedes' characterization of the hydrostatic equilibrium position, [39]. The force (5.44) is the correction to the Archimedes' force (5.47), due to the finite size of the grains.

The motion can be studied in the diffusive limit where we also rescale time $\sim \epsilon^2$. That means to take for example

$$a = \frac{e^{-\beta Mg\epsilon/2}}{\epsilon^2}, b = \frac{e^{\beta Mg\epsilon/2}}{\epsilon^2} \qquad (5.48)$$

and to expand the generator

$$L_\epsilon^{\mathrm{RW}} f(y) = a[1 - d(y+\epsilon)]^N[f(y+\epsilon) - f(y)] + b[1 - d(y-\epsilon)]^N[f(y-\epsilon) - f(y)] \qquad (5.49)$$

(see (5.43)) in orders of $\epsilon$. The result is that $L_\epsilon^{\mathrm{RW}} f(y) \to Lf(y)$ with

$$Lf(y) = (Df')'(y) + \chi(y)F(y)f'(y) \qquad (5.50)$$

with

$$F(y) = Nd(y)mg - Mg, \ D(y) = [1 - d(y)]^N, \chi(y) = \beta D(y)$$

We again have made use of (5.46) in the continuum limit. The result (5.50) is the generator of an overdamped diffusion equation with diffusion coefficient $D(y)$. The corresponding Langevin equation, in the Itô-sense, is given by

$$\dot{y}_t = \chi(y_t)F(y_t) + D'(y_t) + \sqrt{2D(y_t)}\xi_t \qquad (5.51)$$

for white noise $\xi_t$. The force $F$ is exactly the one found in (5.47), as in Archimedes' law. The diffusion $D(y)$ is related to the mobility $\chi(y)$ via the

Einstein equation $k_B T \chi(y) = D(y)$. The term with the derivative $D'(y)$ is due to the Itô-convention.

The above analysis concludes that the two-dimensional lattice model on a lattice with a simple exclusion dynamics, provides a reasonable description of the hydrostatic behavior of granular matter in the limiting (fluidized) case. We have seen above how the discreteness of the vertical lattice-direction makes a first correction, easily studied for small lattice mesh. For the second major type of correction, we study the approach to the fluid limit. The next section is devoted to these questions.

### 5.4.4 Random Walk in a dynamical environment



Figure 5.19: The two-dimensional model is contracted onto a line. The presence of a size $N$ hole is represented by the green color, the absence of the same by a red color.

To this end we propose a contracted description of the model, coarse-graining it to an effective one-dimensional model; see Fig: 5.19. The idea is as follows. The essential aspect of the monomer dynamics as far as regards the rod, is whether there is a hole above or below the rod in which it can jump. We therefore summarize all of the monomer configuration $\eta(x, y)$ by variables $\sigma(y), y \in \mathbb{Z}$, that specify whether or not there is a monomer in the region $A_N(y)$, see (5.38):

$$\sigma(y) \quad = \quad 1 \text{ if there is no hole at } y \tag{5.52}$$

$$= \quad 0 \text{ if there is a hole at } y \tag{5.53}$$

More precisely, there is a hole at $y$ if $\eta(i) = 0$ for all $i \in A_N(y)$. The position of the rod is still denoted by $Y$. We assume as major simplification that the (contracted) system $(\sigma_t(y), Y_t), y \in \mathbb{Z}, t \geq 0$, undergoes a joint Markov process which mimics the original model in the following sense.

The rod moves up $y \to y + 1$ with rate $a$ if there is a hole at $y + 1$, i.e., if $\sigma(y + 1) = 0$. The rod moves down $y \to y - 1$ with rate $b$ if there is a hole at $y - 1$, i.e., if $\sigma(y - 1) = 0$. The rod never moves to a position $y$ where there is no hole, $\sigma(y) = 1$. For the monomer dynamics, we assume that the $\sigma_t(y)$ flip $0 \rightleftarrows 1$ with different rates depending on $y$, and depending on the position of the rod. More precisely, $\sigma_t(y)$ has rate $q(y)$ for the change $1 \to 0$ and has rates $p(y)$ for $0 \to 1$ except when $Y_t = y$ because then it must remain zero; see Fig. 5.20.
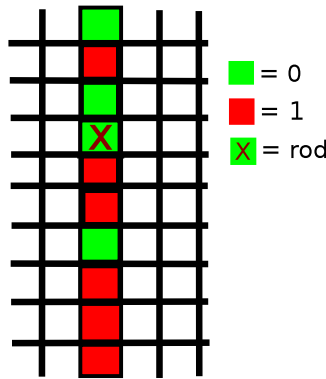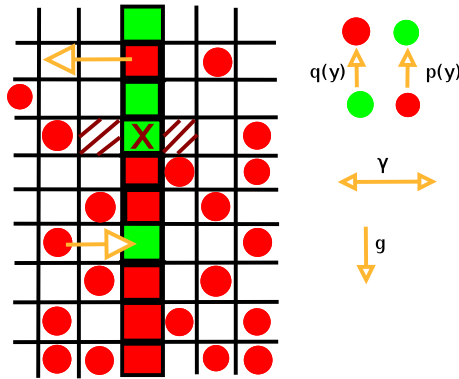


Figure 5.20: The two-dimensional model is contracted onto a line. The presence of a size $N$ hole is represented by the green color, the absence of the same by a red color. There is no particle number conservation anymore. The red and green lights interchange with rates $p(y)$ and $q(y)$ depending on the height.

So formally the backward generator of our new Markov process is

$$\mathcal{L}f(\sigma, Y) = a[1 - \sigma(y + 1)][f(\sigma, y + 1) - f(\sigma, y)]$$

$$+ b[1 - \sigma(y - 1)][f(\sigma, y - 1) - f(\sigma, y)] \tag{5.54}$$

$$+ \sum_{y \in \mathbb{Z}} \big[ [1 - \sigma(y)]\, p(y)(1 - \delta_{y,Y}) + \sigma(y)\, q(y) \big]$$

$$\times [f(\sigma^y, Y) - f(\sigma, Y)] \tag{5.55}$$

where $\sigma^y$ is the hole-configuration obtained after flipping the occupation at $y$: $\sigma^y(y') = \sigma(y')$ if $y \neq y'$ and $\sigma^y(y') = 1 - \sigma(y)$ if $y = y'$. At no point in time could the region occupied by the rod be simultaneously occupied by a monomer and vice versa, so $\sigma_t(Y_t) = 0$ always. This is the influence of the active particle (the rod) on the fast degrees of freedom.

### 5.4.5   Interpretation

Obviously, the rates $p(y), q(y)$ must be interpreted in terms of the monomer density $d(y)$ at $y$ with their dependence on the size $N$ of the rod and on the amount of horizontal shaking $\gamma$. Comparing (5.54) with (5.39) suggests further interpretations.

It remains that $a/b = \exp(-Mg/k_BT)$ where $M$ is the mass of the rod. We can think of the monomers as blinking lights, red ($\sigma(y) = 1$) for no passage of the rod, and green ($\sigma(y) = 0$) for passage allowed. In the original two-dimensional model a hole (green light) $\sigma(y) = 0$ at $y$ represents the fact that there are no monomers at the sites $A_N(y) = \{(0, y), (1, y), \ldots, (N-1, y)\}$, and (red light) $\sigma(y) = 1$ means that some monomer can be found in the region $A_N(y)$. Abbreviating

$$\rho(y) \equiv 1 - (1 - d(y))^N$$

we take therefore

$$p(y) = \gamma \, \rho(y), \quad q(y) = \gamma \, (1 - \rho(y)) \tag{5.56}$$

for the rate at which a hole gets removed, respectively created. Each depend on $N$ and on $y$ but observe that $p(y) + q(y) = \gamma$ which is the horizontal shaking rate. The stationary hole density at $y$ for that two-state Markov process becomes $1 - \rho(y) = (1 - d(y))^N$ which is the correct hole probability in the original monomer-model, cf. (5.41). Of course the weight of the monomer is represented in the density $d(y)$ via (5.40).

Here also, for our simplified model we can take the fluid limit $\gamma \to \infty$. By simpler arguments than in [48], the motion of $Y_t$ decouples from that of the $\sigma_t$ and by our choice (5.56) we find exactly the same limiting motion of the rod as given in (5.43). The two models mathematically agree in the fluid limit but our second model allows more easily to find the most significant contribution before the fluid limit, to which we turn next.

## 5.4.6   Before the fluid limit

Suppose we find the rod at time $u$ in position $y$. Thus, at that time the hole probability at $y$ is equal to 1. When the rod jumps from position $y$ to say position $y + 1$ at time $u$ it leaves a "hole" at position $y$ which remains a hole until it gets occupied by either monomers or by the rod again. In the fluid limit the monomer dynamics is fast enough and they relax to their equilibrium configuration so that at its next jump the rod sees a hole with probability $1 - \rho(y)$. On the other hand if the time of monomer relaxation is longer in comparison to the rod, at the next jump at time $u + t$ the rod sees "no hole" with probability

$$\rho(y)(1 - \exp(-\gamma t)) \tag{5.57}$$

as follows from a simple calculation for the two-state Markov process $\sigma_t(y)$. Note however that the transient density (5.57) is lower than $\leq \rho(y)$ and that (5.57) is only valid under the condition that the rod has not (re-)entered position $y$ during $[u, u + t]$. It implies that at time $u + t$ the rod still sees the hole it left behind at $y$. We conclude that before the fluid limit, the jump rates of the rod depend also on the past and the rod dynamics is by itself non-Markovian for finite $\gamma$.

We make the above statements now more concrete, and more precise. Knowing the rod's motion follows from the evolution equation, for all functions $g$ on $\mathbb{Z}$,

$$\frac{d}{dt} \langle g(Y_t) \rangle = \langle \mathcal{L}g(\sigma_t, Y_t) \rangle$$

with, from (5.54),

$$\mathcal{L}g(\sigma, y) = a[1 - \sigma(y+1)][g(y+1) - g(y)] + b[1 - \sigma(y-1)][g(y-1) - g(y)] \tag{5.58}$$

Consider for example the expectation

$$\langle [1 - \sigma_t(Y_t + 1)]g(Y_t + 1) \rangle = \langle \langle 1 - \sigma_t(Y_t + 1)|Y_s, 0 \leq s \leq t \rangle g(Y_t + 1) \rangle$$

where

$$\langle \sigma_t(Y_t + 1)|Y_s, 0 \leq s \leq t \rangle \tag{5.59}$$

is the conditional probability of having no hole just above the rod, given the full history of the walker $(Y_s, 0 \leq s \leq t)$. Obviously, history matters. Suppose for example that at time $t$ we have $Y_t = y$ and that the rod has been there already for a time $t_1$. The previous position was either $y + 1$ or $y - 1$, from which the rod has moved at time $t - t_1$. Before that, at jump time $t - t_1 - t_2$ the rod has been jumping either from $y - 2$, from $y$ or from $y + 2$, *et cetera*. In this way the whole history of the rod can be parametrized in terms of waiting times and successive positions. We denote such a rod-history by $\omega$. Yet, the

only thing that matters for the expected hole probability at $y + 1$ in (5.59) is the last time $t(\omega, y + 1)$ it was occupied by the rod, since

$$\langle [1 - \sigma_t(Y_t + 1)] \,|\, \omega \rangle = (1 - d(y+1))^N + \rho(y+1) \exp(-\gamma(t - t(\omega, y+1))) \quad (5.60)$$

We put $t(\omega, y) = -\infty$ if the rod has never been in position $y$, to realize the initial condition (5.41).

We must now estimate the conditional expectation

$$\langle e^{-\gamma[t - t(\omega, y+1)]} | (Y_s, s \in [0, t]) = \omega \rangle \quad (5.61)$$

for a history $\omega$ in which $Y_t = y$. Clearly, that equals $\exp -\gamma t_1$ if before $y$ the rod was at $y + 1$; otherwise (if before the rod was at $y - 1$) (5.61) is certainly less than $\exp -\gamma(t_1 + t_2)$, which is much smaller than $e^{-\gamma t_1}$ for large $\gamma$. There are then two cases depending on the sign of the rod's "velocity"

$$V_t = Y_t - Y_{t-t_1} \quad (5.62)$$

We therefore approach the fluid limit by putting (5.61) equal to zero if $V_t$ is positive, and by putting it equal to

$$\mu(\gamma) \equiv \int_0^{+\infty} e^{-\gamma t_1} (a + b) e^{-(a+b)t_1} \, dt_1 = \frac{a + b}{a + b + \gamma} \quad (5.63)$$

if $V_t$ is negative. The integral (5.63) takes the expectation over the exponential waiting time distribution for $t_1$. In (5.63), the sum $a + b = v$ is a good estimate for the average speed of the rod, or $\mu(\gamma) V_t = \frac{v V_t}{v + \gamma} = \nu(\gamma) \vec{v}_t$, where $\nu(\gamma) = 1/(v + \gamma)$ is the friction coefficient and $\vec{v}_t$ is the velocity of the rod before it arrived at $Y_t$. The drag force on a particle immersed in granular matter was studied in various experiments — in [66, 102, 128, 25] a linear dependence on the particle velocity such as proven above was observed and corresponds to low density. Inserting this $\mu(\gamma)$ we have obtained for large but finite $\gamma$ that

$$\begin{aligned}
\frac{d}{dt} \langle g(Y_t) \rangle &= \langle L^{\mathrm{RW}} g(Y_t) \rangle \\[2ex]
&+ a \left\langle \rho(Y_t + 1) \mu(\gamma) \frac{[1 - V_t]}{2} [g(Y_t + 1) - g(Y_t)] \right\rangle \\[2ex]
&+ b \left\langle \rho(Y_t - 1) \mu(\gamma) \frac{[1 + V_t]}{2} [g(Y_t - 1) - g(Y_t)] \right\rangle \quad (5.64)
\end{aligned}$$

always with $\rho(y) = 1 - [1 - d(y)]^N$ and the first line of (5.64) corresponds to the fluid limit (5.43). The $V_t$ is $\pm 1$ as defined in (5.62).

To recapitulate, the approximation in which we replace (5.61) by (5.63) is the following. The rate of the rod's dynamics in comparison to the monomer dynamics is such that for the rod making a jump $y \to y + 1$ it can still "see" the gap it left at $y + 1$ when indeed the rod was at $y + 1$ before it came to $y$. However the rod does not "see" any gaps which were left at $y + 1$ from earlier visits there: the monomer dynamics is fast so that it can erase the trace of the rod's trajectory up to one time step ago. The introduction of the velocity $V_t$ of the rod is a way to re-install the Markov property, where the state of the rod is now defined as its position plus its (previous) velocity. In other words, due to the active nature of the rod it acquires memory before the fluid limit (which results in a drag force, see below), which is most efficiently dealt with by introducing a velocity.

For the position of the rod, $g(y) = y$,

$$
\begin{aligned}
\frac{d}{dt} \langle Y_t \rangle \;=\;\; & \langle a(1 - \rho(Y_t + 1)) - b(1 - \rho(Y_t - 1)) \rangle \\[2mm]
+\;\; & a \left\langle \rho(Y_t + 1)\mu(\gamma)\frac{[1 - V_t]}{2} \right\rangle - b \left\langle \rho(Y_t - 1)\mu(\gamma)\frac{[1 + V_t]}{2} \right\rangle
\end{aligned}
$$

This equation gives the speed of the rod at time $t$ given its current position and previous direction $V_t$. If the rod was moving upwards ($V_t = +1$), then it continues moving up with a rate $a \langle (1 - \rho(Y_t + 1)) \rangle$ and goes down with a rate $\langle b(1 - \rho(Y_t - 1)) \rangle + b\,\mu(\gamma)\,\langle \rho(Y_t - 1) \rangle$. On the other hand if the rod was moving downwards, $V_t = -1$, then it continues moving down with a rate $b \langle (1 - \rho(Y_t - 1)) \rangle$ and goes up with a rate $\langle a(1 - \rho(Y_t + 1)) \rangle + a\,\mu(\gamma)\,\langle \rho(Y_t + 1) \rangle$. In comparison to the fluid-limit there is an increase in the rate of return. The rod has a higher tendency to go back to the site it started from when the bath is not completely fluid. The rate to go forward remains the same as in the fluid limit. This phenomenon of a greater tendency to return with possible subsequent oscillations can be interpreted as a greater dynamical activity which becomes effective as the bath becomes less and less fluid. When the rod has an overall tendency of rising because of buoyancy, the result is friction acting downwards.

As in the fluid limit here also we can make a small mesh analysis and take the diffusive limit. We also need to rescale the shaking $\gamma \to \gamma/\varepsilon^2$ so that with the choice of (5.56), $\mu(\gamma) \to 2/(2 + \gamma)$ and $V_t = \pm\epsilon$. We only need to worry about

the additional last two lines in (5.64), i.e., corresponding to

$$\varepsilon^{-2}\left(1 - \frac{Mg\varepsilon}{2kT}\right)\left[1 - (1 - d(y+\varepsilon))^N\right]\frac{\varepsilon^-}{2+\gamma}[g(y+\varepsilon) - g(y)]$$

$$+ \quad \varepsilon^{-2}\left(1 + \frac{Mg\varepsilon}{2kT}\right)\left[1 - (1 - d(y-\varepsilon))^N\right]\frac{\varepsilon^+}{2+\gamma}[g(y-\varepsilon) - g(y)] \quad (5.65)$$

where $\varepsilon^- = 2\varepsilon$ if the rod was going down and $\varepsilon^- = 0$ when the rod was going up; similarly $\varepsilon^+ = 2\varepsilon$ if the rod was going up and $\varepsilon^+ = 0$ when the rod was going down. Again making the $\varepsilon-$expansion we find, similar to (5.50), the corrected Langevin equation

$$\dot{y}_t = \chi(y_t)\,F(y_t) - \frac{2(1 - D(y_t))}{2+\gamma}v_t + D'(y_t) + \sqrt{2D(y_t)}\,\xi_t \quad (5.66)$$

with memory term in the friction, $v_t = \frac{y_t - y_{t-dt}}{\|y_t - y_{t-dt}\|}$ being the direction of the velocity just before time $t$; the rest of the Langevin equation (5.66) is interpreted in the Itô-sense with, in particular the left-hand side referring to $y_{t+dt} - y_t$. The diffusion coefficient remains the same as before in the fluid limit, see (5.51). The friction $\sim (1 - D(y))$ increases with higher density.

If we look at the origins of drag or friction in common phenomena like Brownian motion, it arises due to a resistance to motion in the form of collisions from the front. The faster a tracer particle moves in a thermal bath the more traffic it finds ahead of itself than behind. Of course friction appears in all directions against motion and exists at shaking of all strengths. The drag force we see here is a variation of this effect. Our system is overdamped and nothing of impact or momentum transfer can be discussed; yet interaction via excluded volume will be sufficient to generate (another) force which opposes motion of the rod. This force appears when granular baths are not completely fluidized.

The higher the intruder dynamics rate, the stronger its memory of its previous position and the greater is the chance of jumping to its old position. The force become weaker and weaker in the fluid limit since the memory of the rod is "instantaneously" being wiped away by the monomers. We believe that the "drag force" dependence on $\gamma$ and intruder velocity as seen in [66, 102] away from the fluid limit are explained by this new kind of opposing force rather than the conventional understanding of friction in fluids, especially in a low density environment where momentum transfer does not play such a big role.

# 5.5   Further remarks

## 5.5.1   Segregation effect

Effects of buoyancy in granular media have been widely studied both theoretically and experimentally. It is not always easy to distinguish between anti-gravity effects and buoyancy as in Archimedes' law. That connects with the variety of segregation effects in granular media upon shaking them. Reference [65] discusses various mechanisms that can work together for the segregation of grains. Buoyancy, i.e., rising/sinking due to pressure gradients, dominates when the fluidization occurs with no convection. Our model does not show boundary effects and inertia is absent. The limiting motion is overdamped in the diffusion limit. Buoyancy is indeed most visible in a vibro-fluidized regime, where only binary collisions are prevalent and there is no long time contact between particles. The medium must have minimal convection, so the boundaries must be far and the interactions with the boundary reduced. In a fluidized regime the effects due to convection as well as inertia are reduced enough for buoyancy to be visible, [65, 81]. In the unfluidized regime, effects like inertia, void filling models (true for vertical shaking) and convection are more important. Another difference to be noted is that buoyancy is not just a phenomenon of the larger particle climbing up to the top of the pile but refers to a specific dependence of height on the relative sizes and densities.

On the other hand, the rising of larger objects in a sea of smaller grains due to the Brazil nut effect, [81, 113, 69], arises in several forms and many competing mechanisms influence the motion of the larger particles within a bath (shape, size, forces between particles, shaking amplitude and direction, interstitial air and humidity). In [4, 3] a similar model to ours was used to investigate the Brazil nut effect. Sometimes segregation is a result of entropic forces which are strong in a gravity free regime and when the frictional forces among bath particles and between bath and intruder are such that the entropy of a segregated state is higher than a highly mixed state, [5].

## 5.5.2   Simulation results

Since the one-dimensional reduction of the full lattice fluid model has undergone some further simplifications, we have tested numerically whether our approximations appear reasonable. In other words, we have compared the trajectories of the rod in our approximations with those of the true model. The simulation was run on a chain of 300 sites and gravity $g$ and $kT$ are taken as unity. In this way we could also numerically verify Archimedes' law in the large
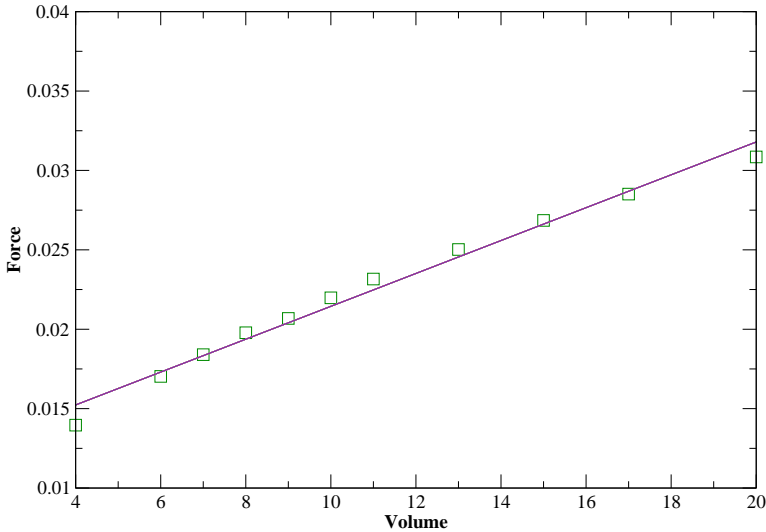
Figure 5.21: The contracted one-d model was simulated. Buoyancy force *vs* rod length $N$ is plotted for $\gamma = 15$ at height $y = 180$ and mass of bath particles $m = 0.02$. $k_B T$ and $g$ taken to be unity. Buoyant force at varying heights in the liquid was measured by finding the weight of the intruding rod such that the rod equilibriates at this height. The squares are the result of simulation in the large $\gamma$ case. This simulation aligns with the behavior predicted in (5.51). The solid line is a guide for the eye.

$\gamma$ limit. In the fluid limit the buoyancy force varies linearly with the size $N$ of the rod, plot 5.21. The straight line indicates that for such a large $\gamma$ the monomer bath is fluid-like. For a given height $y$ buoyancy force is calculated by estimating the weight of the rod which would exactly balance the force from the bath at that height. In the fluid limit at equilibrium then, the weight of the rod is equal to the upward force (called buoyancy).

Before the fluid limit is reached buoyancy force varies with $\gamma$; for large $\gamma$ the buoyancy force tends to a steady value as given by Archimedes' law, see plot 5.22. That must be compared with Fig.3 in [66]. The buoyancy force grows with $\gamma$ and after a certain critical value which in the simulation was $\gamma = 4.0$, it saturates. Plot 5.22 shows the Archimedes' force (5.47) corrected with the

friction term as it acts in (5.66), with the $2/(2+\gamma)$ kind of variation.

### 5.5.3 Longer memory

Instead of considering memory only until one time step before, one could also take two, three or more time steps long memory. That means, to consider again (5.61) and to take into account contributions from alternative histories. These contributions are all of smaller order, with each correction falling as an inverse power of $\gamma$. The power arises from performing the integral like in (5.63) but now the time is a sum of exponential variables, so that we get corrections like $\mu(\gamma)^n$.
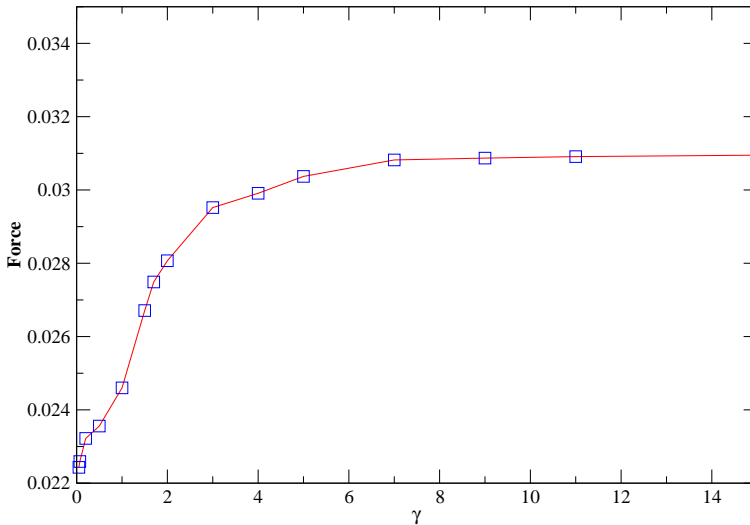


Figure 5.22: Buoyancy force *vs* $\gamma$ for $N = 20$ at height $y = 180$ and mass of bath particles $m = 0.02$. $k_B T$ and $g$ taken to be unity. Buoyant force at varying heights in the liquid was measured by finding the weight of the intruding rod such that the rod equilibriates at this height. The squares are the result of simulation for different values of $\gamma$. This simulation results aligns with the behavior predicted by (5.66). The solid curve is a guide for the eye.

### 5.5.4 Nonequilibrium seas

Another type of correction to Archimedes' law comes from the possible nonequilibrium nature of the medium, even in the fluid limit. Indeed, an essential aspect of our analysis above was that the sea of grains (monomers) reach their equilibrium between two moves of the rod (in the fluid limit), and that equilibrium is the same with or without the rod. In other words, the stationary distribution of the constrained dynamics of the monomers given the rod's position gives exactly the same as conditioning the stationary distribution of the joint monomer–rod dynamics on the position of the rod. That is only valid under the condition of detailed balance, see e.g. Lemma 3.1 in [48]. In the present work detailed balance is forced by the specific choice of density profile (5.40) for which holds that

$$p\, d(y)\, (1 - d(y+1)) = q\, d(y+1)\, (1 - d(y)) \tag{5.67}$$

In the small mesh (continuum) limit this detailed balance condition (5.67) becomes $d'(y) = -mg d(y)\, (1 - d(y))/(kT)$ as repeatedly used in the derivation of the Langevin equations (5.51) and (5.66), and in the validity of the corresponding Einstein relation. When detailed balance is violated and the granular sea shows an irreversible steady behavior, the motion remains much less understood.

### 5.5.5 Collective effects

A final source of corrections to Archimedes' law is due to the interaction with other intruders (rods). Here we are really speaking about a whole new range of phenomena in which pairing of particles, [100] and more general collective effects as flocking [104], can occur. The main underlying reason however is already visible from the simple analysis of the present work. The excluded volume effect of one rod not only creates a bias for itself to return to the place it was before (creating drag, [32]), but also creates space where another intruder can hop into, and thus "attracts" other rods and intruders. This granular-hydrodynamic interaction is long range and is expected to be proportional to the speeds of the rods, but more exploration is needed. This interaction qualitatively resembles the long range hydrodynamic interaction between colloidal particles in suspensions. These interactions come through due to the Stokes-like force applied by the suspension on a moving colloid which results in long-range interaction between two colloids connected through the Oseen tensor. Here, the collective behavior of multiple intruders results from simple exclusion and memory tracks left on the bath.

# Chapter 6

# Entropic Forces in nonequilibrium

*The force is an energy field created by all living things, it surrounds us, it penetrates us, it binds the galaxy together.*

*- Obi-Wan Kenobi to Luke Skywalker*

## 6.1   Introduction

In the last chapter we defined and studied some properties of forces which arise due to fluctuations in the surrounding environment. As illustrated clearly by the last few examples entropic forces arise due the tendency of fluctuating systems to evolve towards a state with maximum entropy. We can derive these forces by studying the large deviation fluctuations of a macroscopic variable. The probability of such fluctuations decays exponentially with a decay parameter which is proportional to the entropy or the free energy of the environment.

For a system composed of large number of microscopic degrees of freedom $x$, the probability of a macroscopic observable $E(x)$ taking value $e$ is

$$\lim_{N \to \infty} \frac{\log P(E(x) = e)}{N} = -I(e)$$

in the asymptotic sense, i.e., in the limit of very large system size $N$. $I(e)$, the rate function is in equilibrium a static fluctuation functional.

Of course, such a result holds true only when the environment is undergoing an equilibrium dynamics.

In the last chapter, where we discussed the emergence of buoyant force on a colloidal particle immersed in a granular medium, a process of coarse-graining was used. An appropriate time-scale separation was assumed, such that the influence of the granular medium on the macroscopic particle was only through its stationary distribution. In this chapter we present a different scenario to study entropic forces. To remind you of the entropic spring in chapter 4, it was a collection of coupled harmonic springs, which were designed to exist in a discrete phase space with just two elements. This collection was attached to a large classical spring which acted as a probe and the entropic force was measured by measuring the average extension of this spring away from its equilibrium length.

In the present scenario, which has been largely inspired by our work in [96], we would look at a collection of $N$ masses, $m$ coupled with springs of spring constant $\kappa$. We call the masses monomers. The whole spring collection, a polymer, is in equilibrium with a heat bath at inverse temperature $\beta$. One of the monomers in this polymer is tagged for observation. The polymer is undergoing fluctuations in its configuration and is diffusing in the heat bath. As far as the observer of the tagged monomer is concerned, the rest of the coupled polymer and the underlying heat bath together constitute a fluctuating environment. Nothing is known to the observer about this environment, which is like a black box, except that which can be deduced by the observed behavior of the tagged monomer.

We study the emergent statistical force on the tagged monomer due to its environment, as the environment is in equilibrium and also, as it is driven away from equilibrium by an external non-conservative force. The first motivation of this work is to study an explicit example of statistical forcing emerging from integrating out a nonequilibrium environment. Yet, the case we study comes with an extra motivation as it opens some questions in the nonequilibrium physics of polymers. In contrast to many ongoing studies of nonequilibrium polymer rheology, of transport through polymers or of mechanical folding and stretching of polymers, the present work considers also steady nonequilibria, i.e., where the driving is constant in time and the condition of detailed balance is broken.

Our working model is the widely studied Rouse model, an ideal chain, where monomers are connected through Gaussian springs, and excluded volume effects

and hydrodynamic interactions are neglected. This model holds a special place, as it is the simplest model which can be exactly solved to describe phenomena like anomalous diffusion of polymers in a bath. Moreover, in the natural context of polymer melts, which are a collection of polymers in a solution, the diffusion of a tagged polymer can be described by Rouse dynamics moving along a one-dimensional tube embedded in a network or mesh of polymers [33, 30]. Our general question can then be asked here, to investigate the effective dynamics of a tagged monomer when the chain is subjected to nonequilibrium driving. We have in mind that the extremal monomers are subject to non-conservative forces e.g. via a small charged particle or optically driven bead attached to them, and we wish to follow a tagged monomer near the middle of the chain.

### 6.1.1   Integrating out: Langevin to generalized Langevin

In this section we illustrate by a simple example of two coupled particles in a thermal bath, the main principle behind the idea of coarse-graining by simple integrating out of the extra degrees of freedom. This technique has been used several times in the discussion of Brownian tagged particles in heat bath, [131, 56].

Consider a system of two particles $X1$ and $X2$ coupled to each other.

$$m\dot{X}1(t) = X2(t) \tag{6.1}$$

$$m\dot{X}2(t) = -m\gamma X2(t) + F(t) + \xi(t) \tag{6.2}$$

$X2$ is surrounded by a heat bath, which is Gaussian distributed and interacts with them through a random force $\xi(t)$. It has the following properties:

$$\langle \xi(t) \rangle = 0; \ \langle \xi(t)\xi(s) \rangle = \frac{2m\gamma}{\beta}\delta(t-s)$$

This system has a Markov dynamics, since the dynamics of each particle at time $t$ is independent of the system configuration before time $t$. Suppose that particle $X1$ is the tagged particle, in whose motion we are interested. We integrate out particle $X2$, by solving its equation of motion, assuming that the initial positions and momenta are sampled from a canonical distribution $\rho^{\text{eq}}(0)$.

We replace $X2$ in equation (6.1) with the solution of equation (6.2) and arrive at the following equation for $X1$:

$$m\dot{X}1(t) = X2(0)e^{-\frac{\gamma}{m}t} + \frac{1}{m}\int_0^t [F(s) + \xi(s)]e^{-\frac{\gamma}{m}(t-s)}ds \qquad (6.3)$$

This is a generalized Langevin equation, governing the equation of the tagged particle $X1$. It is apparent that the equation is non-Markovian, depending on the history of the force $F(s)$ and the noise $\xi(s)$ and initial conditions. This represents the general features of the process of integrating out.

The noise

$$\eta(t) := X2(0)e^{-\frac{\gamma}{m}t} + \int_0^t \frac{\xi(s)}{m}e^{-\frac{\gamma}{m}(t-s)}$$

is colored, with a long time correlation.

$$\langle\eta(t1)\eta(t2)\rangle = \frac{e^{-\frac{\gamma}{m}\tau}}{\beta} := \frac{\mu(\tau)}{\beta}; \ |t1 - t2| = \tau, \ t1 + t2 \to \infty \qquad (6.4)$$

We call $\mu(t)$ the memory of the process, which quantifies long-time correlations in the system.

The definitions from the above example would bear their meaning and function in the analysis which would follow.

## 6.1.2   Rouse dynamics

A polymer can be represented by a set of beads connected along a chain. The dynamics of such a polymer is modeled by the Brownian motion of these beads. This model was first proposed by Prince E. Rouse in [114] and has been a basis to study polymer dynamics in dilute solutions. In the Rouse model excluded volume interactions and hydrodynamic long-ranged effects are disregarded. Hence, it is is also called the *phantom Rouse model*.

The Langevin equation of each bead is a combination of the deterministic elastic force due to the springs, the surrounding fluid provides a local isotropic drag proportional to the local velocity, $\dot{r}$ of the bead, $f_{\mathrm{drag}} = \gamma\dot{r}$, where $\gamma$ is the friction coefficient. A Gaussian white random force $\xi$ (with its mean zero) describes the coupling to the thermal bath.

Because of the harmonic interaction, the nonequilibrium Rouse model is one of the simplest, still physically interesting examples to understand the effective

dynamics in a driven medium. The equilibrium version of integrating out the Rouse model was already carried out by D. Panja [106]. The dynamics of the tagged monomer is shown to be non-Markovian with memory kernel having a power law decay $\mu(t) \propto t^{-1/2}$ for short times and exponential decay asymptotically in time,

$$\mu(t) \propto \frac{1}{\sqrt{t}} \, e^{-t/\tau} \tag{6.5}$$

The kernel $\mu(t)$ is shown to be the mean relaxation response of the polymers to local strain and its behavior gives good information on the nature of the diffusion, which is anomalous for intermediate times, $\Delta x^2 \propto D\sqrt{t}$.

In the present work we start with the phantom Rouse dynamics in the inertial regime and we introduce a nonequilibrium driving. The result of integrating out the (other) polymer degrees of freedom is again a generalized Langevin equation (GLE) for the tagged monomer. We show that in the overdamped limit, the equilibrium results match those of Panja [106]. We discuss the nonequilibrium corrections to the force and memory terms for driving of specific nature to obtain some general information about statistical forces in nonequilibrium.

The more systematic and general approach to integrating out degrees of freedom is commonly referred to as the Mori-Zwanzig approach [129, 101] or the approach via adiabatic elimination [58, 89, 16, 70]. Generalized Langevin equations have also been derived in nonstationary environments [74] and similar in spirit to the present work is also the generalization where a coarse-graining is added upon a coarse-grained description [47], or where one Brownian particle is described in a nonequilibrium bath [118]. In the case of nonequilibrium thermostated dynamics a generalized Langevin equation has also been derived [99].

We do not follow these general schemes here also because we work on the more explicit Langevin (not Fokker-Planck) side of the question, and we take no special limits for macroscopic systems or for the speed of motion of non-conserved versus conserved quantities. Moreover, these general approaches are less explored for starting with open driven polymer dynamics as we do here. An interesting study of the average square displacement of a tagged monomer in Rouse polymer chain subjected to random, layered convection flows both time-independent and time-dependent has been made in [103, 71].

In the next section we introduce the model and the various types of nonequilibrium driving. Sections 6.4, 6.5 and 6.6 summarize the method and the results with a discussion of the effective dynamical behavior. Finally some more essential elements of the computations are collected in Appendix A.1.

## 6.2 Nonequilibrium Rouse dynamics

We consider the positions $\vec{R}_i, i = 1, \ldots, N$, of $N$ point particles (also called monomers) in a three-dimensional domain open to thermal exchanges. The particles are harmonically coupled and some are subject to further forces, some of which are non-conservative. The potential energy is quadratic

$$U(\vec{R}) = \frac{\kappa}{2}(\vec{R}_1 - \vec{R}_2)^2 + \frac{\kappa}{2}(\vec{R}_2 - \vec{R}_3)^2 + \ldots + \frac{\kappa}{2}(\vec{R}_{N-1} - \vec{R}_N)^2 \qquad (6.6)$$

and the force on the $i$th particle is the sum of systematic forces $\vec{K}_i$ and Langevin forces $\vec{L}_i$:

$$\vec{K}_i = -\vec{\nabla}_i U + \vec{F}_i, \quad \vec{L}_i = -m\gamma\dot{\vec{R}}_i + \vec{\xi}_i \qquad (6.7)$$

There is an independent standard white noise $\vec{\xi}_i$ modeling the action of the thermal environment at temperature $T$ and friction $\gamma$, with $\langle \vec{\xi}_{i,\alpha}(t)\vec{\xi}_{j,\beta}(t') \rangle = 2m\gamma k_B T \delta_{i,j}\delta_{\alpha,\beta}\delta(t - t')$, where $\alpha$ and $\beta$ refer to the various spatial directions. The first term in $\vec{K}_i$ is the conservative part of the force. The force $\vec{F}_i$ need not be conservative or constraining and will be specified below; that is what we refer to as the driving. We then have the equation of motion for the time-dependent coordinates $\vec{R}_i(t)$

$$m\frac{d^2\vec{R}_i}{dt^2} = \vec{K}_i + \vec{L}_i \qquad (6.8)$$

with given initial conditions $R_i(0), \dot{R}_i(0)$ at time $t = 0$. In many cases of standard polymer physics the inertial term proportional to the mass in (6.8) can be fairly ignored. That can be done in all following equations and results but there is however no harm in keeping it ; in fact our concern is not in the first place towards a detailed study in polymer physics. In fact, we take the Rouse polymer model for the simple purpose of illustrating effects of statistical forces in a nonequilibrium environment. To have a workable model we can exploit the linearity of the Rouse model and the extra forcing $\vec{F}_i$ will also be assumed linear. We will however not proceed with a diagonalization, and we will not write the solution in terms of modes. After integrating out all particles but the first one, we obtain explicit information about the final equation of the form,

$$m\frac{d^2\vec{R}_1}{dt^2} = -m\int_0^t dt' \mu^{(N)}(t - t')\dot{\vec{R}}_1(t') - m\gamma\dot{\vec{R}}_1(t) + \vec{\eta}^{(N)}(t) + \vec{\xi}_1(t) + \vec{G}^{(N)}(t) \qquad (6.9)$$

Indeed, not surprisingly and as an explicit example of a type of Zwanzig's program [131], we will find the validity of a GLE of the form (6.9). Our model will enable rather explicit memory and friction kernels. We will discuss the memory kernel $\mu(t)$ (more generally a matrix), the noise $\vec{\eta}(t)$ and the statistical forcing $\vec{G}$ (that all depend on $N$) in the cases that we introduce next. Obviously, the case of the effective dynamics on another coordinate, e.g. the middle one around $i = N/2$, can be reduced to that case. The effective force $\vec{G}$ can be of convolution type, as in Eq. (6.28) below, and also contain the memory of the past trajectory of the tagged monomer.

## 6.2.1 Uniform constant driving

The simplest case is to assume that the outer end of the polymer is being driven under a constant external force $f$. That is a mathematical idealization of a polymer say with a charged end, forced under an electric field. As there is no confining force for the polymer, that means the whole system will move in the direction of the field and we discuss that diffusive regime. That is, we take free boundary conditions and $\vec{F}_i = \delta_{N,i}\, f\, \hat{e}_x$, for some constant field $f$ in the $x-$direction. The simplest example corresponds to two linearly coupled degrees of freedom moving in one dimension, with dynamics

$$
\begin{aligned}
m\frac{d^2 R_1}{dt^2} &= -\kappa[R_1 - R_2] - m\gamma\frac{d}{dt}R_1 + \xi_1(t) \\
m\frac{d^2 R_2}{dt^2} &= -\kappa[R_2 - R_1] - m\gamma\frac{d}{dt}R_2 + \xi_2(t) + f
\end{aligned}
\tag{6.10}
$$

for $R_1, R_2 \in \mathbb{R}$. The constant $f$ induces a drift. We give here that dimer-case explicitly also because we have found that for all finite $N$ (size of original polymer) the basic qualitative features of generalized memory and friction are unchanged from $N = 2$, where things are of course much simpler.

## 6.2.2 Non-uniform driving

Here we imagine the motion of a polymer in a 2-dimensional slab of vertical size $L$ in which the outer end is subject to a forcing in the horizontal direction that is linear in the vertical distance. We can imagine that as the result of a shearing at the outer edge of the polymer, but we do not imagine a surrounding fluid as we wish to stick to the Rouse model (ignoring hydrodynamic interactions as e.g. in the Zimm model). In terms of a polymer melt we can realize that by attaching a bead or nanoparticle to the end of the polymer chain, which is

then driven in one direction but non-uniformly with respect to an orthogonal direction. That provides a well known case of a non-conservative force. For explicitness we write out this case again first for a polymer of size $N = 2$. One monomer is being acted on by the non-uniform force which depends on its $y$-coordinate. The equation of motion written in Cartesian coordinates is then

$$\frac{md^2R_{2x}}{dt^2} = k[R_{1x} - R_{2x}] - m\gamma\frac{dR_{2x}}{dt} + \xi_{2x}(t) + f\,R_{2y}$$

$$\frac{md^2R_{2y}}{dt^2} = k[R_{1y} - R_{2y}] - m\gamma\frac{dR_{2y}}{dt} + \xi_{2y}(t)$$

$$\frac{md^2R_{1x}}{dt^2} = -k[R_{1x} - R_{2x}] - m\gamma\frac{dR_{1x}}{dt} + \xi_{1x}(t)$$

$$\frac{md^2R_{1y}}{dt^2} = -k[R_{1y} - R_{2y}] - m\gamma\frac{dR_{1y}}{dt} + \xi_{1y}(t) \tag{6.11}$$

where $f$ is the nonequilibrium amplitude.

Since the external force now does depend on the position, it is useful here to have a comparison or equilibrium reference, where an external potential $U_{\text{ext}}$ is added to the potential energy $U$ so to trap the outer monomer. In other words, again for simplicity of presentation, for the case of a dimer, $F(t) = -f(R_2 - Q)$ which derives from a confining potential around position $Q$ which holds the outer edge of the polymer.

$$m\frac{d^2R_2}{dt^2} = -\kappa(R_2 - R_1) - m\gamma\frac{dR_2}{dt} + \xi_2(t) - f(R_2 - Q)$$

$$m\frac{d^2R_1}{dt^2} = -\kappa(R_1 - R_2) - m\gamma\frac{dR_1}{dt} + \xi_1(t) \tag{6.12}$$

which would replace the dynamics of the $x$-components of the equations (6.11).

## 6.3 General method: induction and recurrence relations

In this section we show the methods and intermediate steps involved in reaching our results that will be summarized in the next three sections. The general method is always to work via iteration and to prove results by induction. More precisely, the tagged particle equation of motion is directly coupled to a second

particle which then is coupled to the other $N - 2$ particles. If we now assume that first, after integrating out these $N - 2$ particles, the effective dynamics on the second particle is of the form (6.9), then we obtain two equations: one is the GLE (6.9) (with $N$ there replaced by $N - 1$) and the other is the original equation of motion of the tagged particle coupled to the second particle. Assuming the structure (6.9) for $N - 1$ with specific properties of the memory kernel, noise and force constitutes the induction hypothesis. The remaining task is then to integrate out that last (second) particle and to prove that the induction hypothesis is indeed reproduced at size $N$. The crucial step to discover what is the correct induction hypothesis is the case $N = 2$. That is also why the essential first step is to be explicit about the case $N = 2$. We next give more details.

After integrating out $N - 2$ particles we arrive at the following GLE for the $N - 1$th monomer, which we label with subscript 2 (second particle). (Note that we skip vector notation, as we can always reduce the problem to more scalar degrees of freedom.)

$$\frac{d^2 R_2^{(N-1)}}{dt^2}(t) = -\frac{k}{m}(R_2^{(N-1)} - R_1) - \gamma \frac{dR_2^{(N-1)}}{dt}(t) + \frac{\xi_2(t)}{m} + \frac{\eta^{(N-1)}(t)}{m}$$

$$- \int_0^t dt' \mu^{(N-1)}(t - t') \frac{dR_2^{(N-1)}}{dt}(t') + \frac{G^{(N-1)}(t)}{m} \qquad (6.13)$$

The tagged monomer $R_1$ is attached to $R_2^{(N-1)}$ by a harmonic spring. The force on which is simply given by

$$\Phi^{(N)}(t) = m \frac{d^2 R_1}{dt^2}(t) = -k(R_1 - R_2^{(N-1)}) - m\gamma \frac{dR_1}{dt}(t) + \xi_1(t) \qquad (6.14)$$

where $\xi_1(t)$ and $\xi_2(t)$ are the independent white noise on monomers 1 and 2. These equations represent a system of 2 monomers, one of which is already a coarse grained variable, with memory kernel $\mu^{(N-1)}(t)$, external force $G^{(N-1)}(t)$ and noise $\eta^{(N-1)}(t)$. A second major ingredient in our computation is quite naturally to take the Laplace transform of (6.13) and (6.14). After integrating out $R_2^{(N-1)}$, we arrive at the following GLE for $R_1$,

$$\tilde{\Phi}^{(N)}(s) = -m\kappa \frac{\tilde{\mu}^{(N-1)}(s) + \gamma + s}{ms\tilde{\mu}^{(N-1)}(s) + ms\gamma + ms^2 + \kappa} [s\tilde{R}_1(s) - R_1(0)]$$

$$- m\gamma[s\tilde{R}_1(s) - R_1(0)] + \frac{\kappa}{ms\tilde{\mu}^{(N-1)}(s) + ms\gamma + ms^2 + \kappa} \tilde{G}^{(N-1)}(s)$$

$$+ m\kappa \frac{\tilde{\mu}^{(N-1)}(s) + \gamma + s}{ms\tilde{\mu}^{(N-1)}(s) + ms\gamma + ms^2 + \kappa} [R_2^{(N-1)}(0) - R_1(0)]$$

$$+ \frac{m\kappa}{ms\tilde{\mu}^{(N-1)}(s) + ms\gamma + ms^2 + \kappa} \dot{R}_2^{(N-1)}(0)$$

$$+ \kappa \frac{(\tilde{\eta}^{(N-1)}(s) + \tilde{\xi}_2(s))}{ms\tilde{\mu}^{(N-1)}(s) + ms\gamma + ms^2 + \kappa} + \tilde{\xi}_1(s) \tag{6.15}$$

That has to be confronted with (6.9) and in particular with each of the terms on the right-hand side. In that way we obtain recurrence relations for the memory kernel $\tilde{\mu}^{(N)}(s)$, the noise $\tilde{\eta}^{(N)}(s)$ and the induced force $\tilde{G}^{(N)}(s)$ on the tagged particle when comparing size $N$ polymers with size $N-1$:

$$\tilde{\mu}^{(N)}(s) = \frac{\kappa(\tilde{\mu}^{(N-1)}(s) + \gamma + s)}{(ms\tilde{\mu}^{(N-1)}(s) + ms\gamma + ms^2 + \kappa)} \tag{6.16}$$

$$\tilde{G}^{(N)}(s) = \frac{\kappa\tilde{G}^{(N-1)}(s)}{(ms\tilde{\mu}^{(N-1)}(s) + ms\gamma + ms^2 + \kappa)} \tag{6.17}$$

$$\tilde{\eta}^{(N)}(s) = m\tilde{\mu}^{(N)}(s)[R_2^{(N-1)}(0) - R_1(0)] + m\kappa \frac{\dot{R}_2^{(N-1)}(0)}{(ms\tilde{\mu}^{(N-1)}(s) + ms\gamma + s^2 + \kappa)}$$

$$+ \frac{\kappa}{(ms\tilde{\mu}^{(N-1)}(s) + ms\gamma + ms^2 + \kappa)} (\tilde{\eta}^{(N-1)}(s) + \tilde{\xi}_2(s)) \tag{6.18}$$

To these we must add "initial" conditions for the recurrence, i.e., to insert the findings for the case $N = 2$. These will enable the correct induction hypothesis. Finally, there are the initial conditions to the dynamics; the initial conditions (positions and momenta) of all the other particles (except the tagged particle) contribute to the noise. Their statistical distribution is in principle a matter of choice but there are of course dynamically more natural choices. We will detail them in Appendix A.1.

## 6.4   Free diffusion under uniform driving

This and the two following sections summarize the main results of the logic explained in the previous Section. We always refer to (6.9) for the notation, that we have obtained after integrating out all but one of the particles.

### 6.4.1   In general

Referring to the dynamics (6.6)–(6.8)–(6.10), we define the frequency $\omega$ as $\omega^2 = \frac{\kappa}{m} - \frac{\gamma^2}{4}$. If $\omega$ is real (inertial case), then the friction kernel $\mu^{(N)}$ is oscillating with frequency $\omega$ with decreasing amplitude. When under high friction, $\omega$ is imaginary (overdamped case), there is monotone decay in time.
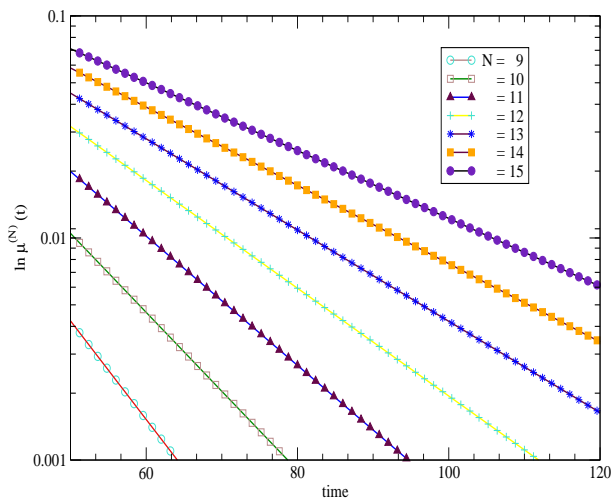


Figure 6.1: Memory vs time for $\kappa = 3, \chi = 1$. The long time limit of memory in a semi-log plot. The data points are a result of a numerical simulation of the eq. (6.16). The solid lines are curves fitting the data. The different colors represent different polymer sizes.

In the long time limit we find that the friction kernel is always exponentially decaying as $\mu^{(N)}(t) \leq e^{-t/\tau_N}$ for large times $t$, where the decay time $\tau_N$ is of

the order $N^2$ for large $N$, see Fig. 6.1. In the figures are represented polymers of different sizes. The discrete data points are solutions of numerical evaluation of analytical results. The lines are fits exhibiting the general nature of these solutions. $\kappa$ is the spring constant and $\chi = m\gamma$. Fig. 6.1 is a semi-log plot, which shows the exponential decay of the friction kernel in long time. The slopes of various lines are proportional to the decay exponent $\tau_N$. It is seen in Fig. 6.1 that $\tau_N$ varies as $N^{-2}$, which is already known to hold in full equilibrium [106]. We show that this remains valid in nonequilibrium. We have also obtained that the time of relaxation is in general bounded from below as $\tau_N > 2/\gamma$, see below in Appendix A.2. This is indeed clear as the time of relaxation grows with the size of the polymer and the tagged particle relaxes fastest when it is connected to just one another monomer, $\tau_N$ then being $2/\gamma$.
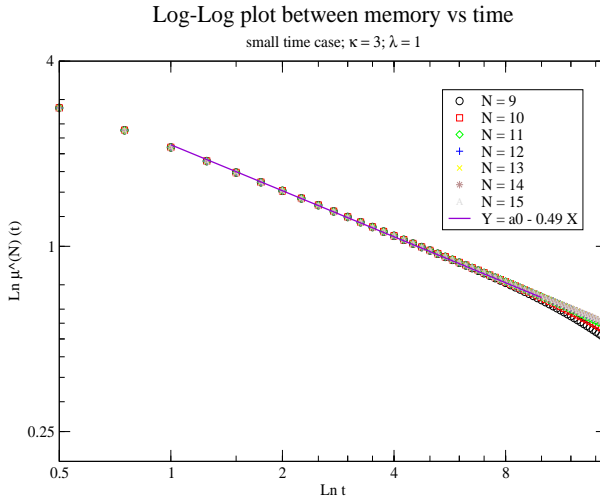


Figure 6.2: The short time behavior of memory in a log-log plot.
The data points are a result of a numerical simulation of the eq. (6.16).
The solid lines are curves fitting the data. The different colors represent different polymer sizes.

As is well known and is also to be expected under nonequilibrium conditions, for short times $t < \tau_N$, the memory kernel has a power law decay $\mu(t) \propto \frac{1}{t^{1/2}}$, see also [33, 30, 106]. Indeed, as seen in the log-log plo 6.2, for short times there is no dependence of memory on system size.

Integrating out the other monomers also creates additional colored noise in the system. The noise $\eta^{(N)}(t)$ is Gaussian with a shifted average and is breaking the second fluctuation–dissipation relation transiently. However asymptotically, the stationary covariance satisfies the second fluctuation-dissipation relation

$$\lim_{t \to \infty} \langle \eta(t + \tau)\eta(t) \rangle = \frac{m}{\beta} \mu(\tau) \tag{6.19}$$

Finally, the external force $f$ on the outer monomer gives rise to a time-dependent statistical force $G(t)$ on the tagged monomer and reaches exponentially-fast a limiting form. The general behavior is exactly similar to what we make explicit in the next subsection; see below in Eq. (6.23).

## 6.4.2  Two monomer case

To give immediately more explicit formula we summarize the results for the dimer-case, which is also used to start the recurrence. First the memory kernel $(N = 2)$,

$$\mu(t) \quad = \quad \frac{\kappa}{m} e^{-\gamma t/2} \left[ \cos \omega t + \frac{\gamma}{2\omega} \sin \omega t \right] \tag{6.20}$$

$$\text{where} \quad \omega^2 = \frac{\kappa}{m} - \frac{\gamma^2}{4} > 0$$

For a dimer, a power law decay for small time is not seen, as can be imagined from the fact that a dimer in one dimension has no conformational degrees of freedom. The mean squared end–to–end distance $\langle R_{ee}^2 \rangle$ is simply equal to the square of the bond length and thus shows only simple diffusion.

The colored noise is

$$\eta(t) \quad = \quad -\kappa [R_1(0) - R_2(0)][\cos(\omega t) + \frac{\gamma}{2\omega} \sin(\omega t)] e^{-\gamma t/2}$$

$$+ \quad \kappa \dot{R}_2(0) \frac{\sin(\omega t)}{\omega} e^{-\gamma t/2}$$

$$+ \quad \frac{\kappa}{m} \int_0^t \frac{\sin(\omega(t - t'))}{\omega} \xi_2(t') e^{-\gamma(t-t')/2} dt' \tag{6.21}$$

It is natural to take the distribution

$$\rho_{st}(R_2, \dot{R}_2) = \frac{1}{Z} e^{-\beta H} \tag{6.22}$$

where $H = \frac{m\dot{R_2}^2}{2} + \frac{\kappa}{2}(R_1 - R_2)^2 - fR_2$ that depends on the position $R_1$ of the tagged particle. When averaged over that initial distribution (6.22) we get a mean

$$\langle \eta(t) \rangle = f[\cos(\omega t) + \frac{\gamma}{2\omega} \sin(\omega t)]e^{-\gamma t/2}$$

which is not zero for $f \neq 0$. Indeed, the monomer $R_2$ is found more on one side than the other due to the force $f$. The effective force is found to be

$$G(t) = f[1 - e^{-\gamma t/2}(\cos(\omega t) + \frac{\gamma}{2\omega} \sin(\omega t))] \tag{6.23}$$

exponentially growing to the applied force $f$. When the force would be time dependent, $f = f_t$, the effective force gets memory and becomes

$$G(t) = k \int_0^t f_s \, e^{-\gamma(t-s)/2} \sin \omega(t - s) \, ds$$

That appears to be a general feature of nonequilibrium forcing; they create effective forces that themselves depend on the forcing at all earlier times. We still emphasize that the nature of nonequilibrium in this work and in the present example of constant forcing is qualitatively different from the case of driving forces discussed in some previous works [105], polymer translocation by an external force being one example. Such driving forces are introduced at the macroscopic level or the level of the GLE and hence do not have effect on the nature of the friction kernel or of the noise. On the other hand the nonequilibrium in our work is introduced microscopically, such that the GLE itself gets modified as a function of the driving.

### 6.4.3 Limiting cases

1. **The long time limit.** Motion after $t \gg \tau_N$, of the tagged particle appears to be diffusive with a constant drift $f$.

2. **Large coupling limit.** A large coupling signifies that the restoring force between any two monomers is very strong and hence the monomers undergo high frequency oscillations given by $\omega \simeq \sqrt{\frac{k}{m}} \to \infty$. Measurements will typically time–average over a few periods. The time-averaged behavior of the tagged monomer is again of a Brownian particle acted on by a constant force. The effective force goes to the constant force $f$. The time averaged total noise goes to white noise $\xi_1(t)$ and the time averaged memory kernel $\mu(t)$ disappears.

3. **The overdamped limit.** The high friction limit refers to the case when the viscosity of the medium is so high that the acceleration of the

monomers is zero, and the only variables which are changing are position. To take the overdamped limit in a meaningful manner, together with taking the friction coefficient $\gamma$ to infinity one has to take the mass $m$ of all monomers to zero, preserving the product $\chi = m\gamma$ to be finite. The memory kernel then reduces to

$$\mu(t) = ke^{-kt/\chi} \tag{6.24}$$

The memory kernel after taking the continuum limit is

$$\mu(t) = 2\sqrt{\frac{\pi\chi k}{t}}e^{-t/\tau} \tag{6.25}$$

where $\tau = N^2\chi/(\pi^2 k)$, as shown before [106] under equilibrium dynamics.

## 6.5 Non-uniform driving

We are now in two dimensions with forcing at one end of the polymer in the horizontal direction with an amplitude that is proportional to the vertical distance. That dependence is similar to a shearing force, but we do not insist here on the presence of a fluid (as we treat the Rouse model and not e.g. the Zimm model). Rather, we have in mind that we can manipulate the outer monomer of a polymer in a melt in a non-uniform way. To a good approximation, that would be the case when nanoparticles are attached to the polymer and undergo non-rigid rotation, where the angular velocity depends on the radial distance (here, the vertical distance). An interesting result here is that the friction kernel $\mu^{(N)}(t)$ is identical to the case of constant forcing (previous section). To be explicit and without loss of essential information we can already state the results for $N = 2$. The memory kernel in each direction is given by

$$\mu_{1x}(t) = \mu_{1y}(t) = \frac{\kappa}{m}e^{-\gamma t/2}[\cos(\omega t) + \frac{\gamma}{2\omega}\sin(\omega t)]$$

which is indeed the same as for a dimer in free space under constant forcing. That is due to the fact that the external forcing does not couple to velocity but only to position. The nature of $\mu$ in the two mutually perpendicular directions and various limits hence remains the same.

The nature of the induced noise however gets modified due to the different nature of the external force. The noise in general is dependent on the initial positions and velocities of all the monomers, and hence picks up additional contributions from the external force which is coupled to the $y$ component of the position of the first monomer. Here is the explicit noise function

$$\eta_{1x}(t) = -\kappa[R_{1x}(0) - R_{2x}(0)](\cos(\omega t) + \frac{\gamma}{2\omega}\sin(\omega t))e^{-\gamma t/2}$$

$$+ \kappa\dot{R}_{2x}(0)e^{-\gamma t/2}\frac{\sin(\omega t)}{\omega}$$

$$+ \frac{\kappa}{m}\int_0^t e^{-\gamma(t-t')/2}\frac{\sin(\omega(t-t'))}{\omega}\xi_{2x}(t')dt'$$

$$+ \frac{f}{m\omega}\kappa\int_0^t dt' e^{-\gamma(t-t')/2}sin(\omega(t-t'))[R_{2y}(0)(\cos(\omega t')+$$

$$\frac{\gamma}{2\omega}\sin(\omega t')) + \dot{R}_{2y}(0)\frac{\sin(\omega t')}{\omega}] \tag{6.26}$$

$$+ \frac{f}{m\omega}\frac{\kappa}{m\omega}\int_0^t\int_0^{t'} dt'dt'' e^{-\gamma(t-t'')/2}\sin(\omega(t-t'))\sin(\omega(t'-t''))\xi_{2y}(t'')$$

Putting $f = 0$ in (6.26) gives us back the noise on a polymer under constant force (6.21). The external force couples the $x$ component of noise to the dynamics in $y$ direction. The initial positions in the $y$-direction as well as the component of the white noise $\xi_{2y}(t)$ in the $y$-direction now play a role in the dynamics in the $x$-direction of the second monomer. The $y$-component of the noise remains unaffected by the force, since the external force does not couple to the motion in the $y$-direction.

$$\eta_{1y}(t) = -\kappa[R_{1y}(0) - R_{2y}(0)](\cos\omega t + \frac{\gamma}{2\omega}\sin\omega t)e^{-\gamma t/2}$$

$$+ \kappa\dot{R}_{2y}(0)e^{-\gamma t/2}\frac{\sin(\omega t)}{\omega}$$

$$+ \frac{\kappa}{m}\int_0^t e^{-\gamma(t-t')/2}\frac{\sin(\omega(t-t'))}{\omega}\xi_{2y}(t')dt'$$

$$\tag{6.27}$$

Now we come to the induced force. The $x-$component of the effective force is

$$
\begin{aligned}
G_{1x}(t) &= f \frac{\kappa^2}{m^2\omega^2} \int_0^t dt' \int_0^{t'} dt'' e^{-\gamma(t-t'')/2} \sin(\omega(t-t')) \\
&\qquad \sin(\omega(t'-t''))R_{1y}(t'')
\end{aligned}
\tag{6.28}
$$

Again, as a nonequilibrium effect, the effective force has memory. On the other hand its $y$-component $G_{1y}(t)$ stays zero. Indeed, since the applied force itself is acting in the $x$-direction, there is no reason why the effective dynamics in the $y$-direction of the tagged monomer should get affected by it.

Let us now go to the results for general $N$. The memory kernels $\tilde{\mu}_x^{(N)}(s)$ and $\tilde{\mu}_y^{(N)}(s)$ look as they did in the case of constant force (6.16), with the same "initial" conditions. The recurrence relation for the colored noise picks up changes due to shearing, similar as discussed under (6.26) and (6.27); they arise due to the fact that the non-uniform forcing couples the $x$ and $y$ components of motion.

$$
\tilde{\eta}_x^{(N)}(s) = m\tilde{\mu}_x^{(N)}(s)[R_x^{(N-1)}(0) - R_x(0)] + \frac{m\kappa}{(ms\tilde{\mu}_x^{(N-1)}(s) + ms\gamma + s^2 + \kappa)}\dot{R}_x^{(N-1)}(0)
$$

$$
+ \frac{\kappa}{(ms\tilde{\mu}_x^{(N-1)}(s) + ms\gamma + ms^2 + \kappa)}(\tilde{\eta}_x^{(N-1)}(s) + \tilde{\xi}_x^{(N-1)}(s))
$$

$$
+ f\frac{\kappa^3}{m^3}\frac{\{[s + \gamma + \tilde{\mu}_y^{(N-1)}(s)]R_y^{(N-1)}(0) + \dot{R}_y^{(N-1)}(0)\}}{[s^2 + \gamma s + \frac{\kappa}{m} + s\tilde{\mu}_x^{(N-1)}][s^2 + \gamma s + \frac{\kappa}{m} + s\tilde{\mu}_y^{(N-1)}][s^2 + \gamma s + \frac{\kappa}{m}]}
$$

$$
+ f\frac{\kappa^3}{m^3}\frac{\{\tilde{\xi}_y^{(N-1)}(s)/m + \tilde{\eta}_y^{(N-1)}(s)/m\}}{[s^2 + \gamma s + \frac{\kappa}{m} + s\tilde{\mu}_x^{(N-1)}][s^2 + \gamma s + \frac{\kappa}{m} + s\tilde{\mu}_y^{(N-1)}][s^2 + \gamma s + \frac{\kappa}{m}]}
$$

The most interesting aspect of the non-uniform case is the appearance of memory in the induced force. We have already seen this in the case of two-monomers (6.28). This behavior persists in general with,

$$
\tilde{F}_x^{(N)}(s) = \tilde{G}_x^{(N)}(s)\tilde{R}_y^{(N)}(s)
\tag{6.29}
$$

$$\tilde{G}_x^{(N)}(s) = \frac{\kappa^2 \tilde{G}_x^{(N-1)}(s)}{[ms^2 + \gamma s + k + ms\tilde{\mu}_x^{(N-1)}(s)][ms^2 + \gamma s + k + ms\tilde{\mu}_y^{(N-1)}(s)]}$$

(6.30)

Starting the recurrence with a single monomer where $\tilde{G}_x^{(1)}(s) = f$, all subsequent forces can be determined using equations (6.29)–(6.30). The initial force on a single monomer in the $y$-direction is zero, hence $\tilde{F}_y^{(N)}(s) = 0$ as also seen in the two monomer case.

We studied the asymptotic behavior of the force-memory kernel $\tilde{G}_x^{(N)}(s)$ in the same spirit as in Appendix A.2. It can be shown easily following the same line of arguments that $\tilde{G}_x^{(N)}(s)$ decays exponentially in time. In the long time limit, for all $N$,

$$G_x^{(N)}(t) < e^{-\gamma t/2}$$

## 6.6 Trapped monomer

Upon introducing an external potential $U_{\text{ext}}$ such that the force in the $x$-direction on the outer edge depends on the $x$-component of the distance of the monomer from a fixed origin, the resulting force is not non-conservative but simply trapping. That is thus an equilibrium reference; the force is conservative in nature. The result a rescaling of the frequency $\Omega^2 = \frac{k+f}{m} - \frac{\gamma^2}{4}$. The effective force on the tagged monomer due to the action of this external potential is

$$F(t) = -\frac{\kappa f}{\kappa + f} R_1(t) + \frac{\kappa f Q}{\kappa + f}\{1 - e^{-\gamma t/2}(\cos \Omega t + \frac{\gamma}{2\Omega} \sin \Omega t)\}$$

(6.31)

We recognize the effective spring replacing two springs connected in series,

$$\frac{1}{\kappa_{eff}} = \frac{1}{\kappa} + \frac{1}{f}$$

This is another way to understand the net restoring force on $R_1$. After all it looks like a trapping potential around the origin but of strength $\kappa_{eff}$. The

colored noise due to unknown initial conditions is

$$
\begin{aligned}
\eta_1(t) \;=\;& \frac{\kappa^2}{\kappa+f}(R_2(0)-R_1(0))e^{-\gamma t/2}(\cos\Omega t + \frac{\gamma}{2\Omega}\sin\Omega t) \\[2mm]
+\;& \frac{\kappa f}{k+f}R_2(0)e^{-\gamma t/2}(\cos\Omega t + \frac{\gamma}{2\Omega}\sin\Omega t) \\[2mm]
+\;& \kappa\dot{R}_2(0)e^{-\gamma t/2}\frac{\sin\Omega t}{\Omega} \\[2mm]
+\;& \frac{\kappa}{m}\int_0^t e^{\gamma(t-t')/2}\xi_2(t')\frac{\sin(\Omega(t-t'))}{\Omega}dt'
\end{aligned}
\tag{6.32}
$$

where $\langle\eta_1(t)\rangle^{R_1}_{\rho_{st}} = \frac{\kappa f Q}{\kappa+f}e^{-\gamma t/2}(\cos(\Omega t) + \frac{\gamma}{2\Omega}\sin\Omega t)$ for distribution

$$
\rho_{st}(R_2) = \frac{1}{Z}e^{-\beta\frac{(\kappa+f)}{2}(R_2 - \frac{(\kappa R_1 + fQ)}{\kappa+f})^2}e^{\beta\frac{(\kappa R_1 + fQ)^2}{2(\kappa+f)}}e^{-\beta\frac{(\kappa R_1^2 + fQ^2)}{2}}
$$

The memory kernel is given as

$$
\mu(t) = \frac{k^2}{m(k+f)}e^{-\gamma t/2}(\cos\Omega t + \frac{\gamma}{2\Omega}\sin\Omega t)
\tag{6.33}
$$

Given the conservative nature of the forces, the second fluctuation-dissipation theorem is seen to hold:

$$
\langle\eta_1(t_1)\eta_1(t_2)\rangle_\rho = \frac{m}{\beta}\mu(\tau)
$$

where $\tau = t_1 - t_2$ and $t_1 + t_2 \longrightarrow \infty$.

## 6.7   Conclusions and outlook

Integrating out degrees of freedom introduces non-Markovian noise, effective forces and memory in a tagged particle dynamics. That is true in equilibrium as in nonequilibrium, and, when starting from coupled diffusion processes, the result is a generalized Langevin equation. Certain more detailed aspects are also unchanged, like the anomalous nature of the memory kernel for short times which goes into pure diffusion for long times, or the $N^2$ dependence of the relaxation times. Other important aspects fundamentally change when the integration is over nonequilibrium degrees of freedom. Naturally, the remaining

and visible degrees of freedom inherit nonequilibrium features and detailed balance gets broken. As a result, the so called second fluctuation-dissipation theorem or Einstein relation gets violated. For the moment however, there is no systematic understanding of exactly *how* that Einstein relation is modified. To put it differently, when considering a diffusion model for a particle (e.g. colloids) in a nonequilibrium environment such as the visco-elastic medium of the cell, we have little idea of how to relate the noise with the friction term, be that they have the same physical origin [18]. The outlook is then to find the analogue of what has been called the frenetic contribution to the first fluctuation-dissipation theorem [11]. Indeed we expect a non-entropic and more kinetic contribution in the breaking of the second fluctuation-dissipation theorem, much like discussed for the modification of the Sutherland-Einstein relation [94]. For the moment however, we must deal with examples and prototypical examples, such as the Rouse model of the present work, where exact computations are possible. There indeed, say in the case of non-uniform driving, the second fluctuation-dissipation relation is broken, but for the uniform driving that is only a transient effect as found in (6.19). A more general theory will of course need to conform to the findings of the present work. A second set of more general research questions really inverts the calculations of the present work. The aim is then to be able to reconstruct the nonequilibrium forcing on the hidden degrees of freedom from the effective motion of the probe or tagged or visible degrees of freedom. The standard example from equilibrium statistical mechanics is the free energy of a thermodynamic system which can be measured from the work on some probe that is coupled to the system. For nonequilibrium statistical mechanical systems there are plenty of nonequilibrium entropies and fluctuation functionals, [91] but so far, no solid and general operational meaning has been attached to them. We would again like to determine these nonequilibrium fluctuation functionals from the effective forces on probes. In the present work it would mean to reconstruct important nonequilibrium features of the full polymer dynamics from the motion and effective dynamics of the tagged monomer. Clearly, before that program can start, the direct question as in the work must be sufficiently understood. We conclude that the Rouse dynamics provides an interesting and important playground for questions that in the future must be addressed in the construction of a nonequilibrium statistical mechanics.

# Chapter 7

# Conclusions & Outlook

## 7.1 Stochastic process and the No-go theorem

We studied some aspects of nonequilibrium forces on effective or coarse grained dynamics of macro observables. This thesis is broadly divided into two parts. In the first part, we explored Stochastic processes in general and time-dependent Markov processes in particular. The action of periodic external driving on systems existing on a finite state space was studied. We considered the jump dynamics such that the external driving makes the escape rates $\lambda_t(x)$ change with time but the transition probabilities $p(i,j)$ of jump remain time-independent,

$$w_t(i,j) = \lambda_t(i)p(i,j)$$

When expressing the rates in the form of the Arrhenius rate law, the time dependent rates can be interpreted as

$$w_t(i,j) = \mathcal{A}(i,j)e^{\beta G_t(i)}, \; \mathcal{A}(i,j) = \mathcal{A}(j,i)$$

with periodic time-dependent energy wells $G_t(i)$ and the constant energy barriers as represented by the symmetric factors $\mathcal{A}(i,j)$.

The dynamics is time dependent and detailed balance is broken. Yet, we show that for this particular time-dependence of the rates, the net time-averaged current over a long time is zero.

$$J(i,j) = \lim_{T \to \infty} \frac{1}{T} \int_0^T j_t(i,j) dt = 0$$

where $j_t(i,j)$ is the instantaneous current.

This is called the No-go Theorem. This effect arises because the specific time-dependent driving is such that the time-averaged dynamics becomes detailed balanced in the long-time limit. If the reference dynamics itself breaks detailed balance, the time-averaged current is a mere *global multiple* of the steady reference current.

## 7.2 Statistical forces in equilibrium and nonequilibrium

In the second part of the thesis we were concerned more generally with the study of coarse grained dynamics of an intruder in a bath and in particular with the nature of Statistical or fluctuation-induced forces that arise due to the action of the bath on the intruder. Statistical forces are a consequence of the action of large numbers. We discussed first some familiar examples of Statistical forces. In Equilibrium Thermodynamics, they have been known to us as Thermodynamic forces, such as pressure and chemical potential.

We pursued the programme in equilibrium in Chaper 5. We systematically studied the variations of Buoyancy in granular media and in particular studied the influence of various time scale separations on Statistical forces. In this context, two cases were considered:

- **In the Fluid limit:** There is a large time scale separation between the bath and the intruder dynamics. The result of which is that the bath dynamics is at all times in stationarity conditioned on the state of the intruder. The effective dynamics was Markovian and the Statistical force on the intruder was recovered as the Buoyant force of a fluid of density $d(y)$ on an intruder of size $N$.

$$F_B = d(y)Ng$$

- **Before the Fluid limit:** The time scales of the bath and the intruder are comparable. As a result an effective non-Markovianity was introduced in the intruder dynamics. The Statistical force consisted of the Buoyant force, corrected by an induced frictional or drag force.

The programme in nonequilibrium was followed in two cases: A Markov jump process and a Diffusion process.

We studied two kinds of forcing on a Rouse polymer in an equilibrium bath: a uniform force $f$ at one end of the polymer, a non-uniform shear force. The observable was a tagged monomer in the polymer, for which an effective equation of motion was arrived at by coarse graining all the other monomers in the polymer. The effective dynamics of the tagged monomer was governed by a Generalized Langevin equation. Additional memory term $\mu(t)$ and colored noise $\eta(t)$ were a consequence of the coarse graining.

In general, for both equilibrium and nonequilibrium driving, in short times, the motion of the tagged monomer was anomalous diffusion, which turned diffusive in long time. The effective force on the tagged monomer is in general time dependent. In equilibrium this force is Markovian. Also, in equilibrium the second fluctuation-dissipation was satisfied for the memory term $\mu(t)$ and colored noise $\eta(t)$.

The most interesting nonequilibrium feature was the appearance of non-Markovianity in the resultant force. A general characteristic of non-conservative or time dependent force is that the effective force depends on the history of the dynamics itself.

We conclude that Statistical forces in general, for Markov jump processes can be expressed

$$F_{\text{Stat}}(x, x') = -\frac{1}{\beta}\log\left[\frac{\chi(\text{x}, \text{x}')}{\chi(\text{x}', \text{x})}\right]$$

where $\chi(x, x')$ are the effective jump rates of the observed process.

In general
$$F_{\text{Stat}}(x) = -\nabla V_f(x) + \nabla \times A_f(x)$$

statistical force can be expressed as a sum of conservative and non-conservative parts. They are both dependent on $f$, the nonequilibrium driving and are not related to the generalized free energies in any simple manner. The effective dynamics in nonequilibrium also depends on the symmetric parts of the rates

and hence the Statistical forces were seen to contain features of average escape rates, which is not true in equilibrium.

In equilibrium

$$F_{\text{Stat}}(x) = -\nabla \mathcal{F}(x)$$

statistical force is the gradient of a generalized free energy.

## 7.3   Looking Ahead

There are several directions to go starting from here. The effective dynamics is arrived at by coarse graining the dynamics of the bath. This coarse graining can be made more systematic so that more than first order corrections around the fluid limit can be obtained. Systematic approaches such as projection operator methods are being put into use to better understand the non-Markovianity in the effective motion of the intruder.

We studied the Statistical force on a single intruder or a single tagged particle in a bath. There exist interesting collective effects, where attractive or repulsive forces arise between multiple intruders in a bath as a result of fluctuations in the bath. These collective effects, as seen in granular media can also be explored when the bath has some nonequilibrium driving in it.

More broadly speaking, Statistical forces are a window to the underlying microscopic dynamics whose fluctuations they mirror. A more generalized frame work starting from Statistical forces can be build, which would render information about the microscopic dynamics. By studying the nature of Statistical forces, information could be gathered about the nature of conservative and non-conservative forces in the bath. Not only that, Statistical forces in nonequilibrium are related to dynamical fluctuations functionals in the bath. A general frame work can be build to relate the two. A related project is to connect the corrections in the second fluctuation theorem in nonequilibrium to the gradient and the non-gradient parts of the Statistical force.

# Appendix A

## A.1 Deriving the long time behavior of statistical force in Laplace space

Let us confine to the case of constant forcing. The initial conditions for the recurrence are $\tilde{\mu}^{(1)}(s) = 0$; $\tilde{G}^{(1)}(s) = f/s$ ; $\tilde{\eta}^{(1)}(s) = 0$.

The stationary distribution of $R_2^{(N-1)}(0)$ given $R_1(0)$ is given by

$$\rho_{st} = \frac{1}{Z} e^{-\beta H_{st}}$$

where

$$H_{st} = \frac{\kappa}{2}[R_2^{(N-1)}(0) - R_1(0)]^2 - G_{st}^{(N-1)} R_2^{(N-1)}(0)$$

where we take it that external force has always been on. Of course, it is also important here to separate transient from stationary behavior. For example, for the force on $q_2$, we have at stationarity $G_{st}^{(N-1)} = \lim_{t\to\infty} G^{(N-1)}(t)$ and as an illustration we will show using recurrence that in the case of constant forcing it always equals the originally applied force $G_{st}^{(N-1)} = f$.

We start from the relation

$$\lim_{t \longrightarrow \infty} G^{(N-1)}(t) = \lim_{s \longrightarrow 0} s\tilde{G}^{(N-1)}(s)$$

141

The recurrence relation for the force (6.17) starts from a dimer,

$$\tilde{G}^{(2)}(s) = \frac{\kappa \tilde{G}^{(1)}(s)}{(ms\tilde{\mu}^{(1)}(s) + ms\gamma + ms^2 + \kappa)}$$

$$= \frac{\kappa f}{s(ms\gamma + ms^2 + \kappa)}$$

By a simple calculation it is seen that

$$\lim_{s \longrightarrow 0} s\tilde{G}^{(2)}(s) = f$$

If now for a polymer of size $N - 2$ (induction hypothesis)

$$\lim_{s \longrightarrow 0} s\tilde{G}^{(N-2)}(s) = f$$

We can use the recurrence relation and the property $\lim_{s \longrightarrow 0} s\tilde{\mu}^{(N)}(s) = 0$ shown in A.2, to see that also

$$\lim_{s \longrightarrow 0} s\tilde{G}^{(N-1)}(s) = f$$

as wanted. The stationary distribution thus is given by

$$\rho_{st} = \frac{1}{Z} e^{-\beta(\frac{\kappa}{2}(R_2^{(N-1)}(0) - R_1(0)^2) - fR_2^{(N-1)}(0))} \tag{A.1}$$

The mean noise is

$$\langle \tilde{\eta}_1^{(N)}(s) \rangle_{st} = m\frac{f}{\kappa} \tilde{\mu}_1^{(N)}(s)$$

## A.2   Asymptotic behavior of memory

We show here that the memory kernel $\tilde{\mu}^{(N)}(s)$ decays exponentially in the long time limit, again by recurrence. We take the constant force case as simplest example. From (6.20) we see that for a dimer

$$\lim_{t \to \infty} e^{\lambda t} \mu^{(2)}(t) = 0 \text{ for } \lambda < \gamma/2$$

which translates to

$$\lim_{s \to 0} s\tilde{\mu}^{(2)}(s - \lambda) = 0 \tag{A.2}$$

in the Laplace space. Let us assume that for a polymer of size $N - 1$

$$\lim_{s \to 0} s\tilde{\mu}^{(N-1)}(s - \lambda) = 0 \text{  (induction hypothesis)} \tag{A.3}$$

and let us choose $\lambda = \gamma/4$. That would show that for a polymer of size $N$,

$$\lim_{s \to 0} s\tilde{\mu}^{(N)}(s - \gamma/4) = \lim_{s \to 0} s \frac{\kappa(\tilde{\mu}^{(N-1)}(s - \gamma/4) + \gamma + s - \gamma/4)}{(s - \gamma/4)(m\tilde{\mu}^{(N-1)}(s - \gamma/4) + m\gamma + m(s - \gamma/4) + \frac{\kappa}{(s-\gamma/4)})}$$

$$= \lim_{s \to 0} 3s\gamma/4 = 0 \tag{A.4}$$

where we have used recurrence relation (6.16) and hypothesis (A.3) and the fact that $\lim_{s \to 0} \tilde{\mu}^{(N)}(s)$ is a constant, as is easy to show. The above result translates to

$$\lim_{t \to \infty} e^{\gamma t/4} \mu^{(N)}(t) = 0$$

Hence in the long time limit, for all $N$,

$$\mu^{(N)}(t) < e^{-\gamma t/2}$$

which also proves the claim made in 6.4.1 that the time of relaxation is bounded from below by $2/\gamma$.

## A.3 Second fluctuation-dissipation relation in Laplace Space

The second fluctuation–dissipation relation says that the stationary noise auto-correlation function is proportional to the memory kernel $\mu(t)$ through inverse temperature $\beta$,

$$\langle \eta(t)\eta(t + \tau) \rangle = \frac{m}{\beta}\mu(\tau) + O(\frac{1}{t}, \tau) \tag{A.5}$$

such that in the long time limit all terms of the order $1/t$ or greater drop out. We continue by deriving that relation in Laplace space. Let $s$ be the variable in the Laplace space, domain $|Re\{s\}| < \gamma/2$, such that the Laplace transform is well defined; see Appendix A.2.

$$\langle\tilde{\eta}(s)\tilde{\eta}(s')\rangle = \int_0^\infty \int_0^\infty e^{-st}e^{-s't'}\langle\eta(t)\eta(t')\rangle dtdt'$$

Let $t' = t + \tau$

$$= \int_0^\infty e^{-st}dt \int_{-t}^\infty e^{-s't}e^{-s'\tau}\langle\eta(t)\eta(t+\tau)\rangle d\tau$$

$$= \int_0^\infty e^{-(s+s')t}dt \int_{-t}^\infty e^{-s'\tau}\langle\eta(t)\eta(t+\tau)\rangle d\tau$$

Let $(s + s')t = T$ (A.6)

$$= \frac{1}{s+s'} \int_0^\infty e^{-T}dT \int_{-\frac{T}{s+s'}}^\infty e^{-s'\tau}\langle\eta(\frac{T}{s+s'})\eta(\frac{T}{s+s'}+\tau)\rangle d\tau$$

Rewriting (A.5) and plugging in the result in (A.6)

$$\langle\eta(\frac{T}{s+s'})\eta(\frac{T}{s+s'}+\tau)\rangle = \frac{m}{\beta}\mu(\tau) + O(s+s')$$

$$\langle\tilde{\eta}(s)\tilde{\eta}(s')\rangle = \frac{1}{s+s'} \int_0^\infty e^{-T}dT \int_{-\frac{T}{s+s'}}^\infty e^{-s'\tau}(\frac{m}{\beta}\mu(\tau) + O(s+s'))d\tau$$

Hence,

$$\lim_{s+s'\to 0}(s+s')\langle\tilde{\eta}(s)\tilde{\eta}(s')\rangle = \frac{m}{\beta} \int_{-\infty}^\infty e^{-s'\tau}\mu(\tau)d\tau$$

$$= \frac{m}{\beta}(\tilde{\mu}(s) + \tilde{\mu}(-s)) \tag{A.7}$$

is the form of the second fluctuation-dissipation relation in Laplace space.

## A.3.1 Proof by induction

We prove our claim that the second fluctuation-dissipation relation holds in case of constant force, for a polymer of general size $N$. We give the explicit calculation for the case of a dimer. Given memory kernel (6.16) and noise

(6.18), which is distributed as $\rho_{st}(R_2, \dot{R}_2)$ as given in (A.1), one can calculate the correlation function $\langle \tilde{\eta}^{(2)}(s)\tilde{\eta}^{(2)}(s')\rangle_{st}$. Using the relation

$$\lim_{s+s'\to 0}(s+s')\langle \tilde{\xi}_i(s)\tilde{\xi}_j(s')\rangle = \frac{2m\gamma}{\beta}\delta_{ij} \tag{A.8}$$

it is shown by a simple calculation that

$$\lim_{s+s'\to 0}(s+s')\langle \tilde{\eta}^{(2)}(s)\tilde{\eta}^{(2)}(s')\rangle = \frac{m}{\beta}\{\tilde{\mu}_2(s) + \tilde{\mu}_2(-s)\} \tag{A.9}$$

which proves the result. To prove it for a general polymer, we use the induction hypothesis that for a polymer of size $N-1$ the second fluctuation-dissipation relation holds:

$$\lim_{s+s'\to 0}(s+s')\langle \tilde{\eta}^{(N-1)}(s)\tilde{\eta}^{(N-1)}(s')\rangle_{st} = \frac{m}{\beta}\{\tilde{\mu}^{(N-1)}(s) + \tilde{\mu}^{(N-1)}(-s)\}$$

From the recurrence relations (6.18) and from (A.8), one easily shows that

$$J = m(s(\tilde{\mu}^{(N-1)}(s) + \gamma + s) + \frac{\kappa}{m})(-s(\tilde{\mu}^{(N-1)}(-s) + \gamma - s) + \frac{\kappa}{m})$$

$$\langle \tilde{\eta}^{(N)}(s)\tilde{\eta}^{(N)}(s')\rangle_{st} = \frac{k_B T\kappa^2(\tilde{\mu}^{(N-1)}(s) + \tilde{\mu}^{(N-1)}(-s))}{J}$$

$$+ \frac{2k_B T\gamma\kappa^2}{J}$$

with $s + s' \to \infty$.

Using the recurrence relations for memory (6.16),

$$\tilde{\mu}^{(N)}(s) + \tilde{\mu}^{(N)}(-s) = \frac{\kappa^2(\tilde{\mu}^{(N-1)}(s) + \tilde{\mu}^{(N-1)}(-s))/m^2}{J}$$

$$+ \frac{2\kappa^2\gamma/m^2}{J}$$

which proves the claim. Therefore, the second fluctuation-dissipation relation holds for a polymer of arbitrary size under the action of a constant force.

In the case of non-uniform forcing, we are in two dimensions and the computations become more involved, but the basic recurrence relations remain in place.

# Bibliography

[1] ALAM, M., TRUJILLO, L., AND HERRMANN, H. J. Hydrodynamic theory for reverse brazil nut segregation and the non-monotonic ascension dynamics. *Journal of statistical physics 124*, 2-4 (2006), 587–623.

[2] ALBERTI, P., AND MERGNY, J.-L. Dna duplex–quadruplex exchange as the basis for a nanomolecular machine. *Proceedings of the National Academy of Sciences 100*, 4 (2003), 1569–1573.

[3] ALEXANDER, F., AND LEBOWITZ, J. On the drift and diffusion of a rod in a lattice fluid. *Journal of Physics A: Mathematical and General 27*, 3 (1994), 683.

[4] ALEXANDER, F. J., AND LEBOWITZ, J. L. Driven diffusive systems with a moving obstacle: a variation on the brazil nuts problem. *Journal of Physics A: Mathematical and General 23*, 8 (1990), L375.

[5] ARANSON I.S., T. L. *Granular Patterns.* Oxford University Press, 2009.

[6] ARCHIMEDES. On the equilibrium of planes or the centers of gravity of planes.

[7] ASAKURA, S., AND OOSAWA, F. Interaction between particles suspended in solutions of macromolecules. *Journal of Polymer Science 33*, 126 (1958), 183–192.

[8] ASTUMIAN, R. D. Adiabatic pumping mechanism for ion motive atpases. *Phys. Rev. Lett. 91*, 11 (2003), 118102.

[9] ASTUMIAN, R. D. Adiabatic operation of a molecular machine. *Proc. of the Nat. Acad. of Sc. 104*, 50 (2007), 19715–19718.

[10] ASTUMIAN, R. D., AND DERÉNYI, I. Towards a chemically driven molecular electron pump. *Phys. Rev. Lett. 86*, 17 (2001), 3859–3862.

[11] BAIESI, M., AND MAES, C. An update on nonequilibrium linear response. *New Journal of Physics 15* (2013), 013004.

[12] BATH, J., GREEN, S. J., AND TURBERFIELD, A. J. A free-running dna motor powered by a nicking enzyme. *Angewandte Chemie 117*, 28 (2005), 4432–4435.

[13] BECHINGER, G. Depletion forces. *http://www.pi2.uni-stuttgart.de/contact/index.php?articleid=19* (University of Stuttgart).

[14] BECKER, T. Statistical forces in and out of equilibrium.

[15] BERG, J. M., TYMOCZKO, J. L., AND STRYER, L. *Biochemistry: International edition.* WH Freeman & Co. New York, 2006.

[16] BERRY, M., AND ROBBINS, J. Chaotic classical and half-classical adiabatic reactions: geometric magnetism and deterministic friction. *Proceedings of the Royal Society of London. Series A: Mathematical and Physical Sciences 442*, 1916 (1993), 659–672.

[17] BOERSMA, S. L. A maritime analogy of the casimir effect. *American Journal of Physics 64*, 5 (1996), 539–540.

[18] BOHEC, P., GALLET, F., MAES, C., SAFAVERDI, S., VISCO, P., AND VAN WIJLAND, F. Probing active forces via a fluctuation-dissipation relation. *arXiv:1203.3571* (2012).

[19] BOKSENBOJM, E. Response and heat in nonequilibrium.

[20] BOWMAN, G. R., BEAUCHAMP, K. A., BOXER, G., AND PANDE, V. S. Progress and challenges in the automated construction of markov state models for full protein systems. *The Journal of chemical physics 131*, 12 (2009).

[21] BOYER, P. D. Molecular motors: What makes atp synthase spin? *Nature 402*, 6759 (1999), 247–249.

[22] BRAY, D. *Cell Movements: From Molecules to Motility.* Garland Publishing, 2001.

[23] BROWN, R. Additional remarks on active molecules. *The Philosophical Magazine 6*, 33 (1829), 161–166.

[24] BROWNE, W. R., AND FERINGA, B. L. Making molecular machines work. *Nature nanotechnology 1*, 1 (2006), 25–35.

[25] CANDELIER, R., AND DAUCHOT, O. Creep motion of an intruder within a granular glass close to jamming. *Physical review letters 103*, 12 (2009), 128001.

[26] CHANDRASEKHAR, S. Stochastic problems in physics and astronomy. *Reviews of modern physics 15*, 1 (1943), 1–89.

[27] CHERNYAK, V., AND SINITSYN, N. Pumping restriction theorem for stochastic networks. *Phys. Review Lett. 101*, 16 (2008), 160601.

[28] CHERNYAK, V., SINITSYN, N., ET AL. Robust quantization of a molecular motor motion in a stochastic environment. *The Journal of chemical physics 131*, 18 (2009), 181101.

[29] CROCKER, J., MATTEO, J., DINSMORE, A., AND YODH, A. Entropic attraction and repulsion in binary colloids probed with a line optical tweezer. *Physical review letters 82*, 21 (1999), 4352–4355.

[30] DE GENNES, P. *Scaling concepts in polymer physics*. Cornell University Press, 1979.

[31] DE ROECK, W., MAES, C., AND NETOČNÝ, K. H-theorems from macroscopic autonomous equations. *Journal of statistical physics 123*, 3 (2006), 571–584.

[32] DÉMERY, V., AND DEAN, D. S. Drag forces on inclusions in classical fields with dissipative dynamics. *The European Physical Journal E 32*, 4 (2010), 377–390.

[33] DOI, M., AND EDWARDS, S. *The theory of polymer dynamics*, vol. 73. Oxford University Press, USA, 1988.

[34] DONSKER, M., AND VARADHAN, S. Asymptotic evaluation of certain markov process expectations for large time-iii. *Communications on pure and applied Mathematics 29*, 4 (1976), 389–461.

[35] DONSKER, M., AND VARADHAN, S. Asymptotic evaluation of certain markov process expectations for large time. iv. *Communications on Pure and Applied Mathematics 36*, 2 (1983), 183–212.

[36] DONSKER, M., AND VARADHAN, S. S. Asymptotic evaluation of certain markov process expectations for large time, i. *Communications on Pure and Applied Mathematics 28*, 1 (1975), 1–47.

[37] DOOB, J. L. Markoff chains – denumerable case. *Trans. Amer. Math. Soc 58*, 3 (1945), 455–473.

[38] DOOB, J. L. *Stochastic processes*, vol. 101. New York, Wiley, 1953.

[39] EDITED BY HEATH T.L. ARCHIMEDES. *On Floating Bodies I, section 5, Works of Archimedes*. Cambridge: Cambridge University Press, 1897.

[40] EINSTEIN, A. On the motion, required by the molecular-kinetic theory of heat, of particles suspended in a fluid at rest. *Ann. Phys 17* (1905), 549–560.

[41] EINSTEIN, A. Zur theorie der brownschen bewegung. *Annalen der physik 324*, 2 (1906), 371–381.

[42] EINSTEIN, A. *Investigations on the Theory of the Brownian Movement*. Dover publications, 1956.

[43] ELLIS, R. S. Large deviations and statistical mechanics.

[44] ELLIS, R. S. An overview of the theory of large deviations and applications to statistical mechanics. *Scandinavian Actuarial Journal 1995*, 1 (1995), 97–142.

[45] ELLIS, R. S. The theory of large deviations: from boltzmann's 1877 calculation to equilibrium macrostates in 2d turbulence. *Physica D: Nonlinear Phenomena 133*, 1 (1999), 106–136.

[46] ELMER, S. P., PARK, S., AND PANDE, V. S. Foldamer dynamics expressed via markov state models. i. explicit solvent molecular-dynamics simulations in acetonitrile, chloroform, methanol, and water. *The Journal of chemical physics 123* (2005), 114902.

[47] ESPAÑOL, P., AND VÁZQUEZ, F. Coarse graining from coarse-grained descriptions. *Philosophical Transactions of the Royal Society of London. Series A: Mathematical, Physical and Engineering Sciences 360*, 1792 (2002), 383–394.

[48] FERRARI, P. A., MAES, C., RAMOS, L., AND REDIG, F. On the hydrodynamic equilibrium of a rod in a lattice fluid. *Journal of Physics A: Mathematical and General 33*, 26 (2000), 4725.

[49] FEYNMAN, R. P. There's plenty of room at the bottom. *Engineering and Science 23*, 5 (1960), 22–36.

[50] FEYNMAN. RICHARD, P. The pleasure of finding things out. *Cambridge: Perseus Books 178* (1999), 19.

[51] FICK, A. On liquid diffusion. *The London, Edinburgh, and Dublin Philosophical Magazine and Journal of Science 10*, 63 (1855), 30–39.

[52] FLETCHER, S. P., DUMUR, F., POLLARD, M. M., AND FERINGA, B. L. A reversible, unidirectional molecular rotary motor driven by chemical energy. *Science 310*, 5745 (2005), 80–82.

[53] FOKKER, A. The median energy of rotating electrical dipoles in radiation fields. *Annalen Der Physik 43* (1914), 810–820.

[54] FORD, B. J. Brownian movement in clarkia pollen: a reprise of the first observations. *The Microscope 40*, 4 (1992), 235–241.

[55] FORD, G., KAC, M., AND MAZUR, P. Statistical mechanics of assemblies of coupled oscillators.

[56] FORD, G., KAC, M., AND MAZUR, P. Statistical mechanics of assemblies of coupled oscillators. *Journal of Mathematical Physics 6* (1965), 504.

[57] FULINSKI, A., GRZYWNA, Z., MELLOR, I., SIWY, Z., AND USHERWOOD, P. Non-markovian character of ionic current fluctuations in membrane channels. *Physical Review E 58* (1998), 919–924.

[58] GARDINER, C. Adiabatic elimination in stochastic systems. i: Formulation of methods and application to few-variable systems. *Physical review. A, General physics 29*, 5 (1984), 2814–2822.

[59] GENG, J., AND BEHRINGER, R. P. Slow drag in two-dimensional granular media. *Physical Review E 71*, 1 (2005), 011302.

[60] HARVEY GOULD, J. T. Statistical and thermal physics. *http://stp.clarku.edu/notes/* (2010).

[61] HERNÁNDEZ, J. V., KAY, E. R., AND LEIGH, D. A. A reversible synthetic rotary molecular motor. *Science 306*, 5701 (2004), 1532–1537.

[62] HESS, H., AND BACHAND, G. D. Biomolecular motors. *Materials Today 8*, 12 (2005), 22–29.

[63] HESS, H., AND VOGEL, V. Molecular shuttles based on motor proteins: active transport in synthetic environments. *Reviews in Molecular Biotechnology 82*, 1 (2001), 67–85.

[64] HOROWITZ, J. M., AND JARZYNSKI, C. Exact formula for currents in strongly pumped diffusive systems. *J. of Stat. Phys. 136*, 5 (2009), 917–925.

[65] HUERTA, D., AND RUIZ-SUÁREZ, J. Vibration-induced granular segregation: a phenomenon driven by three mechanisms. *Physical review letters 92*, 11 (2004), 114301.

[66] HUERTA, D., SOSA, V., VARGAS, M., AND RUIZ-SUÁREZ, J. Archimedes' principle in fluidized granular systems. *Physical Review E 72*, 3 (2005), 031307.

[67] IN: J. POPIELAWSKI J. GORECKI (EDS.) W. STILLER, E. M. Far-from-equilibrium dynamics of chemical systems. *World Scientific, Singapore 99*, 2 (1990), 578.

[68] ITÔ, K. Stochastic integral. *Proceedings of the Japan Academy, Series A, Mathematical Sciences 20*, 8 (1944), 519–524.

[69] JAEGER, H. M., NAGEL, S. R., AND BEHRINGER, R. P. Granular solids, liquids, and gases. *Reviews of Modern Physics 68*, 4 (1996), 1259–1273.

[70] JARZYNSKI, C. Thermalization of a brownian particle via coupling to low-dimensional chaos. *Physical Review Letters 74*, 15 (1995), 2937–2940.

[71] JESPERSEN, S., OSHANIN, G., AND BLUMEN, A. Polymer dynamics in time-dependent matheron-de marsily flows: An exactly solvable model. *Physical Review E 63*, 1 (2000), 011801.

[72] KAC, M. Random walk and the theory of brownian motion. *The American Mathematical Monthly 54*, 7 (1947), 369–391.

[73] KAC, M. On distributions of certain wiener functionals. *Trans. Amer. Math. Soc 65*, 1 (1949), 1–13.

[74] KAWAI, S., AND KOMATSUZAKI, T. Derivation of the generalized langevin equation in nonstationary environments. *The Journal of Chemical Physics 134* (2011), 114523.

[75] KEIZER, J. *Statistical thermodynamics of nonequilibrium processes.* Springer-Verlag, 1987.

[76] KELLY, T. R., DE SILVA, H., AND SILVA, R. A. Unidirectional rotary motion in a molecular system. *Nature 401*, 6749 (1999), 150–152.

[77] KINBARA, K., AIDA, T., ET AL. Toward intelligent molecular machines: directed motions of biological and artificial molecules and assemblies. *Chemical Reviews-Columbus 105*, 4 (2005), 1377–1400.

[78] KLEIN, O. *Zur statistischen Theorie der Suspensionen und Lösungen.* PhD thesis, Stockholm, 1921.

[79] KOLMOGOROV, A. On the theory of markov chains. *Mathematische Annalen 112* (1936), 155.

[80] KRAMERS, H. A. Brownian motion in a field of force and the diffusion model of chemical reactions. *Physica 7*, 4 (1940), 284–304.

[81] KUDROLLI, A. Size separation in vibrated granular matter. *Reports on progress in Physics 67*, 3 (2004), 209.

[82] KURZYNSKI, M. The thermodynamic machinery of life. *The Thermodynamic Machinery of Life, by Michal Kurzynski. 2006 XIV, 431 p. 193 illus. 3-540-23888-3. Berlin: Springer, 2006. 1* (2006).

[83] LANDFORD, O. Entropy and equilibrium states in classical statistical mechanics, in: A> lenard(ed.), statistical mechanics and mathematical problems. *Lecture Notes in Physics 20* (1973), 1–113.

[84] LANGEVIN, P. Sur la théorie du mouvement brownien. *CR Acad. Sci. Paris 146*, 530-533 (1908).

[85] LEBON, G., JOU, D., AND VÁZQUEZ, J. C. *Understanding non-equilibrium thermodynamics: foundations, applications, frontiers.* Springer, 2008.

[86] LEIGH, D. A., WONG, J. K., DEHEZ, F., ZERBETTO, F., ET AL. Unidirectional rotation in a mechanically interlocked molecular rotor. *Nature 424*, 6945 (2003), 174–179.

[87] LÉVY, P. Processus stochastiques et mouvement brownien. *Loeve.(French) Gauthier-Villars, Paris* (1948).

[88] LEWIS, J. T., PFISTER, C.-E., AND SULLIVAN, W. G. Large deviations and the thermodynamic formalism: A new proof of the equivalence of ensembles, in: M. fannes, c. maes, a. verbeure(eds.). 183–192.

[89] MACKAY, R. Langevin equation for slow degrees of freedom of hamiltonian systems. *Nonlinear Dynamics and Chaos: Advances and Perspectives, Understanding Complex Systems 1* (2010), 89–102.

[90] MAES, C. Lectures on markov processes for physics students. *http://itf.fys.kuleuven.be/ christ/markovLECT123.pdf* (2012).

[91] MAES, C. Nonequilibrium entropies. *Physica Scripta 86*, 5 (2012), 058509.

[92] MAES, C., NETOČNÝ, K., AND THOMAS, S. R. General no-go condition for stochastic pumping. *The Journal of chemical physics 132* (2010), 234116.

[93] MAES, C., NETOČNÝ, K., AND WYNANTS, B. On and beyond entropy production: the case of markov jump processes. *Markov Processes and Related Fields* (2008), 445–464.

[94] MAES, C., SAFAVERDI, S., VISCO, P., AND VAN WIJLAND, F. Fluctuation-response relations for nonequilibrium diffusions with memory. *arXiv:1211.2181* (2012).

[95] MAES, C., AND THOMAS, S. R. Archimedes' law and its corrections for an active particle in a granular sea. *Journal of Physics A: Mathematical and Theoretical 44*, 28 (2011), 285001.

[96] MAES, C., AND THOMAS, S. R. From langevin to generalized langevin equations for the nonequilibrium rouse model. *Physical Review E 87*, 2 (2013), 022145.

[97] MAHADEVAN, L., AND YONG, E. H. Probability, physics, and the coin toss. *Physics Today 64* (2011), 66.

[98] MARKOV, A. An example of statistical analysis of the text of eugene onegin illustrating the association of trials into a chain. *Bulletin de l, Acadamie Imperiale des Sciences de St. Petersburg, ser 6*, 7 (1913), 153–162.

[99] MCPHIE, M., DAIVIS, P., SNOOK, I., ENNIS, J., AND EVANS, D. Generalized langevin equation for nonequilibrium systems. *Physica A: Statistical Mechanics and its Applications 299* (2001), 412–426.

[100] MEJÍA-MONASTERIO, C., AND OSHANIN, G. Bias-and bath-mediated pairing of particles driven through a quiescent medium. *Soft Matter 7*, 3 (2011), 993–1000.

[101] MORI, H. Transport, collective motion, and brownian motion. *Progress of Theoretical Physics 33* (1965), 423–455.

[102] NICHOL, K., ZANIN, A., BASTIEN, R., WANDERSMAN, E., AND VAN HECKE, M. Flow-induced agitations create a granular fluid. *Physical review letters 104*, 7 (2010), 078302.

[103] OSHANIN, G., AND BLUMEN, A. Rouse chain dynamics in layered random flows. *Physical Review E 49*, 5 (1994), 4185–4191.

[104] PACHECO-VÁZQUEZ, F., AND RUIZ-SUÁREZ, J. Cooperative dynamics in the penetration of a group of intruders in a granular medium. *Nature communications 1* (2010), 123.

[105] PANJA, D. Anomalous polymer dynamics is non-markovian: memory effects and the generalized langevin equation formulation. *Journal of Statistical Mechanics: Theory and Experiment 2010*, 06 (2010), P06011.

[106] PANJA, D. Generalized langevin equation formulation for anomalous polymer dynamics. *Journal of Statistical Mechanics: Theory and Experiment 2010* (2010), L02001.

[107] PARK, S., AND PANDE, V. S. Validation of markov state models using shannon's entropy. *The Journal of chemical physics 124*, 5 (2006), 054118–054118.

[108] PAULI, W. Sommerfeld festschrift. *S. Hirzel, Oxford* (1928), 30.

[109] PLANCK, M. Fokker-planck equation. *Sitzber, Preub. Akad. Wiss* (1917), 324.

[110] PUSHKIN, A., AND ELTON, O. Evgeny onegin. *The Slavonic and East European Review* (1936), 249–269.

[111] RAHAV, S., HOROWITZ, J., AND JARZYNSKI, C. Directed flow in nonadiabatic stochastic pumps. *Phys. Rev. Lett. 101*, 14 (2008), 140602.

[112] REIMANN, P. Brownian motors: noisy transport far from equilibrium. *Physics Reports 361*, 2 (2002), 57–265.

[113] ROSATO, A., STRANDBURG, K. J., PRINZ, F., AND SWENDSEN, R. H. Why the brazil nuts are on top: Size segregation of particulate matter by shaking. *Physical Review Letters 58*, 10 (1987), 1038–1040.

[114] ROUSE JR, P. A theory of the linear viscoelastic properties of dilute solutions of coiling polymers. *The Journal of Chemical Physics 21* (1953), 1272.

[115] RUELLE, D., AND MECHANICS, S. *Rigorous Results,*. World Scientific, 1969.

[116] SCHLIWA, M. *Molecular motors*. Wiley-VCH, 2006.

[117] SCHROEDER, D. V. *An Introduction to Thermal Physics*. Pearson Education, India, 2007.

[118] SHEA, J., AND OPPENHEIM, I. Fokker-planck equation and langevin equation for one brownian particle in a nonequilibrium bath. *Journal of Physical Chemistry 100* (1996), 19035–19042.

[119] SHISHODIA, N., AND WASSGREN, C. R. Particle segregation in vibrofluidized beds due to buoyant forces. *Physical Review Letters 87*, 8 (2001), 084302.

[120] SHORE, S. N. *Forces in physics: A Historical Perspective*. Greenwood Press, Westport, 2008.

[121] SINITSYN, N., AND NEMENMAN, I. Universal geometric theory of mesoscopic stochastic pumps and reversible ratchets. *Phys. Rev. Lett. 99*, 22 (2007), 220408.

[122] STIRZAKER, D. R., AND GRIMMETT, G. *Probability and Random Processes*. Oxford University Press, Oxford, 2002.

[123] THOULESS, D. Quantization of particle transport. *Physical Review B 27*, 10 (1983), 6083.

[124] TOUCHETTE, H. The large deviation approach to statistical mechanics. *Physics Reports 478*, 1 (2009), 1–69.

[125] TSONG, T. Y. Na, k-atpase as a brownian motor: Electric field-induced conformational fluctuation leads to uphill pumping of cation inthe absence of atp. *Journal of Biological Physics 28*, 2 (2002), 309–325.

[126] WYNANTS, B. Structures of nonequilibrium fluctutaions: dissipation and activity. *arXiv preprint arXiv:1011.4210* (2010).

[127] YAN, H., ZHANG, X., SHEN, Z., AND SEEMAN, N. C. A robust dna mechanical device controlled by hybridization topology. *Nature 415*, 6867 (2002), 62–65.

[128] ZIK, O., STAVANS, J., AND RABIN, Y. Mobility of a sphere in vibrated granular media. *EPL (Europhysics Letters) 17*, 4 (1992), 315.

[129] ZWANZIG, R. Memory effects in irreversible thermodynamics. *Physical Review 124*, 4 (1961), 983.

[130] ZWANZIG, R. Nonlinear generalized langevin equations. *Journal of Statistical Physics 9*, 3 (1973), 215–220.

[131] ZWANZIG, R. *Nonequilibrium Statistical Mechanics*. Oxford University Press, USA, 2001.

# Curriculum Vitae

## Personal Details

- **Address:** Institute for Theoretical Physics, 200D Celestijnenlaan 3001, Heverlee, Belgium.
- **Date of Birth:** 29, March 1984 **Place of Birth:** Ghaziabad, India
- **Citizenship:** Indian
- **email** simi.thomas@fys.kuleuven.be **Mobile** +32474061016

## Professional Experience

- **PhD in physics (2009 - 2013)**, Institute for Theoretical Physics, KU Leuven Belgium.
- **Teaching Duties**
  - Quantum Physics (2012-2013)
  - Kwantummechanica (2010 - 2012)
  - Nonequilibrium Statistical Physics (2009 - 2010)
- **Schools and Conferences attended**
  - German – Belgian "Energiewende" Symposium, September 2012, KU Leuven Belgium
  - Foundations and Applications of Non-Equilibrium Statistical Mechanics, September 2011, NORDITA Stockholm
  - Belgian Physical Society Meeting, May 2011, Namur
  - Foundations of Nonequilibrium Statistical Physics: from basic science to future challenges, September 2010, Granada
  - Fluctuations, information flow and experimental measurements, January 2010, Institut des Systèmes Complexes, Paris
  - Journées de physique statistique January 2010, l'Ecole Supérieure de Physique et Chimie de Paris, Paris

- – Understanding and exploiting complexity at the nanoscale, January 2010, ULB Brussels
- – International Summer School : Fundamental Problems in Statistical Physics XII, August 2009 KU Leuven.
- **Couses Attended**
  - – Plasma Physics, June 2012, ITF Leuven
  - – Advanced Quantum Monte Carlo methods, June 2011, ITF Leuven
  - – Feynman diagrams for solid state physics, April 2011, ITF Leuven
  - – Introduction to homogeneous and inhomogeneous liquids, February 2010, ITF Leuven

## Education

- Research project (2008-2009), Fluctuation effects in soft matter, Raman Research Institute, India
- Master of physics (2005-2007), University of Delhi, India
- Bachelor of physics (2002-2005), St Stephen's college, University of Delhi, India

## Scholarships

- Joint Research Fellowship, University Grants Commission, India (2007)
- Top 2% in Joint Entrance Screening Test (JEST), India (2007)

**Languages**     English, Hindi, Malayalam, French, Dutch

# List of publications

(Authors in alphabetical order)

1. Christian Maes and Simi R. Thomas,
   From Langevin to generalized Langevin equations for the nonequilibrium Rouse model,
   Physical Review E **87**, 022145, (2013)

2. Christian Maes and Simi R. Thomas,
   Archimedes' law and its corrections for an active particle in a granular sea,
   Journal of Physics A: Mathematical and Theoretical **44**, 285001, (2011)

3. Christian Maes, Karel Netočný, Simi R. Thomas,
   General no-go condition for stochastic pumping,
   The Journal of chemical physics **132**, 234116 (2010)
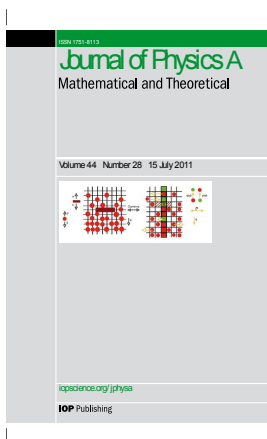
FACULTY OF SCIENCE
DEPARTMENT OF PHYSICS AND ASTRONOMY
INSTITUUT VOOR THEORETISCHE FYSICA
Celestijnenlaan 200D
B-3001 Heverlee
simi.thomas@fys.kuleuven.be
https://itf.fys.kuleuven.be